SLENDER-BODY THEORY FOR STOKES FLOW AND FLAGELLAR HYDRODYNAMICS

Thesis by

Robert Edward Johnson

In Partial Fulfillment of the Requirements

for the Degree of

Doctor of Philosophy

California Institute of Technology

Pasadena, California

1977

(Submitted May 17, 1977)

ACKNOWLEDGMENTS

I sincerely thank Professor Theodore Y. T. Wu for his continual guidance and enthusiasm which made this research not only a rewarding experience, but an enjoyable one as well. Much appreciation is also extended to Professor Christopher Brennen for having always been available for the many enlightening discussions on various aspects of this work.

I am greatly indebted to Helen Burrus for her masterful preparation of this manuscript which involved a generous donation of her own time. My sincere gratitude also goes to Cecilia Lin for the skillful preparation of the figures.

To my wife, Mary, go my deepest thanks for her constant personal support and for the many sacrifices she made in order that I might complete this work.

Finally, sincere thanks are due Rockwell International, the National Science Foundation, the Office of Naval Research and the California Institute of Technology for the financial assistance that supported this investigation.

ABSTRACT

The singularity method for Stokes flow is used to examine the flow past slender bodies possessing finite centerline curvature, in a viscous, incompressible fluid without any appreciable inertia effects. The motion of a slender toroidal ring in Stokes flow is considered first. The symmetry of the geometry and absence of ends has made an accurate analysis possible; the result of this problem elucidates the general flow characteristics present for bodies moving in an arbitrary manner with a finite centerline curvature. Using the methods developed here it is possible to calculate the force/length to higher orders in the slenderness parameter, ϵ, than has previously been possible. In particular, we find the Stokeslet strength with an error of $O(\epsilon^2)$. The solution of the torus problem serves as an effective guide in extending the theory to slender bodies of circular cross section with arbitrary centerline configurations and spheroidal ends. In all the cases considered, the no-slip boundary condition is satisfied by distributing appropriate Stokeslets, doublets, rotlets, sources, stresslets, and quadrupoles on the body centerline up to an error term of $O(\epsilon^2 \ln\epsilon)$, which is sufficient for practical application. From the general slender body analysis we find an integral equation which determines the Stokeslet strength up to the term of $O(\epsilon^2)$. The general theory is then applied to examine the propulsion of flagellated microorganisms, including an approximate solution for the interaction between cell body and flagella. A final brief note is made on the thrust enhancing capabilities of oscillating non-spherical cell bodies.

TABLE OF CONTENTS

LIST OF FIGURES

I. INTRODUCTION

The hydromechanics of slender body theory in the Stokes flow regime plays a fundamental role in the study of micro-organism locomotion, sedimentation, aerosol physics, and many other areas of biophysics and geophysics. In recent years this area of fluid mechanics has received considerable attention (Tuck, 1964; Cox, 1970; Tillett, 1970; Batchelor, 1970; Keller & Rubinow, 1976). Yet most of the available literature consider only bodies with straight centerlines. Those few authors examining the general case account only for the lowest order effects of body-centerline curvature and exclude any consideration of body ends.

Here we will construct solutions to bodies of circular cross section by distributing flow singularities along the body centerline. We restrict our attention to bodies whose cross-sectional radius, b, is small compared to its length, 2ℓ, and its radius of centerline curvature, $1/\kappa$. The velocity field is obtained in a neighborhood of the body surface as an expansion in the slenderness parameter, $\epsilon = b/\ell$. Application of the no-slip boundary condition produces a set of simultaneous integral equations for the Stokeslet strength. In the previous theories the method of matched asymptotic expansions has been applied to determine the force/length, or equivalently the Stokeslet strength as a series in $(\ln\epsilon)^{-n}$, $n = 1, 2, \ldots$. Because of the analytical complexity, however, only the first two or three terms have been obtained. Solution of the integral equations found here has higher accuracy, as we are able to calculate the Stokeslet strength up to an error of $O(\epsilon^2)$. In order to achieve this

accuracy numerical computation is in general required. However, for the special case of a slender toroidal ring, which is characterized by its unique rotational symmetry and lack of ends, a completely analytic analysis is possible. This spendid example will serve as a guide in constructing the solution to the general case.

It may be pointed out here that in all of the existing theories for slender bodies with a curved centerline moving in Stokes flow, the local curvature effect has been neglected as an approximation, but this effect will be accounted for here. For example, Cox's inner expansion is, at the order of approximation found there, simply the solution for flow past a straight circular cylinder. This is also true for the analysis of Keller & Rubinow. By satisfying the boundary condition to higher orders in the slenderness parameter we will correct the solution for the effect of local body curvature. The boundary condition will in fact be satisfied neglecting $O(\epsilon^2 \ln \epsilon)$ by using appropriate distributions of Stokeslets, doublets, rotlets, sources, stresslets, and quadrupoles. Furthermore, the boundary conditions will be satisfied at the body ends provided the body has a spheroidal cross section near the ends.

Our investigation will begin in Chapter II with a study of the arbitrary motion of a torus. The linearity of the Stokes equations allows us to divide the arbitrary motion of torus into five fundamental problems: a translation along and a translation perpendicular to the generating or longitudinal axis, a rotation about an axis perpendicular to the longitudinal axis and intersecting the torus centerline, a rotation about the longitudinal axis, and a torus in a radial flow. At the

outset of this study an elementary discussion will be presented describing the various methods available for expanding the integrals that result from using the singularity method.

In Chapter III we consider an extension of the methods developed for the torus problem to arbitrary slender bodies. We shall first consider bodies with circular cross sections along a curved centerline and with cross-sectional area satisfying a spheroidal distribution, and then proceed to consider bodies with cross sections that need only be spheroidal in the vicinity of the ends. Chapter III is then concluded with an application to the flow past a partial torus.

The final chapter is addressed to the important problem of flagellar hydromechanics by applying the present theory to a flagellum performing a prescribed planar motion of finite amplitude. Data are chosen for the spermatoza of Chaetopterus and oyster, for which comparisons are made between the present slender body theory and the classical theories. The interaction between cell body and flagellum is further evaluated in an approximate sense, for the special case of spherical bodies, by applying the method introduced by Burgers (1938). The chapter is then concluded with a brief study of the thrust enhancement that can be achieved by organisms which have non-spherical cell bodies that oscillate in the direction transverse to the direction of propulsion.

II. STOKES FLOW PAST A SLENDER TORUS

The torus is chosen for the primary investigation of the body-centerline-curvature effects in Stokes flow because it possesses two desirable features. First, it has a constant finite curvature since the radius of the centerline, or major radius, is comparable to the total body length. Second, it has no ends. These two characteristics along with the body symmetry render the problem tractable by analytical methods. This example will provide valuable information that proves to be enlightening in constructing the solution for the general case.

Figure (2. 1. 1) shows the torus and the coordinates to be used. It is assumed henceforth that the cross-sectional radius, b, is small compared with the major radius a, i. e., $\epsilon = b/a \ll 1$.

The governing equations for the Stokes flow and boundary conditions are

$$\nabla p = \mu \nabla^2 \underline{u}$$

$$\nabla \cdot \underline{u} = 0$$

$$\underline{u} = \underline{U} \qquad (\underline{x} \text{ on } S_b)$$

$$\underline{u} \to 0 \qquad \text{as } \underline{x} \to \infty$$

where $\underline{u}$ is the velocity field, p the pressure, $\underline{U}$ the velocity of the body and S_b the body surface. The solution will be constructed by applying the method of singularities which was extensively studied for bodies which are not necessarily slender by Chwang & Wu (1974, 1975).

2.1 A torus in translation along its longitudinal axis

We consider a torus moving with velocity U along its longitudinal axis which is taken to be the z-axis in a cylindrical coordinate system (r, θ, z). Motivated by the results available for slender bodies with straight centerlines we represent the flow field, as a first approximation, by a distribution of Stokeslets and doublets directed parallel to the z-axis, along the body centerline $r = a$. The velocity at $\theta = \theta'$ is given by

$$\underline{u} = \underline{u}_S + \underline{u}_D = \int_{\theta'}^{\theta'+2\pi} \{\underline{U}_S(\underline{R};\underline{a}) + \underline{U}_D(\underline{R};\underline{\beta})\}\, a\,d\theta \quad ,$$

where the fundamental Stokeslet and doublet are given respectively by

$$\underline{U}_S = \frac{\underline{a}}{R} + \frac{(\underline{a}\cdot\underline{R})\underline{R}}{R^3} \quad ,$$

$$\underline{U}_D = \frac{\underline{\beta}}{R^3} - \frac{3(\underline{\beta}\cdot\underline{R})\underline{R}}{R^5} \quad , \qquad (2.1.1)$$

$$\underline{R} = \underline{x} - \underline{\xi} = (r\cos\theta' - a\cos\theta)\underline{e}_x + (r\sin\theta' - a\sin\theta)\underline{e}_y + z\underline{e}_z \, ,$$

$$R = |\underline{R}| = (r^2 + a^2 + z^2 - 2ar\cos\varphi)^{1/2} \quad ,$$

$$\varphi = \theta - \theta' \, ,$$

(see figures 2.1.1 and 2.1.2).

The no-slip boundary condition $\underline{u} = U\underline{e}_z$ on $r_1 = b$, where $r_1 = [(r-a)^2 + z^2]^{1/2}$, will produce an integral equation for the Stokeslet strength $\underline{a}(\theta)$ and the doublet strength $\underline{\beta}(\theta)$. However, from the flow symmetry we assume a priori that

$\underline{\alpha} = \alpha \underline{e}_z$ and $\underline{\beta} = \beta \underline{e}_z$ where α, β are constants. This assumption will in fact be verified a posteriori when the boundary condition is satisfied.

In terms of the unit vectors $\underline{e}'_r$, $\underline{e}'_\theta$, $\underline{e}_z$ at $\theta = \theta'$ (see figures 2. 1. 1 and 2. 1. 2) we may write

$$\underline{R} = (r - a\cos\varphi)\underline{e}'_r - a\sin\varphi\,\underline{e}'_\theta + z\underline{e}_z \,. \qquad (2.1.2)$$

Furthermore, by introducing the curvilinear orthogonal coordinate system (r_1, θ, ψ) defined by (see figures 2. 1. 1 and 2. 1. 2)

$$x = r\cos\theta = (a + r_1\cos\psi)\cos\theta$$

$$y = r\sin\theta = (a + r_1\cos\psi)\sin\theta$$

$$z = r_1\sin\psi \,,$$

we have

$$R = [2a^2(1 + r_1/a\cos\psi)(1 - \cos\varphi) + r_1^2\,]^{1/2} \,. \qquad (2.1.3)$$

This first torus problem will be examined in detail in order that the methods are fully presented; however, in the remaining examples much of the tedious analysis will be curtailed.

We next attempt to integrate equation (2. 1. 1) and apply the boundary condition on $r_1 = b$. Before doing so, it is appropriate first to discuss more generally the methods available. For the special case of a torus, where it is possible to presuppose the functional form of the singularity distributions, the integrals may be expressed in terms of complete elliptic integrals, as was shown by Wu & Yates (1976) for the analogous potential flow problem.

The well-known asymptotic expansions can then be used to evaluate the velocity on $r_1 = b$. However for the general case where the functional forms of the singularity distributions are not known a priori, a more general approach is needed, as will be discussed below.

For the torus problem it is sufficient to consider the integral

$$I = \int_{\theta'}^{\theta'+2\pi} \frac{f(\theta)d\theta}{R} \quad , \qquad (2.1.4)$$

where R is given in (2.1.3) and $f(\theta)$ is continuously differentiable for as many times as necessary. Similar integrals arising for the torus problems and those to be found when considering the general slender body case can be evaluated by following the same basic procedure as that to be developed here. The objective is to expand the integrand in equation (2.1.4) in a neighborhood of the body surface, i.e., $r_1 \ll a$, with the resulting expansion being easily integrated termwise. The method is essentially a generalization of that used by Handelsman & Keller (1967), and Tillett (1970) for axisymmetric slender bodies.

The integral above can be rewritten as

$$I = (ar)^{-1/2} \int_0^{\pi} \frac{f(\theta'+\varphi) + f(\theta'-\varphi)}{\sqrt{2(1-\cos\varphi) + r_1^2/ar}} \, d\varphi \quad , \qquad (2.1.5)$$

where $r = a + r_1\cos\psi$. In the neighborhood of the torus surface, $r_1/a = O(\epsilon)$ and $r_1^2/ar = O(\epsilon^2)$. Consequently, if $f(\theta)$ is a sufficiently smooth function of $O(1)$, we clearly see that the

integrand is of order ϵ^{-1} at $\varphi = 0$ and decreases monotonically and rather rapidly to O(1) when φ moves away from $\varphi = 0$. We note that the two terms in the square root, namely $1 - \cos\varphi$ and r_1^2/ar, become of the same order when φ is of $O(\epsilon)$. This suggests that we construct an inner expansion of the integrand near $\varphi = 0$ and an outer expansion for $\varphi = O(1)$. For this purpose we introduce the inner or stretched variable

$$\sigma = \varphi/\epsilon \ , \qquad (2.1.6)$$

for expansion of the integrand in the 'inner region' near $\varphi = 0$. We can then construct a uniformly valid or composite expansion from the inner expansion about $\varphi = 0$ and the outer expansion for $\varphi = O(1)$, using the standard methods of perturbation theory (Kaplun, 1967; Van Dyke, 1975; Cole, 1968).

For convenience we define

$$h(\varphi, \theta';\epsilon) = \frac{f(\theta'+\varphi)+f(\theta'-\varphi)}{[2(1-\cos\varphi)+\epsilon^2\eta^2]^{1/2}} \ , \qquad (2.1.7)$$

where $\epsilon^2\eta^2 = r_1^2/ar$. The inner expansion of h to n terms is then given for $\epsilon \to 0$, holding σ fixed, by

$$E_n^{(i)}h = \lim_{\substack{\epsilon\to 0 \\ \sigma \text{ fixed}}} h(\epsilon\sigma, \theta';\epsilon) = \sum_{j=o}^{n-1} \mu_j(\epsilon)h_j(\sigma, \theta') \ ,$$

where the coefficients $\mu_j(\epsilon)$ form an asymptotic sequence of functions such that

$$\mu_{n+1}(\epsilon) = o(\mu_n(\epsilon)) \qquad \text{as } \epsilon \to 0 \ .$$

For $\epsilon \to 0$, with φ held fixed, we express the outer expansion of h up to n terms as

$$E_n^{(o)}h = \lim_{\substack{\epsilon \to 0 \\ \varphi \text{ fixed}}} h(\varphi;\theta',\epsilon) = \sum_{j=o}^{n-1} \nu_j(\epsilon) g(\varphi;\theta') \quad ,$$

where $\nu_j(\epsilon)$ form another asymptotic sequence of functions, namely $\nu_{j+1}(\epsilon) = o(\nu_j(\epsilon))$ as $\epsilon \to 0$. In our case we will in fact find $\mu_j(\epsilon) = \epsilon^{2j-1}$, $\nu_j(\epsilon) = \epsilon^{2j}$, by virtue of h being even in φ. The uniformly valid expansion is then formed in the usual manner and is given by

$$E_n^{(c)}h = E_n^{(i)}h + E_n^{(o)}h - E_n^{(i)} E_n^{(o)}h \, . \qquad (2.1.8)$$

The last term represents an inner expansion and outer expansion operated on h in succession, regardless of order, and is often referred to as the common-part expansion. This uniformly valid expansion as the name implies, holds uniformly for $0 \leqslant \varphi \leqslant \pi$, with error of order ϵ^{2n-1}. Substituting (2.1.8) into (2.1.5) then allows termwise integration, resulting in an asymptotic expansion for I as $\epsilon \to 0$. We note that the integration will modify the error of the final result.

The algebra involved in this method is quite complex but can be reduced for the case of a torus, where the body shape has no ends, by following a somewhat simplified procedure. We write the integral I as follows

$$I = (ar)^{-1/2}\{\int_o^{\gamma} E_n^{(i)}h\,d\varphi + \int_{\gamma}^{\pi} E_n^{(o)}h\,d\varphi + O(\epsilon^{2n-1})\} \, ,$$

with γ chosen to be $\epsilon \ll \gamma \ll \pi$. A particularly useful choice is to restrict γ to $O(1) > O(\gamma^2) > O(\epsilon)$. The above integration procedure is justified by considering the uniformly valid expansion of h. We regroup the terms in (2. 1. 8) as follows,

$$E_n^{(c)}h = E_n^{(i)}h + R_n^{(i)}h \qquad (0 \leqslant \varphi \leqslant \gamma)$$

$$= E_n^{(o)}h + R_n^{(o)}h \qquad (\gamma \leqslant \varphi \leqslant \pi)$$

where

$$R_n^{(i)}h = E_n^{(o)}(h - E_n^{(i)}h) \quad ,$$

$$R_n^{(o)}h = E_n^{(i)}(h - E_n^{(o)}h) \quad .$$

We observe that both 'residual expansion' $R_n^{(i)}h$ and $R_n^{(o)}h$ are of $O(\epsilon^{2n-1})$ in their respective regions of φ, when the inner and outer regions overlap. It therefore follows that

$$\int_o^\pi h d\varphi = \int_o^\pi E_n^{(c)}h d\varphi + \int_o^\pi (h - E_n^{(c)}h)d\varphi$$

$$= \int_o^\gamma (E_n^{(i)}h + R_n^{(i)}h)d\varphi + \int_\gamma^\pi (E_n^{(o)}h + R_n^{(o)}h)d\varphi + O(\epsilon^{2n-1})$$

$$= \int_o^\gamma E_n^{(i)}h d\varphi + \int_\gamma^\pi E_n^{(o)}h d\varphi + O(\epsilon^{2n-1}) \quad .$$

This method also implies that the resulting expansion of I will not involve γ, provided it is appropriately chosen so that the regions overlap. This process will be employed in expanding the integrals encountered for various motions of a torus. Later, for the general

case, it will be necessary to employ the general uniformly valid expansion procedure in order to construct solutions valid everywhere, including the body ends. Another comment in order is that the above method enables one to distinguish between short and long range contributions to the velocity field, whereas the elliptic integral technique does not readily offer such physical information about the solution.

Returning now to the motion of a torus we separate equation (2. 1. 1) as just discussed

$$\underline{u} = \int_{\theta'+\gamma}^{\theta'+2\pi-\gamma} (\underline{U}_S + \underline{U}_D) a d\theta + \int_{\theta'-\gamma}^{\theta'+\gamma} (\underline{U}_S + \underline{U}_D) a d\theta \quad . \qquad (2.1.9)$$

With respect to the region of integration in the above two integrals we will refer to them as follows: the first will be called the far-field singularity distribution and the second the near-field singularity distribution.

The outer and inner expansions of R in terms of φ are respectively given by

$$R = \sqrt{2}a(1+\tilde{\epsilon}\cos\psi)^{1/2}(1-\cos\varphi)^{1/2}\{1+O(\frac{\tilde{\epsilon}^2}{1-\cos\varphi})\} \quad , \qquad (2.1.10)$$

$$\text{for } \gamma < \varphi < 2\pi-\gamma$$

$$R = a\Delta\{1 - \frac{\varphi^4}{24\Delta^2} + O(\frac{\epsilon\varphi^4}{\Delta^2}, \frac{\varphi^6}{\Delta^2})\} \quad , \qquad (2.1.11)$$

$$\text{for } -\gamma < \varphi < \gamma$$

where $\tilde{\epsilon} = r_1/a$, $\Delta = [(1+\tilde{\epsilon}\cos\psi)\varphi^2 + \tilde{\epsilon}^2]^{1/2}$.

We retain the actual form of the error terms in order to obtain an accurate final error estimate, since the integration, as already mentioned, will modify that error.

In satisfying the boundary condition on the torus we will always consider the three components of velocity at $\theta = \theta'$ in a cylindrical coordinate system, namely

$$\begin{aligned} u &= \underline{u} \cdot \underline{e}'_r && \text{(radial component)} \\ v &= \underline{u} \cdot \underline{e}'_\theta && \text{(tangential component)} \\ w &= \underline{u} \cdot \underline{e}_z && \text{(axial component)} \end{aligned} \qquad (2.1.12)$$

By examining the far-field singularity distribution, or equivalently the outer expansion, we observe that up to an error of $O(\epsilon^2 \ln \epsilon)$, the contribution to the velocity field from the far-field doublet distribution can be neglected. In fact, the integrand of the doublet in the outer expansion is proportional to β/a^3, we easily see then that its contribution to the velocity in the near field will be, upon integration, of order β/a^2. If we expect the doublet strength to leading order to be the same as found for a straight slender spheroid (as will be verified later), namely $\beta = ab^2/2$, we can then conclude that this contribution to the velocity will be $O(a\epsilon^2)$. Therefore the far-field doublet distribution may be neglected. Actual integration of the far-field doublet is straightforward and the result confirms our expectation that the far-field doublet contribution to the velocity field is of $O(a\epsilon^2)$. Equation (2.1.9) then becomes

$$\underline{u} = \int_{\gamma}^{2\pi-\gamma} \underline{U}_S a d\varphi + \int_{-\gamma}^{\gamma} (\underline{U}_S + \underline{U}_D) a d\varphi + O(a\epsilon^2) \ . \qquad (2.1.13)$$

We first consider the velocity field induced by the Stokeslet distribution, $\underline{U}_S$. For the near field, the inner expansion of $\underline{R}$, which is simply the expansion for small φ, is given in terms of the (r_1, θ, ψ) coordinate system and the unit vectors $(\underline{e}'_r, \underline{e}'_\theta, \underline{e}_z)$ at $\theta = \theta'$ by

$$\underline{R} = a\{(\tilde{\epsilon}\cos\psi + \varphi^2/2 + O(\varphi^4))\underline{e}'_r - (\varphi - \varphi^3/6 + O(\varphi^5))\underline{e}'_\theta + \tilde{\epsilon}\sin\psi\,\underline{e}_z\}. \qquad (2.1.14)$$

Using this and equation (2.1.11) in $\underline{U}_S$ given in (2.1.1), and recalling that for this case $\underline{a} = a\underline{e}_z$, we find the inner expansion to be,

$$\underline{U}_S^{(i)} = \frac{a\underline{e}_z}{a\Delta}\left[1 + \frac{\varphi^4}{24\Delta^2} + O\left(\frac{\tilde{\epsilon}\varphi^4}{\Delta^2}, \frac{\varphi^6}{\Delta^2}\right)\right] + \frac{az}{a^2\Delta^3}\left[(\tilde{\epsilon}\cos\psi + \varphi^2/2 + O(\varphi^4))\underline{e}'_r - (\varphi - \varphi^3/6 + O(\varphi^5))\underline{e}'_\theta + \tilde{\epsilon}\sin\psi\,\underline{e}_z\right]\left(1 + O\left(\frac{\varphi^4}{\Delta^2}\right)\right) .$$

The velocity components of the integral of this near-field Stokeslet (which is the first part of the second integral in equation 2.1.13), when expressed in the cylindrical coordinates as (u, v, w), at $\theta = \theta'$ are given by (after using the integrals defined in Appendix A and noting that odd functions of φ integrate to zero),

$$u_S^{(i)} = 2a\sin\psi\{\cos\psi + \tfrac{1}{2}\tilde{\epsilon}\ln 2\gamma/\tilde{\epsilon} - \tfrac{1}{2}\tilde{\epsilon}(1+\cos^2\psi) + O(\epsilon^2\ln\epsilon)\},$$

$$v_S^{(i)} = 0,$$

$$w_S^{(i)} = 2a\{(1 - \tfrac{1}{2}\tilde{\epsilon}\cos\psi)\ln 2\gamma/\tilde{\epsilon} + \tfrac{\tilde{\epsilon}}{2}\cos\psi + \tfrac{1}{48}\gamma^2 + \sin^2\psi(1 - \tfrac{1}{2}\tilde{\epsilon}\cos\psi) + O(\epsilon^2\ln\epsilon)\}.$$

The outer expansion of the Stokeslet distribution is given, using equations (2. 1. 10) and (2. 1. 1), by

$$\underset{\sim}{U}_S^{(o)} = \{\frac{a\underset{\sim}{e}_z}{ac(1-\cos\varphi)^{1/2}} + \frac{az\underset{\sim}{R}}{a^3c^3(1-\cos\varphi)^{3/2}}\}(1+O(\frac{\tilde{\epsilon}^2}{1-\cos\varphi})),$$

where $c = \sqrt{2}(1+\tilde{\epsilon}\cos\psi)^{1/2}$

and $\underset{\sim}{R}$ is given in equation (2. 1. 2). Using the integrals in Appendix A, and again noting that odd functions of φ give zero, we have

$$u_S^{(o)} = a\{\sin\psi\,\tilde{\epsilon}\ln\frac{4}{\gamma} + O(\epsilon^2)\},$$

$$v_S^{(o)} = 0,$$

$$w_S^{(o)} = 2a\{(1 - \tfrac{\tilde{\epsilon}}{2}\cos\psi)\ln\frac{4}{\gamma} - \frac{1}{48}\gamma^2 + O(\epsilon^2\ln\epsilon)\}.$$

Combining the velocity fields at $\theta = \theta'$ due to both Stokeslets gives the following result, which is independent of γ as expected.

$$u_S = a \sin\psi \{2\cos\psi + \tilde{\epsilon} \ln \frac{8}{\tilde{\epsilon}} - \tilde{\epsilon}(1 + \cos^2\psi) + O(\epsilon^2 \ln \epsilon)\} ,$$

$$v_S = 0 ,$$

$$w_S = 2a\{(1 - \frac{\tilde{\epsilon}}{2}\cos\psi) \ln \frac{8}{\tilde{\epsilon}} + \frac{\tilde{\epsilon}}{2}\cos\psi + \sin^2\psi(1 - \frac{\tilde{\epsilon}}{2}\cos\psi)$$

$$+ O(\epsilon^2 \ln \epsilon)\} .$$

As already discussed, we need only consider the contribution of the near-field doublet distribution, which is given by

$$\underline{u}_D = \int_{-\gamma}^{\gamma} \{ \frac{\beta \underline{e}_z}{R^3} - \frac{3\beta z \underline{R}}{R^5} \} \, a d\varphi .$$

Substituting for $\underline{R}$ and R from (2.1.11) and (2.1.14) gives the inner expansion

$$\underline{u}_D = \int_{-\gamma}^{\gamma} \{ \frac{\beta \underline{e}_z}{a^3 \Delta^3} - \frac{3\beta z}{a^4 \Delta^5} [(\tilde{\epsilon}\cos\psi + \frac{\varphi^2}{2} + O(\varphi^4)) \underline{e}'_r - (\varphi - \frac{\varphi^3}{6}$$

$$+ O(\varphi^5)) \underline{e}'_\theta + \tilde{\epsilon} \sin\psi \underline{e}_z]\}(1 + O(\frac{\varphi^4}{\Delta^2})) \, a d\varphi .$$

Upon integration we obtain the cylindrical components of $\underline{u}_D$ as

$$u_D = - \frac{\beta}{r_1^2} \{2\cos\psi \sin\psi + \tilde{\epsilon} \sin\psi(1 - 2\cos^2\psi) + O(\epsilon^2)\} ,$$

$$v_D = 0 ,$$

$$w_D = \frac{2\beta}{r_1^2} \{1 - 2\sin^2\psi - \frac{\tilde{\epsilon}}{2} \cos\psi(1 - 2\sin^2\psi) + O(\epsilon^2 \ln \epsilon)\} .$$

The total velocity field produced near the body surface by the Stokeslet and doublet distribution is then given by

$$u = u_S + u_D = 2\cos\psi\sin\psi\,(a - \frac{2\beta}{r_1^2}) + a\sin\psi\,\tilde{\epsilon}\ln\frac{8}{\tilde{\epsilon}}$$

$$- \tilde{\epsilon}\sin\psi\,[a + \frac{\beta}{r_1^2} + \cos^2\psi(a - \frac{2\beta}{r_1^2})] + O(a\epsilon^2\ln\epsilon,\ \frac{\beta}{r_1^2}\epsilon^2)\ ,$$

$$v = v_S + v_D = 0, \qquad (2.1.15)$$

$$w = w_S + w_D = 2a\ln\frac{8}{\tilde{\epsilon}} + \frac{2\beta}{r_1^2} + 2\sin^2\psi(a - \frac{2\beta}{r_1^2}) - a\cos\psi\,\tilde{\epsilon}\ln\frac{8}{\tilde{\epsilon}}$$

$$+ \tilde{\epsilon}\cos\psi\,[a - \frac{\beta}{r_1^2} - \sin^2\psi(a - \frac{2\beta}{r_1^2})] + O(a\epsilon^2\ln\epsilon,\ \frac{\beta}{r_1^2}\epsilon^2\ln\epsilon).$$

The no-slip boundary condition on $r_1 = b$,

$u = v = 0, \quad w = U$,

can be satisfied by the velocity given in equation (2.1.15), neglecting terms of $O(a\epsilon\ln\epsilon)$, if we take

$$\beta = \frac{1}{2}ab^2\ , \qquad (2.1.16)$$

$$a = \frac{U}{2(\ln\frac{8}{\epsilon} + \frac{1}{2})}\ , \qquad (\epsilon = \frac{b}{a})\ . \qquad (2.1.17)$$

As expected, we see that equation (2.1.16) is essentially the same result obtained for a straight slender spheroid moving perpendicular to its generating axis. For that case (see Chwang & Wu, 1975) the doublet strength normal to the body axis is given by

$$\beta = \delta^2(c^2 - \xi^2)\frac{a}{2} \; ; \qquad \delta = \frac{b}{\ell} \ll 1$$

where ℓ is the body half length, ξ is the position along the body axis and c is the focal point. Since $c = \ell - O(\delta^2)$,

$$\beta = b^2\left[1 - \left(\frac{\xi}{\ell}\right)^2 + O(\delta^2)\right]\frac{a}{2} \; .$$

We see that in both cases the normal doublet strength is, to the lowest order, equal to one half the Stokeslet strength times the square of the local cross-sectional radius. We might now expect that even for bodies with a finite centerline curvature this result may have a general validity.

With the Stokeslet density a and doublet density β already determined, the remaining terms in the boundary value of the radial and axial velocity components reduce to a higher order and may be written using equation (2. 1. 16) and (2. 1. 17) as

$$u = a\sin\psi\,\epsilon\left[\left(\ln\frac{8}{\epsilon} - 1\right) - \frac{1}{2}\right] + O(a\epsilon^2\ln\epsilon) \; ,$$

$$w - U = a\cos\psi\,\epsilon\left[-\left(\ln\frac{8}{\epsilon} - 1\right) - \frac{1}{2}\right] + O(a\epsilon^2\ln\epsilon) \; . \qquad (2.1.18)$$

In order to satisfy the no-slip boundary condition to higher orders in ϵ we must therefore incorporate other appropriate fundamental singularities into our solution.

A physical interpretation of those velocity terms in equation (2. 1. 18) will clearly suggest our choice of the higher order singularities to be used. If we combine the remaining radial and axial velocity components given by (2. 1. 18), using the (r_1, θ, ψ) coordinate

system so that

$$\underline{e}_r = \cos\psi\, \underline{e}_{r_1} - \sin\psi\, \underline{e}_\psi$$

$$\underline{e}_z = \sin\psi\, \underline{e}_{r_1} + \cos\psi\, \underline{e}_\psi \quad ,$$

(see figure 2. 1. 2), the combined velocity defined as $\underline{q} = (u, o, w-U)$ is given by

$$\underline{q} = \underline{q}_1 + \underline{q}_2 \quad , \tag{2. 1. 19}$$

where $\underline{q}_1 = -\alpha\epsilon(\ln\frac{8}{\epsilon} - 1)\underline{e}_\psi$,

$$\underline{q}_2 = -\frac{1}{2}\alpha\epsilon(\sin 2\psi\, \underline{e}_{r_1} + \cos 2\psi\, \underline{e}_\psi) \quad .$$

The velocity vector $\underline{q}_1$ represents, in the neighborhood of the body, a "rotational like" flow about the torus surface (see figure 2. 1. 3). This description suggests that we will be able to eliminate this term by distributing along the centerline a constant rotlet in the $\underline{e}_\theta$ direction. The fact that $\underline{q}_1$ tends to increase the velocity in the $\underline{e}_z$ direction on the inside surface of the torus and decrease it on the outside is a manifestation of the local centerline curvature. The distance from the singularity distribution to the inside surface is shorter than the distance to the outside surface, thus creating the indicated departure from the required velocity.

Examining the velocity vector $\underline{q}_2$ we see that it describes an "extensional-like" flow near the body surface in the cross-sectional plane of the torus (see figure 2. 1. 3). It also tends to increase the induced velocity on the inside surface and decrease it on the outside surface. Motivated by the exact solution for a two-dimensional

circular cylinder in an extensional flow (Chwang & Wu, 1975) we envisage the need for a stresslet and quadrupole to eliminate these terms in order to satisfy the boundary condition.

We now proceed to calculate the velocity field induced by these additional singularity distributions just mentioned. The required rotlet distribution along the body centerline has a velocity field given by

$$\underline{u}_R = \int_{\theta'}^{\theta'+2\pi} \underline{U}_R(\underline{R};\underline{\delta})\, a\, d\theta \; ; \quad \underline{U}_R(\underline{R};\underline{\delta}) = \frac{\underline{\delta} \times \underline{R}}{R^3} \; , \tag{2.1.20}$$

with the rotlet strength assumed to be of the form

$$\underline{\delta} = \delta \underline{e}_\theta = \delta(-\sin\varphi\, \underline{e}'_r + \cos\varphi\, \underline{e}'_\theta) \; ,$$

where δ is a constant. Using (2.1.2) and retaining only even functions of φ gives

$$\underline{u}_R = 2a\delta \int_0^{\pi} \frac{z\cos\varphi\, \underline{e}'_r + (a - r\cos\varphi)\, \underline{e}_z}{R^3}\, d\varphi \; .$$

Proceeding as we did for the far-field doublet distribution, we note that for the rotlet the outer expansion is of order $\frac{\delta}{a^2}$, which upon integration will give a contribution to the velocity field of order $\frac{\delta}{a}$. We will neglect a priori the velocity induced by this outer expansion and show later that $\frac{\delta}{a}$ is indeed of $O(\epsilon^2 \ln\epsilon a)$, thereby verifying our supposition.

Considering then the near-field rotlet distribution we have

$$\underline{u}_R = 2a\delta \int_0^{\gamma} \frac{z\cos\varphi\, \underline{e}'_r + (a - r\cos\varphi)\underline{e}_z}{R^3}\, d\varphi \; .$$

Integrating the inner expansion of the integrand as explained before gives

$$\underline{u}_R = \frac{2\delta}{b} \{ \sin\psi \, \underline{e}'_r - \cos\psi \, \underline{e}_z + O(\epsilon \ln \epsilon) \} \ .$$

The velocity term $\underline{q}_1$ in equation (2. 1. 19) is canceled by including a rotlet distribution into our solution of strength

$$\delta = \epsilon (1 - \ln \frac{8}{\epsilon}) \frac{ab}{2} \ .$$

With this result we see as already mentioned that the far-field contribution from the rotlet distribution to the velocity field is of order $\epsilon^2 \ln \epsilon a$.

We next examine the distribution of stresslets and quadrupoles necessary to eliminate the velocity term $\underline{q}_2$ in (2. 1. 19). To the leading order, the effect of the higher order singularity distribution can be expected to be confined to a small neighborhood of the point in question. Therefore the quidelines for choosing the appropriate singularities come from inspecting the flow field of a constant straight line distribution and the previously mentioned exact solutions of Chwang & Wu (1975). From these considerations we are led to try constant stresslet and quadrupole distributions with velocity fields $\underline{u}_{SS}(\underline{e}_r, \underline{e}_z)$ and $\underline{u}_Q(\underline{e}_r, \underline{e}_z)$, where $\underline{e}_r$ and $\underline{e}_z$ are the characteristic directions associated with these singularities (see Chwang & Wu, 1975).

In general the stresslet velocity field is given by

$$\underline{u}_{SS}(\underline{\rho}_1, \underline{\rho}_2) = \int_0^{2\pi} \underline{U}_{SS}(\underline{R}; \underline{\rho}_1, \underline{\rho}_2) a \, d\varphi \ , \qquad (2. 1. 21)$$

where

$$\underline{U}_{SS}(R;\underline{\rho}_1,\underline{\rho}_2) = \{-\frac{\underline{\rho}_1 \cdot \underline{\rho}_2}{R^3} + \frac{3(\underline{\rho}_1 \cdot \underline{R})(\underline{\rho}_2 \cdot \underline{R})}{R^5}\}\,\underline{R}\ ,$$

which for our case becomes, using $\underline{e}_r = \cos\varphi\,\underline{e}'_r + \sin\varphi\,\underline{e}'_\theta$ and equation (2. 1. 2),

$$\underline{u}_{SS}(\underline{e}_r, \underline{e}_z) = 3Aa\int_0^{2\pi} \frac{z(r\cos\varphi - a)\underline{R}}{R^5}\,d\varphi\ .$$

As was done in the calculation of the doublet and rotlet distribution we again neglect the contribution of the far-field distribution here, since we can argue likewise that the velocity induced near the body by this far-field distribution will be of $O(\alpha\epsilon^2)$.

Thus we need consider only the near-field stresslet. After substituting (2. 1. 2) for $\underline{R}$ and neglecting odd functions of φ we obtain the velocity components in cylindrical coordinates as

$$u_{SS} = 6Aaz\int_0^{\gamma} \frac{(r\cos\varphi - a)(r - a\cos\varphi)}{R^5}\,d\varphi\ ,$$

$$v_{SS} = 0\ ,$$

$$w_{SS} = 6Aaz^2\int_0^{\gamma} \frac{r\cos\varphi - a}{R^5}\,d\varphi\ .$$

Constructing the inner expansion using equation (2. 1. 11) and integrating, we find

$$u_{SS} = \frac{2A}{r_1}\sin\psi\,(1 + \cos 2\psi + O(\epsilon))\ ,$$

$$v_{SS} = 0\ ,$$

$$w_{SS} = \frac{2A}{r_1}\cos\psi\,(1 - \cos 2\psi + O(\epsilon))\ .$$

This velocity field combined with the following quadrupole velocity will correct for the velocity term $\underline{q}_2$.

The quadrupole velocity can be readily deduced from a doublet as follows

$$\underline{u}_Q(\beta\underline{e}_r, \eta\underline{e}_z) = \eta \frac{\partial}{\partial z} \underline{u}_D(\beta\underline{e}_r). \qquad (2.1.22)$$

Therefore we first calculate the doublet velocity given by

$$\underline{u}_D(\beta\underline{e}_r) = \int_0^{2\pi} \{ \frac{\underline{\beta}}{R^3} - \frac{3(\underline{\beta} \cdot \underline{R})\underline{R}}{R^5} \} \, a d\varphi \ ,$$

where $\underline{\beta} = \beta\underline{e}_r = \beta \cos\varphi \, \underline{e}'_r + \beta \sin\varphi \, \underline{e}'_\theta$. As has been discussed before, we may neglect the far-field quadrupole since it falls off like $\frac{B}{R^4}$, where B is its strength, and is even a weaker singularity than the already neglected stresslet and doublet. Equivalently, then we neglect the far-field of the above doublet. It is readily seen that, after obtaining the quadrupole strength, the contribution to the velocity by the far-field distribution will be $O(a\epsilon^4)$.

The components of the doublet field are therefore given by

$$u_D = 2\int_0^{\gamma} \{\frac{\beta\cos\varphi}{R^3} - \frac{3\beta(r\cos\varphi - a)(r - a\cos\varphi)}{R^5} \} \, a d\varphi \ ,$$

$$v_D = 0 \ ,$$

$$w_D = -6\beta\int_0^{\gamma} \frac{z(r\cos\varphi - a)}{R^5} \, a d\varphi \ .$$

Constructing the inner expansion as usual and integrating we find

$$u_D = \frac{2\beta}{r_1^2}\{1 - 2\cos^2\psi + O(\epsilon)\} ,$$

$$v_D = 0 ,$$

$$w_D = -\frac{4\beta}{r_1^2}\{\sin\psi\cos\psi + O(\epsilon)\} .$$

The quadrupole, which is the quantity of interest here, is given by (2. 1. 22), where in the (r_1, θ, ψ) coordinate system we have

$$\frac{\partial}{\partial z} = \frac{\partial r_1}{\partial z}\frac{\partial}{\partial r_1} + \frac{\partial \psi}{\partial z}\frac{\partial}{\partial \psi} + \frac{\partial \theta}{\partial z}\frac{\partial}{\partial \theta} = \sin\psi\frac{\partial}{\partial r_1} + \frac{\cos\psi}{r_1}\frac{\partial}{\partial \psi} .$$

Differentiating the doublet velocity field then gives the result for the quadrupole,

$$u_Q = \frac{2B}{r_1^3}\sin\psi\,(2 + 4\cos 2\psi + O(\epsilon)) ,$$

$$v_Q = 0 ,$$

$$w_Q = \frac{2B}{r_1^3}\cos\psi\,(2 - 4\cos 2\psi + O(\epsilon)) ,$$

where $B = \eta\beta$. Combining the stresslet and quadrupole velocity field we have

$$u_{SS} + u_Q = \frac{2\sin\psi}{r_1}\{(A + \frac{2B}{r_1^2}) + (A + \frac{4B}{r_1^2})\cos 2\psi + O(A\epsilon, \frac{B}{r_1^2}\epsilon)\} ,$$

$$v_{SS} + v_Q = 0 , \qquad (2. 1. 23)$$

$$w_{SS} + w_Q = \frac{2\cos\psi}{r_1}\{(A + \frac{2B}{r_1^2}) - (A + \frac{4B}{r_1^2})\cos 2\psi + O(A\epsilon, \frac{B}{r_1^2}\epsilon)\} .$$

Including these singularity distributions, i. e., stresslet and quadrupole, into our solution will allow us to counter balance the velocity terms $\underline{q}_2$ in (2. 1. 19), and thus satisfy the boundary condition, if we require

$$A = \frac{1}{2}\epsilon ba \ ,$$

$$B = -\frac{1}{4} Ab^2 = -\frac{1}{8}\epsilon b^3 a \ .$$

Summarizing, we see that we have satisfied the boundary condition neglecting $O(\epsilon^2 \ln \epsilon)$ by using line distributions of Stokeslets, doublets, rotlets, stresslets, and quadrupoles on the body centerline with strengths given respectively by

$$a = \frac{U}{2(\ln \frac{8}{\epsilon} + \frac{1}{2})} \ ,$$

$$\beta = \frac{1}{2} ab^2 \ ,$$

$$\delta = \frac{1}{2}\epsilon ba \, (1 - \ln \frac{8}{\epsilon}) \ ,$$

$$A = \frac{1}{2}\epsilon ba \ ,$$

$$B = -\frac{1}{4} Ab^2 = -\frac{1}{8} \epsilon b^3 a \ .$$

The above procedure, by which the accuracy of the solution can be improved stepwise, is a further indication that the method of singularities for Stokes flows can be a powerful tool when coupled with simple physical considerations of the flow field. Furthermore, with the solution found here the error in the Stokeslet strength is of $O(\epsilon^2)$.

This is a considerably improved estimate over what has been possible, i. e., $O(\frac{1}{\ln\epsilon})^3$, using the method of matched asymptotic expansions demonstrated by Cox (1970).

As a note for the arbitrary body case we see that in the far-field, only the Stokeslet was required for the order of accuracy desired here. The leading-order effect of local centerline curvature, i. e., the terms of $O(a\epsilon \ln\epsilon)$ in the velocity field, only require inclusion of a rotlet with a strength of $O(a\epsilon \ln\epsilon)$. The stresslet, quadrupole and remainder of the rotlet render the boundary condition satisfied through $O(a\epsilon)$. We also observe that all the singularity strengths are determined in terms of the Stokeslet strength.

We now compute the viscous stresses and pressure on the body surface. The pressure is found by integrating the individual pressures associated with the various singularities involved, whereas the viscous stress in the vicinity of the body is calculated from derivatives of the complete velocity field in the neighborhood of the body.

Combining all the velocities induced by the singularity distribution we have for r_1 near b the solution

$$u = 2(a - \frac{2\beta}{r_1^2}) \sin\psi\cos\psi + [\,a\tilde{\epsilon}(\ln\frac{8}{\tilde{\epsilon}} - 1) + \frac{2\delta}{r_1}\,] \sin\psi$$

$$+ \sin\psi[\,-\tilde{\epsilon}\frac{\beta}{r_1^2} + \tilde{\epsilon}\cos^2\psi(\frac{2\beta}{r_1^2} - a) + \frac{2}{r_1}(A + \frac{2B}{r_1^2})$$

$$+ \frac{2\cos 2\psi}{r_1}(A + \frac{4B}{r_1^2})] + O(\epsilon^2) \ ,$$

$$v = 0 \ , \qquad (2.1.24)$$

$$w = 2a\ln\frac{8}{\tilde{\epsilon}} + \frac{2\beta}{r_1^2} + 2(a - \frac{2\beta}{r_1^2})\sin^2\psi - [\,a\tilde{\epsilon}(\ln\frac{8}{\tilde{\epsilon}} - 1) + \frac{2\delta}{r_1}\,]\cos\psi$$

$$+ \cos\psi[\,-\tilde{\epsilon}\frac{\beta}{r_1^2} + \tilde{\epsilon}\sin^2\psi(\frac{2\beta}{r_1^2} - a) + \frac{2}{r_1}(A + \frac{2B}{r_1^2})$$

$$- \frac{2\cos 2\psi}{r_1}(A + \frac{4B}{r_1^2})] + O(\epsilon^2\ln\epsilon) \ .$$

Now the stress is given by

$$\underset{\sim}{\tau} = -p\,\underset{\sim}{I} + \mu\,\underset{\sim}{e} \ , \qquad (2.1.25)$$

$$\underset{\sim}{e} = [\nabla\underline{u} + (\nabla\underline{u})^T]$$

(note $(\nabla\underline{u})^T$ is the transpose of $\nabla\underline{u}$).

Using the (r_1, θ, ψ) coordinate system we have

$$\nabla = \underset{\sim}{e}_i \frac{\partial}{\partial x_i} = \underline{e}_{r_1}\frac{\partial}{\partial r_1} + \underline{e}_\psi \frac{1}{r_1}\frac{\partial}{\partial\psi} + \underline{e}_\theta \frac{1}{a(1 + \tilde{\epsilon}\cos\psi)}\frac{\partial}{\partial\theta}$$

and therefore

$$e_{r_1 r_1} = 2\frac{\partial u_{r_1}}{\partial r_1} ,$$

$$e_{r_1 \psi} = \frac{1}{r_1}\frac{\partial u_{r_1}}{\partial \psi} + \frac{\partial u_\psi}{\partial r_1} - \frac{u_\psi}{r_1} , \qquad (2.1.26)$$

$$e_{r_1 \theta} = \frac{1}{a(1+\tilde{\epsilon}\cos\psi)}\left(\frac{\partial u_{r_1}}{\partial \theta} - u_\theta \cos\psi\right) + \frac{\partial u_\theta}{\partial r_1} ,$$

where in the (r_1, θ, ψ) coordinate system the velocity

$$\underline{u} = (u_{r_1}, u_\theta, u_\psi) .$$

Using

$$u_{r_1} = u\cos\psi + w\sin\psi$$

$$u_\psi = -u\sin\psi + w\cos\psi$$

$$u_\theta = v$$

and equation (2.1.24) the velocity in the (r_1, θ, ψ) coordinates become

$$u_{r_1} = \left[2a(\ln\frac{8}{\tilde{\epsilon}} + 1) - \frac{2\beta}{r_1^2}\right]\sin\psi + \left[\frac{2}{r_1}(A + \frac{2B}{r_1^2}) - \frac{\tilde{\epsilon}a}{2}\right]\sin 2\psi + O(\epsilon^2 \ln\epsilon) ,$$

$$u_\theta = 0 , \qquad (2.1.27)$$

$$u_\psi = (2a\ln\frac{8}{\tilde{\epsilon}} + \frac{2\beta}{r_1^2})\cos\psi - a\tilde{\epsilon}(\ln\frac{8}{\tilde{\epsilon}} - 1) - \frac{2\delta}{r_1} - (\tilde{\epsilon}\frac{\beta}{r_1^2} + \frac{4B}{r_1^3})\cos 2\psi + O(\epsilon^2 \ln\epsilon).$$

Substituting (2.1.27) into (2.1.26) we find

$$e_{r_1 r_1} = (-\frac{2a}{r_1} + \frac{4\beta}{r_1^3}) \sin\psi - [\frac{2A}{r_1^2} + \frac{12B}{r_1^4} + \frac{a}{2a}] \sin 2\psi + O(\frac{\epsilon \ln\epsilon}{a}) ,$$

$$e_{r_1 \psi} = -\frac{8\beta}{r_1^3} \cos\psi + \frac{a}{a} + \frac{4\delta}{r_1^2} + [\frac{4A}{r_1^2} - \frac{a}{a} + \frac{3\tilde{\epsilon}\beta}{r_1^3} + \frac{24B}{r_1^4}] \cos 2\psi + O(\frac{\epsilon \ln\epsilon}{a}) ,$$

$$e_{r_1 \theta} = 0 .$$

On the torus surface, i.e., $r_1 = b$, we have after substituting for the singularity strengths and neglecting $O(\frac{\epsilon \ln\epsilon}{a})$

$$e_{r_1 r_1} = e_{r_1 \theta} = 0 ,$$

$$e_{r_1 \psi} = C_1 + C_2 \cos\psi + C_3 \cos 2\psi$$

where

$$C_1 = \frac{\epsilon a}{b} (3 - 2 \ln \frac{8}{\epsilon}),$$

$$C_2 = \frac{4a}{b} ,$$

$$C_3 = -\frac{a\epsilon}{2b} .$$

The pressure fields accompanying the various flow singularities are given by (Chwang & Wu, 1975)

$$P_S = 2\mu \frac{\underline{a} \cdot \underline{R}}{R^3} ,$$

$$P_D = P_R = P_Q = 0 ,$$

$$P_{SS} = 2\mu \{ -\frac{\underline{\rho}_1 \cdot \underline{\rho}_2}{R^3} + \frac{3(\underline{\rho}_1 \cdot \underline{R})(\underline{\rho}_2 \cdot \underline{R})}{R^5} \} .$$

For our case the Stokeslet pressure field becomes

$$p_S = 4\mu \int_0^{\pi} \frac{az}{R^3}\, a\,d\varphi$$

$$= 4\mu \{ \int_0^{\gamma} \frac{az}{R^3}\, a\,d\varphi + \int_{\gamma}^{\pi} \frac{az}{R^3}\, a\,d\varphi \} .$$

Constructing the inner and outer expansions as usual using (2. 1. 10) and (2. 1. 11) gives

$$p_S = 4\mu \frac{a}{b} \tilde{\epsilon}^2 \sin\psi \{ \int_0^{\gamma} \frac{1}{\Delta^3} (1 + O(\frac{\varphi 4}{\Delta^2}))\, d\varphi$$

$$+ \int_{\gamma}^{\pi} \frac{1}{c^3 (1 - \cos\varphi)^{3/2}} [\, 1 + O(\frac{\epsilon^2}{1 - \cos\varphi}) \,]\, d\varphi \} .$$

Upon integrating and evaluating on $r_1 = b$ we have

$$p_S = 4\mu \frac{a}{b} \{ \sin\psi - \frac{\epsilon}{4} \sin 2\psi + O(\epsilon^2 \ln\epsilon) \} .$$

Similarly for the stresslet pressure field we find

$$p_{SS} = 4\mu \frac{A}{b^2} (\sin\psi + O(\epsilon)) .$$

The total pressure on the torus surface is then given by

$$p = p_S + p_{SS} = 4\mu \{ \frac{a}{b} \sin\psi + (\frac{A}{b^2} - \frac{a}{4a}) \sin 2\psi + O(\frac{\epsilon \ln\epsilon}{a}) \} .$$

And thus the stresses on $r_1 = b$ become

$$\tau_{r_1 r_1} = -p + \mu e_{r_1 r_1}$$

$$= -4\mu\{\frac{a}{b}\sin\psi + (\frac{A}{b^2} - \frac{a}{4a})\sin 2\psi + O(\frac{\epsilon \ln\epsilon}{a})\} \ ,$$

$$\tau_{r_1\theta} = \mu e_{r_1\theta} = 0 \ , \qquad (2.1.28)$$

$$\tau_{r_1\psi} = \mu e_{r_1\psi} = \mu\{C_1 + C_2\cos\psi + C_3\cos 2\psi + O(\frac{\epsilon\ln\epsilon}{a})\} \ .$$

The force per unit length $\underline{f}$ on the torus defined as the total force divided by $ad\theta$ can now be computed. An infinitesimal surface area element of the torus is given by

$$dS = bd\psi\, a(1 + \epsilon\cos\psi)d\theta.$$

Thus in cylindrical coordinates we have for the force per unit length

$$f_r = \int_0^{2\pi} (\tau_{r_1 r_1}\cos\psi - \tau_{r_1\psi}\sin\psi)b(1 + \epsilon\cos\psi)d\psi \ ,$$

$$f_\theta = \int_0^{2\pi} \tau_{r_1\theta}\, b(1 + \epsilon\cos\psi)d\psi \ , \qquad (2.1.29)$$

$$f_z = \int_0^{2\pi} (\tau_{r_1 r_1}\sin\psi + \tau_{r_1\psi}\cos\psi)b(1 + \epsilon\cos\psi)d\psi \ .$$

Substituting (2.1.28) into (2.1.29) and integrating gives, neglecting terms of $O(\epsilon^2 \ln\epsilon)$

$$f_r = f_\theta = 0 \ ,$$

$$f_z = -8\pi\mu a \ .$$

This yields the result we might expect; however, the force/length being equal to $8\pi\mu a$ does not follow immediately from the singularity method. What does follow directly is that the total force on the fluid should equal the total Stokeslet strength times $8\pi\mu$. This does not exclude the possibility, in this case, of having a constant force/length acting in the radial direction, which would not contribute to the total force on the fluid. We will, for the arbitrary body case, carry out the calculation in general and, in fact, find to the order of approximation here, that the force/length is directly proportional to the Stokeslet strength. The actual computation here gives us added confidence in our result for the velocity field.

As is frequently done in resistive force theory we define a drag coefficient, C_n, as

$$\text{Drag} = \mu C_n U = 8\pi\mu a \ ,$$

where

$$C_n = \frac{4\pi}{\ln \frac{8}{\epsilon} + \frac{1}{2}} \ .$$

This then allows us to compare our result to those for straight slender bodies, thereby determining the effect of finite centerline curvature. We see from figure (2. 1. 4) that the drag coefficients for our torus deviate only slightly (less than 15% for $\epsilon < 0.2$) from the results for the two straight bodies given. In both cases, however, the drag on the torus is seen to be less than that on the straight bodies. This result owes itself to the fact that the actual distance separating two points on the body centerline of equal arc length away is less for

the torus than for the straight centerline bodies. The fluid dragged along by one point is felt more strongly at another point in the case of a torus where the separation distance is decreased. The apparent fluid velocity impinging at a point is thereby reduced, resulting in decreased drag. Although for this case the deviation is small, we might now suspect that for cases where points on the centerline move in opposite directions, such as in the case of a rotating torus, there may be considerable deviation.

With the stresses on the body available we can proceed further and obtain the torque/length exerted on the torus about the body centerline. Defining this torque/length ($\underline{M}$) as the total torque divided by $ad\theta$ we have

$$M_r = -\int_0^{2\pi} \sin\psi \, \tau_{r_1\theta} b^2(1 + \epsilon \cos\psi)d\psi \ ,$$

$$M_\theta = -\int_0^{2\pi} \tau_{r_1\psi} b^2(1 + \epsilon \cos\psi)d\psi \ , \qquad (2.1.30)$$

$$M_z = \int_0^{2\pi} \cos\psi \, \tau_{r_1\theta} b^2(1 + \epsilon \cos\psi)d\psi \ .$$

Substituting (2.1.28) in (2.1.30) gives

$$M_r = M_z = 0, \qquad \text{since } \tau_{r_1\theta} = 0 \ ;$$

$$M_\theta = -2\pi\mu b(\epsilon a + \frac{4\delta}{b} + \frac{\epsilon 4\beta}{b^2})$$

$$= -2\pi\mu b\epsilon(2\ln\frac{8}{\epsilon} - 1)a \ .$$

From the above result we see that not only does the rotlet distribution yield a torque/length, as should have been expected, but the Stokeslet and doublet distributions also produce a torque/length. More precisely, the leading contribution to the total torque/length is from the rotlet, and is of $O(\alpha\epsilon \ln\epsilon)$, while those contributions from the Stokeslet and doublet are of $O(\alpha\epsilon)$. This torque/length is a direct result of the motion of a body possessing finite centerline curvature, and we should anticipate this feature of the flow field to be present in the general case.

2.2 A torus in translation perpendicular to its longitudinal axis

Having pursued the first case in a rather detailed fashion, we will now examine the remaining cases more briefly since the major concepts and methods are identical and should now be clear. For the present case our torus is assumed to move in the $\underline{e}_y$ direction in its own plane. The boundary condition is

$$\underline{u} = U\underline{e}_y ,$$

$$= U(\sin\theta\,\underline{e}_r + \cos\theta\,\underline{e}_\theta) \quad \text{on} \quad r_1 = b .$$

We again represent, as a first approximation, the velocity field by a distribution of Stokeslets and doublets with strengths assumed a priori to be

$$\underline{a} = a_n \underline{e}_r + a_s \underline{e}_\theta \ ,$$

where

$$a_n = K_n \sin\theta \ ,$$

$$a_s = K_s \cos\theta \ , \qquad (K_n,\ K_s \text{ constant}) \ ,$$

and

$$\underline{\beta} = \beta_n \underline{e}_r \ , \qquad (2.2.1)$$

where

$$\beta_n = B_n \sin\theta \ , \qquad (B_n \text{ constant}) \ ,$$

This choice, which will be verified to satisfy the boundary condition, is motivated by the fact that we might expect the Stokeslet strength in the normal and tangential directions to be proportional to the local normal and tangential centerline velocities, i.e.,

$$a_n \propto U_n = U \sin\theta \ , \qquad a_s \propto U_s = U \cos\theta$$

The velocity field at $\theta = \theta'$ induced by the Stokeslet distribution is given, after using (2.1.2), (2.2.1) and eliminating odd functions of φ, in cylindrical coordinates by

$$u_s = 2a \sin\theta' \int_0^\pi \{(K_n \cos^2\varphi + K_s \sin^2\varphi)\frac{1}{R} + [K_n \cos\varphi(r\cos\varphi - a) + K_s r \sin^2\varphi] (r - a\cos\varphi)\frac{1}{R^3}\} \, d\varphi \ ,$$

$$v_s = 2a \cos\theta' \int_0^\pi \{(K_n \sin^2\varphi + K_s \cos^2\varphi)\frac{1}{R} - a\sin^2\varphi \ [K_n(r\cos\varphi - a) - K_s r\cos\varphi]\frac{1}{R^3}\} d\varphi \ ,$$

$$w_s = 2a \sin\theta' \int_0^\pi z[K_n \cos\varphi(r\cos\varphi - a) + K_s r \sin^2\varphi] \frac{d\varphi}{R^3} \ .$$

where we have used

$$\alpha_n = K_n \sin\theta = K_n(\sin\theta' \cos\varphi + \cos\theta' \sin\varphi) \ ,$$

$$\alpha_s = K_s \cos\theta = K_s(\cos\theta' \cos\varphi - \sin\theta' \sin\varphi) \ .$$

Separating the integrals into the inner and outer regions, expanding the integrands appropriately and carrying out the integrations gives

$$u_s = \sin\theta' \{2K_n(\ln\frac{8}{\tilde{\epsilon}} - 1) + 4K_s + 2\cos^2\psi\, K_n + 2\tilde{\epsilon}\cos\psi(\ln\frac{8}{\tilde{\epsilon}})(K_s - \frac{K_n}{2})$$
$$+ 2\tilde{\epsilon}\cos\psi[(1 - \frac{\cos^2\psi}{2})K_n - 3K_s] + O(K\epsilon^2\ln\epsilon)\} \ ,$$

$$v_s = \cos\theta' \{4K_s(\ln\frac{8}{\tilde{\epsilon}} - 2) + 4K_n - 2\tilde{\epsilon}\cos\psi(\ln\frac{8}{\tilde{\epsilon}})(K_n + K_s)$$
$$+ 2\tilde{\epsilon}\cos\psi(K_n + 3K_s) + O(K\epsilon^2\ln\epsilon)\} \ ,$$

$$w_s = 2\sin\theta' \sin\psi\{K_n\cos\psi + \tilde{\epsilon}(\ln\frac{8}{\tilde{\epsilon}})(K_s - \frac{K_n}{2})$$
$$+ \tilde{\epsilon}[\frac{K_n}{2}(3 - \cos^2\psi) - 2K_s] + O(K\epsilon^2\ln\epsilon)\} \ ,$$

where

$$K = O(K_n, K_s) \ .$$

For precisely the same reasons as used in the last case we neglect the far field or outer expansion of the doublet distribution. The velocity field from the doublet distribution after using

$$\beta_n = B_n \sin\theta = B_n(\sin\theta' \cos\varphi + \cos\theta' \sin\varphi) \ ,$$

equation (2. 1. 2), and omitting odd functions of φ is

$$u_D = 2a \sin\theta' \int_0^\gamma \{ \frac{B_n \cos^2\varphi}{R^3} - 3B_n \cos\varphi[(r^2 + a^2)\cos\varphi - ra(1+\cos^2\varphi)] \frac{1}{R^5} \} d\varphi ,$$

$$v_D = 2a \cos\theta' \int_0^\gamma \{ \frac{B_n \sin^2\varphi}{R^3} + \frac{3B_n a \sin^2\varphi(r\cos\varphi - a)}{R^5} \} d\varphi ,$$

$$w_D = 2az \sin\theta' \int_0^\gamma \frac{3B_n(a - r\cos\varphi)}{R^5} d\varphi .$$

Generating the inner expansion for φ near zero and then integrating gives

$$u_D = 2 \sin\theta' \frac{B_n}{r_1^2} \{1 - 2\cos^2\psi + \tilde{\epsilon} \cos\psi(\cos^2\psi - \frac{1}{2}) + O(\epsilon^2 \ln\epsilon)\} ,$$

$$v_D = 2 \cos\theta' \frac{B_n}{r_1^2} \{\tilde{\epsilon} \cos\psi + O(\epsilon^2 \ln\epsilon)\} ,$$

$$w_D = 2 \sin\psi \sin\theta' \frac{B_n}{r_1^2} \{-2\cos\psi + \tilde{\epsilon}(\frac{1}{2} + \cos^2\psi) + O(\epsilon^2)\} .$$

The boundary condition at $\theta = \theta'$ on $r_1 = b$ is

$$\underline{u} = U \underline{e}_y = U (\sin\theta' \underline{e}'_r + \cos\theta' \underline{e}'_\theta) .$$

Combining the expansions of the velocity field due to the Stokeslet and doublet and equating to the boundary condition gives, after some simple algebra and neglecting terms of $O(K\epsilon^2 \ln\epsilon, \frac{B_n}{b^2}\epsilon^2 \ln\epsilon)$,

$$U \sin\theta' = \sin\theta' \{2K_n(\ln\frac{8}{\epsilon} - 1) + 4K_s + \frac{2B_n}{b^2} + 2\cos^2\psi(K_n - \frac{2B_n}{b^2})$$

$$+ 2\cos\psi\epsilon[(\ln\frac{8}{\epsilon})(K_s - \frac{K_n}{2}) + K_n - 3K_s - \frac{B_n}{2b^2} + \frac{\cos^2\psi}{2}(\frac{2B_n}{b^2} - K_n)]\},$$

$$U\cos\theta' = \cos\theta'\{4K_s(\ln\frac{8}{\epsilon} - 2) + 4K_n + 2\cos\psi\epsilon[(-\ln\frac{8}{\epsilon})(K_n + K_s)$$

$$+ K_n + 3K_s + \frac{B_n}{b^2}]\} \ ,$$

$$0 = 2\sin\theta'\sin\psi\{(K_n - \frac{2B_n}{b^2})\cos\psi + \epsilon[(\ln\frac{8}{\epsilon})(K_s - \frac{K_n}{2}) + \frac{3}{2}K_n - 2K_s$$

$$+ \frac{B_n}{2b^2} + \frac{\cos^2\psi}{2}(\frac{2B_n}{b^2} - K_n)]\}.$$

The three boundary conditions can be satisfied, neglecting terms of $O(K\epsilon\ln\epsilon)$, by taking

$$B_n = \frac{K_n b^2}{2} \qquad (2.2.2)$$

and solving the following equations for K_n and K_s

$$U = 2K_n(\ln\frac{8}{\epsilon} - \frac{1}{2}) + 4K_s \ ,$$

$$U = 4K_n + 4K_s(\ln\frac{8}{\epsilon} - 2)$$

giving

$$K_n = \frac{(\ln\frac{8}{\epsilon} - 3)U}{2[(\ln\frac{8}{\epsilon} - \frac{1}{2})(\ln\frac{8}{\epsilon} - 2) - 2]} \ ,$$

$$K_s = \frac{(\ln\frac{8}{\epsilon} - \frac{5}{2})U}{4[(\ln\frac{8}{\epsilon} - \frac{1}{2})(\ln\frac{8}{\epsilon} - 2) - 2]} \ . \qquad (2.2.3)$$

We see here that the radial doublet strength is related to the radial Stokeslet strength (equation 2. 2. 2) in precisely the same way as we had in the previous case for the axial doublet and Stokeslet strengths. This reinforces the proposition that this relationship between doublet and Stokeslets strengths normal to the body centerline may be true in general.

As before we will satisfy the boundary condition to higher orders by including other singularity distributions into the solution. But first a physical interpretation of those higher order terms to guide our selection will be provided. We define those higher order velocity terms that do not satisfy the boundary condition as $\tilde{u}, \tilde{v}, \tilde{w}$ and, realize as before, that the new singularity distributions to be used must cancel them. Thus we obtain, using (2. 2. 2),

$$\tilde{u} = 2 \sin\theta' \cos\psi \epsilon \left[(\ln\frac{8}{\epsilon})(K_s - \frac{K_n}{2}) + \frac{3}{4} K_n - 3K_s \right] ,$$

$$\tilde{v} = 2 \cos\theta' \cos\psi \epsilon \left[-(\ln\frac{8}{\epsilon})(K_n + K_s) + \frac{3}{2} K_n + 3K_s \right] ,$$

$$\tilde{w} = 2 \sin\theta' \sin\psi \epsilon \left[(\ln\frac{8}{\epsilon})(K_s - \frac{K_n}{2}) + \frac{7}{4} K_n - 2K_s \right] .$$

The radial and normal components, i. e., $\tilde{u}, \tilde{w}$, which will combine for easy interpretation in the cross section plane, may be written as

$$\tilde{u} = 2 \sin\theta' \cos\psi \epsilon (D_1 - D_2) ,$$

$$\tilde{w} = 2 \sin\theta' \sin\psi \epsilon (D_1 + D_2) ,$$

where

$$D_1 = (\ln \frac{8}{\epsilon} - \frac{5}{2})(K_s - \frac{K_n}{2}) = \frac{K_s}{2} ,$$

$$D_2 = \frac{1}{2}(K_s + K_n) .$$

The resultant vector of the two velocities $\tilde{u}$ and $\tilde{w}$, which we will define as $\underline{q}$, assumes in the (r_1, θ, ψ) coordinate system the form

$$\underline{q} = \tilde{u}\,\underline{e}'_r + \tilde{w}\,\underline{e}_z = \sin\theta'(\underline{q}_1 + \underline{q}_2) , \qquad (2.2.4)$$

where

$$\underline{q}_1 = 2\epsilon D_1 \underline{e}_{r_1} ,$$

$$\underline{q}_2 = -2\epsilon D_2(\cos 2\psi\, \underline{e}_{r_1} - \sin 2\psi\, \underline{e}_\psi) .$$

The velocity term $\underline{q}_1 \sin\theta'$ represents a pure "radial-like" flow in the meridian plane (see figure 2.2.1) which exhibits a constant flow for all angles ψ in the $\underline{e}_{r_1}$ direction for any θ and as such obviously suggests the use of a source distribution or equivalently a tangential doublet. Similar to what we had in the last case, $\underline{q}_2 \sin\theta'$ represents an "extensional-like" flow, although here its principal axes are rotated and it is modulated by $\sin\theta'$ (see figure 2.2.1). As before, a stresslet and quadrupole will account for these terms. The sum of the two velocities, i.e., $\underline{q}$, produces the local curvature effect mentioned in section 2.1 by effectively increasing the velocity in the direction of torus motion on the inside torus surface and decreasing it on the outside surface. This is again due to the over-all singularity distribution being essentially closer to the inside surface than the outside surface, and thus inducing larger velocities near the former.

The remaining tangential velocity $\tilde{v}$ has, for $\theta < \theta' < \frac{1}{2}\pi$ as a typical region to examine, a positive contribution in the $\underline{e}_\theta$ direction on the inside torus surface and a negative contribution on the outside surface which we shall call (see figure 2. 2. 2) a "shear-like" flow on the $\underline{e}_\theta$ direction, with the shear gradient in the $\underline{e}_r$ direction. This shear flow also tends to increase the velocity induced by the singularity distribution on the inside surface. We can produce a velocity opposite to $\tilde{v}$ by a line distribution of rotlets in the $\underline{e}_z$ direction.

We first consider the rotlet distribution that will correct the tangential velocity boundary condition through the terms of $O(\alpha\epsilon)$. Examining the behavior of $\tilde{v}$ for various θ' leads us to assume a rotlet strength given by

$$\underline{\delta} = \delta \cos\theta \, \underline{e}_z$$

$$= \delta(\cos\theta' \cos\varphi - \sin\theta' \sin\varphi)\underline{e}_z \ .$$

The rotlet velocity field is given in general by (2. 1. 20) which for this case becomes

$$u_R = \int_0^{2\pi} \frac{\delta_z a^2 \sin\varphi \, d\varphi}{R^3} \ ,$$

$$v_R = \int_0^{2\pi} \frac{\delta_z a^2 (r - a\cos\varphi)}{R^3} \, d\varphi \ ,$$

$$w_R = 0 \ , \qquad \text{since } (\underline{\delta} \times \underline{R}) \cdot \underline{e}_z = 0 \ ,$$

where $\delta_z = \delta \cos\theta$.

As explained before, only the near field distributions need be considered, i. e., the inner expansions and we find

$$u_R = -2 \sin\theta' \frac{\delta}{r_1} \tilde{\epsilon}\{\ln \frac{8}{\tilde{\epsilon}} - 2 + O(\epsilon \ln \epsilon)\} , \qquad (2.2.5)$$

$$v_R = 2 \cos\theta' \frac{\delta}{r_1} \{\cos\psi + \frac{\tilde{\epsilon}}{2} \ln \frac{8}{\tilde{\epsilon}} - \frac{\tilde{\epsilon}}{2}(3 + \cos^2\psi) + O(\epsilon^2 \ln \epsilon)\} ,$$

$$w_R = 0 .$$

And therefore the tangential velocity term $\tilde{v}$ in the boundary condition is corrected for by taking the rotlet strength to be

$$\delta = \epsilon b\{(\ln \frac{8}{\epsilon})(K_n + K_s) - 3(K_s + \frac{K_n}{2})\} .$$

With this result we then see that the rotlet far field distribution will give a contribution to the velocity field of $O(\epsilon^2)$. Furthermore, the radial velocity component u_R in (2.2.5) is of $O(K\epsilon^2 \ln^2 \epsilon)$ and is therefore of higher order and will be neglected.

Studying the velocity term $\underline{q}_1$ we observe that this term is a source for $\theta < \theta' < \pi$ and a sink for $\pi < \theta' < 2\pi$ since it is modulated by $\sin\theta'$. The required source distribution strength is appropriately taken to be

$$\hat{m} = m \sin\theta = m(\sin\theta' \cos\varphi + \cos\theta' \cos\varphi) .$$

The velocity field is

$$\underline{u}_m = \int_0^{2\pi} U_m(\underline{R};\hat{m}) a d\varphi ; \quad U_m(\underline{R};\hat{m}) = \frac{\hat{m}\underline{R}}{R^3} . \qquad (2.2.6)$$

For the outer expansion we see that the integrand is of $O(\frac{m}{a})$. Knowing a priori that the source strength will be $O(\epsilon bK)$, we thus note that the contribution to the velocity field from the far field source distribution is of $O(\epsilon^2 K)$ and can be neglected. Thus we have the velocity field given by

$$u_m = 2m \sin\theta' a \int_o^\gamma \frac{(r - a\cos\varphi)\cos\varphi}{R^3}\, d\varphi \quad ,$$

$$v_m = -2m \cos\theta' a^2 \int_o^\gamma \frac{\sin^2\varphi}{R^3}\, d\varphi \quad ,$$

$$w_m = 2m \sin\theta' az \int_o^\gamma \frac{\cos\varphi}{R^3}\, d\varphi \quad .$$

Integrating the inner expansions of these integrands gives

$$u_m = \frac{2m}{r_1} \sin\theta'(\cos\psi + O(\epsilon \ln\epsilon)) \quad ,$$

$$v_m = O(\frac{m}{r_1} \epsilon \ln\epsilon) \quad ,$$

$$w_m = \frac{2m}{r_1} \sin\theta' \sin\psi(1 + O(\epsilon)) \quad .$$

With this velocity field added to the solution, taking

$$m = -\frac{1}{2} \epsilon bK_s \quad ,$$

we are able to eliminate the $\underline{q}_1$ term in the boundary condition.

The equivalence of a source and tangential doublet distribution alluded to earlier is easily seen by considering the familiar potential

function Φ where $\underline{u} = \nabla\Phi$. For a line of tangential doublets on $r = a$ we have

$$\Phi = \int_0^{2\pi} -\beta_s \frac{\partial}{\partial\theta}\left(\frac{1}{R}\right) d\theta$$

$$= \int_0^{2\pi} \left\{-\frac{\partial}{\partial\theta}\left(\frac{\beta_s}{R}\right) + \frac{1}{R}\ \frac{\partial}{\partial\theta}\ \beta_s\right\} d\theta \ .$$

The first term is identically zero, and the second term is a source with strength

$$\hat{m} = \frac{1}{a}\ \frac{\partial\beta_s}{\partial\theta} \ .$$

Therefore in our case where $\hat{m} = m \sin\theta$ the equivalent tangential doublet strength is $\beta_s = -ma\cos\theta$. Using m we have

$$\beta_s = \frac{K_s b^2}{2}\ \cos\theta = \frac{b^2}{2}\ \alpha_s \ .$$

Once again that frequently observed relationship between doublet strength and Stokeslet appears, even here where it relates the tangential doublet and Stokeslets.

We now proceed to satisfy the no-slip boundary conditions through terms of $O(\epsilon^2 \ln\epsilon)$ by correcting for the velocity term $\underline{q}_2$. We consider the stresslet and quadrupole velocity fields $\underline{u}_{SS}(\underline{e}_r, \underline{e}_r)$ and $\underline{u}_Q(\underline{e}_r, \underline{e}_r)$ the stresslet velocity field from (2. 1. 21) is given by

$$\underline{u}_{SS}(\underline{e}_r, \underline{e}_r) = \int_0^{2\pi} \hat{A}(\theta)\left\{-\frac{1}{R^3} + 3\left[\cos\varphi(r - a\cos\varphi) - a\sin^2\varphi\right]^2 \frac{1}{R^5}\right\} \underline{R}\, a d\varphi \ .$$

The stresslet strength is assumed to be

$$\hat{A}(\theta) = A \sin\theta = A(\sin\theta' \cos\varphi + \cos\theta' \sin\varphi), \qquad A \text{ being a constant.}$$

The far-field contribution will again be small and, considering only the near-field, we find after integrating the inner expansion,

$$u_{SS} = \frac{2A}{r_1} \sin\theta' (\cos\psi \cos 2\psi + O(\epsilon \ln\epsilon)) ,$$

$$v_{SS} = 0(\frac{A}{r_1} \epsilon \ln\epsilon) ,$$

$$w_{SS} = \frac{2A}{r_1} \sin\theta' (\sin\psi \cos 2\psi + O(\epsilon)) .$$

The quadrupole velocity is in general given by

$$\underline{u}_Q(\underline{\mu}_1, \underline{\mu}_2) = \int_0^{2\pi} \underline{U}_Q(\underline{R};\underline{\mu}_1,\underline{\mu}_2) a d\varphi ,$$

where

$$\underline{U}_Q(\underline{R};\underline{\mu}_1,\underline{\mu}_2) = \frac{3(\underline{\mu}_1 \cdot \underline{R})\underline{\mu}_2 + 3(\underline{\mu}_2 \cdot \underline{R})\underline{\mu}_1 + 3(\underline{\mu}_1 \cdot \underline{\mu}_2)\underline{R}}{R^5}$$

$$- \frac{15(\underline{\mu}_1 \cdot \underline{R})(\underline{\mu}_2 \cdot \underline{R})\underline{R}}{R^7} . \qquad (2.2.7)$$

For our case where $\underline{\mu}_1 = \underline{\mu}_2 = \mu \underline{e}_r$, with $\hat{B} = \mu^2$, we have

$$\underline{u}_Q(\underline{e}_r, \underline{e}_r) = \int_0^{2\pi} 3\hat{B} \{[2(r\cos\varphi - a)(\cos\varphi \underline{e}'_r + \sin\varphi \underline{e}'_\theta) + \underline{R}] \frac{1}{R^5}$$

$$- 5(r\cos\varphi - a)^2 \frac{\underline{R}}{R^7}\} a d\varphi .$$

Assuming $\hat{B} = B \sin\theta$, neglecting the quadrupole far field since it is of higher order, and then integrating the inner expansion we find

$$u_Q = \frac{2B}{r_1^3} \sin\theta' \{ \cos\psi(2 - 4\cos 2\psi) + O(\epsilon) \} ,$$

$$v_Q = O(\frac{B}{r_1^3} \epsilon) ,$$

$$w_Q = -\frac{2B}{r_1^3} \sin\theta' \sin\psi \{2 + 4\cos 2\psi + O(\epsilon)\} .$$

The combined stresslet plus quadrupole velocity gives

$$u_{SS} + u_Q = 2 \sin\theta' \cos\psi \{\frac{2B}{r_1^3} + \frac{\cos 2\psi}{r_1} (A - \frac{4B}{r_1^2}) + O(\frac{A}{r_1} \epsilon \ln\epsilon, \frac{B}{r_1^3} \epsilon)\} ,$$

$$v_{SS} + v_Q = O(\frac{A}{r_1} \epsilon \ln\epsilon , \frac{B}{r_1^3} \epsilon) ,$$

$$w_{SS} + w_Q = 2 \sin\theta' \sin\psi \{-\frac{2B}{r_1^3} + \frac{\cos 2\psi}{r_1} (A - \frac{4B}{r_1^2}) + O(\frac{A}{r_1} \epsilon, \frac{B}{r_1^3} \epsilon)\} .$$

Recalling the term $\underset{\sim}{q}_2$ (see equation 2. 2. 4) we see that it is eliminated from the boundary condition after taking

$$A = \epsilon(K_s + K_n)b ,$$

$$B = \frac{Ab^2}{4} = \epsilon(K_s + K_n) \frac{b^3}{4} .$$

Here we observe the possibility of another general relationship, this time between stresslet and quadrupole strengths. Both in the present case and in the last case we found that the quadrupole strength, B, is proportional to one-half the cross-sectional radius squared times the

stresslet strength, A. The expression for the stresslet strength is also very much alike in the two cases, being proportional to ϵb times the sum of the stokeslet strengths, which in the previous case was simply a.

We briefly summarize the result by saying that through the use of a Stokeslet, doublet, rotlet, source, stresslet, and quadrupole distributions we have satisfied the no-slip boundary condition neglecting terms of $O(\epsilon^2 \ln\epsilon)$. The complete velocity field in the neighborhood of the torus, i.e., r_1 near b, may be written in the (r_1, θ, ψ) coordinates, with the terms of $O(\epsilon^2 \ln\epsilon)$ neglected, as

$$u_{r_1} = 2\sin\theta\{(K_n L + 2K_s - \frac{B_n}{r_1^2})\cos\psi - \frac{\tilde{\epsilon}}{2} K_n(L - 2) + \tilde{\epsilon} K_s(L - \frac{5}{2})$$

$$+ \frac{m}{r_1} + \frac{\tilde{\epsilon} B_n}{2r_1^2} + \cos 2\psi[-\frac{\tilde{\epsilon}}{2}(K_n + K_s) + \frac{A}{r_1} - \frac{2B}{r_1^3}]\} ,$$

$$u_\theta = 2\cos\theta\{2K_s(L - 2) + 2K_n + \cos\psi[-\tilde{\epsilon} K_n(L - 1) - \tilde{\epsilon} K_s(L - 3)$$

$$+ \frac{\tilde{\epsilon} B_n}{r_1^2} + \frac{\delta}{r_1}]\} , \qquad (2.2.8)$$

$$u_\psi = 2\sin\theta\{-[K_n(L - 1) + 2K_s + \frac{B_n}{r_1^2}]\sin\psi$$

$$+ \cos\psi\sin\psi[\tilde{\epsilon}\frac{K_n}{2} + \tilde{\epsilon} K_s + \frac{\tilde{\epsilon} B_n}{r_1^2} - \frac{4B}{r_1^3}]\} ,$$

where

$$L = \ln\frac{8}{\tilde{\epsilon}} .$$

It is easily verified that these velocity fields satisfy the no-slip boundary condition in the (r_1, θ, ψ) coordinates, namely

$$u_{r_1} = U \sin\theta \cos\psi$$

$$u_\theta = U \cos\theta \qquad \text{on } r_1 = b$$

$$u_\psi = U \sin\theta \sin\psi \ .$$

Using (2. 1. 26) and (2. 2. 8) and neglecting the terms of $O(\frac{\epsilon \ln\epsilon}{a})$ we find the rate of strain tensor on $r_1 = b$ as

$$e_{r_1 r_1} = \frac{4\sin\theta}{b} \{-K_n \epsilon (L - \frac{5}{2}) + 2K_s \epsilon (L - 3)\} \ ,$$

$$e_{r_1 \psi} = \frac{2 \sin\theta}{b} \{2K_n \sin\psi + \epsilon (2K_s + \frac{3}{2} K_n) \sin 2\psi\} \ ,$$

$$e_{r_1 \theta} = \frac{2 \cos\theta}{b} \{- 2K_s - \cos\psi [K_s \epsilon (4L - 13) + K_n \epsilon (L - \frac{1}{2})]\} \ .$$

The pressure is given by $p = p_s + p_{ss}$ which for our case gives

$$p_S = 4\mu a \sin\theta \int_0^\pi [K_n \cos\varphi (r\cos\varphi - a) + K_s r \sin^2\varphi] \frac{1}{R^3} \, d\varphi \ ,$$

$$p_{SS} = 2\mu a \sin\theta A \int_0^\pi [- \frac{\cos\varphi}{R^3} + \frac{3(r\cos\varphi - a)^2 \cos\varphi}{R^5}] d\varphi \ .$$

Integrating the inner and outer expansions of the integrands gives

$$p = \frac{4\mu\sin\theta}{b}\{K_s\epsilon(L - 2) - \frac{K_n}{2}\epsilon(L - \frac{5}{2}) + K_n\cos\psi$$

$$+ \cos 2\psi\,\epsilon(K_s + \frac{3}{4}K_n) + O(\epsilon^2)\} \quad .$$

The stresses on the torus neglecting terms of $O(\frac{\epsilon\ln\epsilon}{a})$ are

$$\tau_{r_1 r_1} = -\frac{4\mu\sin\theta}{b}\{\frac{K_n}{2}\epsilon(L - \frac{5}{2}) - K_s\epsilon(L - 4) + K_n\cos\psi$$

$$+ \epsilon(K_s + \frac{3}{4}K_n)\cos 2\psi\} \quad ,$$

$$\tau_{r_1\psi} = \frac{4\mu\sin\theta}{b}\{K_n\sin\psi + \epsilon(K_s + \frac{3}{4}K_n)\sin 2\psi\} \quad ,$$

$$\tau_{r_1\theta} = -\frac{4\mu\cos\theta}{b}\{K_s + \frac{\epsilon}{2}[K_s(4L - 13) + K_n(L - \frac{1}{2})]\cos\psi\} \quad .$$

Using (2. 1. 29) we find the somewhat expected results for the force per unit length

$$f_r = -8\pi\mu a_n + O(\epsilon^2\ln\epsilon) \quad ,$$

$$f_\theta = -8\pi\mu a_s + O(\epsilon^2\ln\epsilon) \quad ,$$

$$f_z = O(\epsilon^2\ln\epsilon) \quad .$$

Similarly the torque/length about the body centerline is obtained from (2. 1. 30) as

$$M_r = M_\theta = 0 \quad ,$$

$$M_z = 2\pi\mu b\cos\theta\epsilon[K_s(4L - 11) + K_n(L - \frac{1}{2})] \quad .$$

As in the previous case, the torque/length on the torus is not simply $8\pi\mu$ times the rotlet strength/length as for straight bodies, but also includes the contribution from the Stokeslet and other singularities due to the effect of centerline curvature.

We again define drag coefficients C_n, and C_s in order to compare the present results with classical theory. We take

$$\underline{f} = 8\pi\mu\underline{a} = \mu C_n U_n \underline{e}_r + \mu C_s U_s \underline{e}_\theta ,$$

where

$$U_n = U \sin\theta ,$$

$$U_s = U \cos\theta ,$$

and so

$$C_n = 8\pi K_n = \frac{4\pi(L - 3)}{(L - \frac{1}{2})(L - 2) - 2} ,$$

$$C_s = 8\pi K_s = \frac{2\pi(L - 5/2)}{(L - \frac{1}{2})(L - 2) - 2} .$$

We should note the rather new form these coefficients take in comparison to what has always been assumed in resistive force theory. Further, since our Stokeslet strength is accurate up to and including terms of $O(\epsilon^2 \ln\epsilon)$, we have in fact summed the entire series of terms $f_n/(\ln\epsilon)^n$ which result from the method of matched asymptotic expansions. A numerical comparison between the straight body results and the exact results for a torus are given in figure (2. 2. 3). Again the difference is rather small for moderate ranges of the slenderness parameter. The unusual behavior for increasing ϵ is

due to the difference in functional form between the coefficients here and the classical theory which are proportional to $(\ln\epsilon + c)^{-1}$, c being a constant.

The total force on the torus is

$$\underline{F} = -8\pi\mu \int_0^{2\pi} \underline{a}\, a\, d\theta$$

which gives

$$F_x = 0 ,$$

$$F_y = -4\pi^2 \mu U a (K_n + K_s) .$$

This may be compared to Cox's result for this case by defining the drag coefficient, C_y,

$$F_y = -2\pi a\, C_y \mu U.$$

From the results for K_n and K_s we have

$$C_y = \pi \left\{ \frac{3L - \frac{17}{2}}{(L - \frac{1}{2})(L - 2) - 2} \right\} + O(\epsilon^2 \ln\epsilon) .$$

Approximating this by neglecting terms $O(\frac{1}{\ln\epsilon})^3$ we find

$$C_y = \frac{3\pi}{L + \frac{1}{3}} + O(\frac{1}{\ln\epsilon})^3$$

which is precisely the result found by Cox (1970). Our result, however, is greatly improved over that due to Cox, being accurate neglecting terms of order $\epsilon^2 \ln\epsilon$.

2.3 On-edge rotation

In this case our torus rotates with angular velocity $\Omega \underline{e}_x$ so that the no-slip boundary condition becomes for $\theta = \theta'$

$$\underline{u} = -\Omega(z\,\underline{e}_y - r\sin\theta'\,\underline{e}_z)$$

$$= -\Omega(b\sin\psi\sin\theta'\,\underline{e}'_r + b\sin\psi\cos\theta'\,\underline{e}'_\theta - r\sin\theta'\,\underline{e}_z)\ ,$$

$$\text{on}\quad r_1 = b$$

recalling that

$$r = a(1 + \epsilon\cos\psi).$$

To avoid much of the same analysis as has already been done we will now include all of the needed singularities from the start. The velocity field here will be given by a line distribution of Stokeslets, doublets, rotlets, stresslets, and quadrupoles. As always, only the Stokeslet far field need be retained since only its far field distribution has a contribution of order greater or equal to $O(\epsilon\,a)$ where a is the magnitude of the Stokeslet strength. This will not be further pursued here since the precise results follow easily from the methods used earlier in doing similar calculations.

The velocity field is given by

$$\underline{u} = \int_{\gamma}^{2\pi-\gamma} \underline{U}_S^{(o)}(\underline{R};\underline{a})\,a\,d\varphi + \int_{-\gamma}^{\gamma} \{\underline{U}_S^{(i)}(\underline{R};\underline{a}) + \underline{U}_D^{(i)}(\underline{R};\underline{\beta}) + \underline{U}_R^{(i)}(\underline{R};\underline{\delta})$$

$$+ \hat{A}\underline{U}_{SS}^{(i)}(\underline{R};\underline{e}_r,\underline{e}_z) + \hat{B}\underline{U}_Q^{(i)}(\underline{R};\underline{e}_r,\underline{e}_z)\}\,a\,d\varphi\ ,$$

where the general form of the terms in the integrand above can be found in the previous two sections 2. 1 and 2. 2. The strengths/length of the Stokeslet, doublet, rotlet, stresslet, and quadrupole using the same notation as before are respectively given by

$$\underline{a} = a \sin\theta \, \underline{e}_z \ ,$$

$$\underline{\beta} = \beta \sin\theta \, \underline{e}_z \ ,$$

$$\underline{\delta} = \delta_n \cos\theta \, \underline{e}_r + \delta_s \sin\theta \, \underline{e}_\theta \ ,$$

$$\hat{A} = A \sin\theta \ ,$$

$$\hat{B} = B \sin\theta \ ,$$

where

$a, \beta, \delta_n, \delta_s, A, B$ are constants.

Carrying out the integration we find the velocity field in the vicinity of the torus, with terms of $O(\epsilon^2 \ln\epsilon)$ neglected, as

$$u = 2\sin\theta' \{ (a - \frac{2\beta}{r_1^2})\cos\psi\sin\psi - \sin\psi [-\frac{a}{2}\tilde{\epsilon} (\ln\frac{8}{\tilde{\epsilon}} - 3) + \frac{\tilde{\epsilon}\beta}{2r_1^2} + \frac{\tilde{\epsilon}}{2}\cos^2\psi (a - \frac{2\beta}{r_1^2}) - \frac{\delta_s}{r_1} - \frac{A}{r_1} - \frac{2B}{r_1^3} - \cos 2\psi (\frac{A}{r_1} + \frac{4B}{r_1^3})] \} \ ,$$

$$v = 2\cos\theta' \sin\psi \{ -\tilde{\epsilon} a (\ln\frac{8}{\tilde{\epsilon}} - 2) + \frac{\tilde{\epsilon}\beta}{r_1^2} - \frac{\delta_n}{r_1} \} \ ,$$

$$w = 2\sin\theta' \{ a(\ln\frac{8}{\tilde{\epsilon}} - 2) + \frac{\beta}{r_1^2} + \sin^2\psi (a - \frac{2\beta}{r_1^2}) - \cos\psi [\frac{a}{2}\tilde{\epsilon} (\ln\frac{8}{\tilde{\epsilon}} - 3) + \frac{\tilde{\epsilon}\beta}{2r_1^2} + \frac{\epsilon \sin^2\psi}{2} (a - \frac{2\beta}{r_1^2}) + \frac{\delta_s}{r_1} - \frac{A}{r_1} - \frac{2B}{r_1^3} + \cos 2\psi (\frac{A}{r_1} + \frac{4B}{r_1^3}) \} \ .$$

The boundary conditions on $r_1 = b$ become six equations for the six unknowns $\alpha, \beta, \delta_s, \delta_n$, A and B. The solution of the above equations is,

$$\alpha = \frac{\Omega a}{2(\ln \frac{8}{\epsilon} - \frac{3}{2})} ,$$

$$\beta = \frac{\alpha b^2}{2} ,$$

$$\delta_s = -\frac{3}{2} \epsilon b \alpha (\ln \frac{8}{\epsilon} - 2) ,$$

$$\delta_n = \epsilon b \alpha ,$$

$$A = \frac{\epsilon b \alpha}{2} ,$$

$$B = -\frac{Ab^2}{4} = -\frac{\epsilon b^3 \alpha}{8} .$$

We see here once more that the doublet strength equals one-half the Stokeslet strength times the cross-sectional radius squared. Furthermore we find, as in the previous two cases, that the quadrupole strength is proportional to the stresslet strength times one-half the cross-sectional radius squared. And we should note that both stresslet and quadrupole strengths are precisely the same as found in section 2. 1. This is due to the fact that in both cases these higher order singularities are required to correct for precisely the same type of "extensional-like" flow induced by the Stokeslet and doublet distributions alone as discussed in section 2. 1. This common flow is reasonable since both motions are similar in that the velocity of the body centerline is moving normal to the plane of the torus centerline.

The solution presented then satisfies the boundary condition, neglecting terms of $O(\epsilon^2 \ln\epsilon)$. It is then straightforward to obtain the components of the velocity field in the (r_1, θ, ψ) coordinate system from which we can calculate the needed terms in the rate of strain tensor. We find, retaining the terms through $O(\frac{a}{b}\epsilon)$ on $r_1 = b$,

$$e_{r_1 r_1} = 0 \ ,$$

$$e_{r_1 \psi} = 2\sin\theta \frac{a}{b} \{ -\epsilon(3\ln\frac{8}{\epsilon} - \frac{13}{2}) - 2\cos\psi - \frac{\epsilon}{4}\cos 2\psi \} \ ,$$

$$e_{r_1 \theta} = 4\cos\theta\sin\psi \, \epsilon \frac{a}{b} \ .$$

As for the pressure we find on $r_1 = b$,

$$p = p_S + p_{SS} = 4\mu \frac{a}{b} \sin\theta \sin\psi \{1 + \frac{\epsilon}{2}\cos\psi\} \ .$$

We are now able to calculate the stress $\underline{\tau}$ and thus find the force/length and torque/length as

$$f_r = f_\theta = 0 \ ,$$

$$f_z = -8\pi\mu a \sin\theta \ ,$$

$$M_r = -4\pi\mu ab\epsilon\cos\theta \ ,$$

$$M_\theta = 4\pi\mu ab \sin\theta \, \epsilon(3L - \frac{11}{2}) \ ,$$

$$M_z = 0 \ .$$

In figure (2. 3. 1) we have a comparison between the drag coefficient for our torus and the straight body case. Defining the drag coefficient in the traditional manner gives

$$f_z = -\mu C_n U \ ,$$

where

$$U = \Omega a \ ,$$

$$C_n = \frac{4\pi}{(L - \frac{3}{2})} \ .$$

We see that the deviations from the classical resistive-force theory are now quite large (as much as 40% for $\epsilon < 0.1$), with the torus experiencing an increased drag/length. The cause, as suggested in the first case, is explained by observing that two points of equal arc lengths from the axis of rotation are moving in opposite directions, dragging fluid with them and producing an increased apparent flow at the corresponding point on the other half of the torus. This increased incident velocity results in increased drag.

2.4 Spinning torus

A spinning torus refers to a torus rotating about its longitudinal axis (of symmetry), with angular velocity Ω. The boundary condition on $r_1 = b$ now requires

$$\underline{u} = \Omega r \underline{e}_\theta = \Omega a(1 + \epsilon \cos\psi)\underline{e}_\theta \ .$$

The solution is here constructed by a line distribution of Stokeslets and rotlets with strengths

$$\underline{a} = a \underline{e}_\theta \ ,$$

$$\underline{\delta} = \delta \underline{e}_z \ . \qquad (a, \delta, \text{ constant})$$

With the lack of motion normal to the centerline there is no need to include stresslets and quadrupoles in our solution, as was necessary in the previous cases where motion of the centerlines in the normal direction was always present.

The velocity field is

$$\underline{u} = \int_0^{2\pi} (\underline{U}_S(\underline{R};\underline{a}) + \underline{U}_R(\underline{R};\underline{\delta}))ad\varphi ,$$

where $\underline{U}_S$ and $\underline{U}_R$ are given in (2. 1. 1) and (2. 1. 20). After constructing the inner and outer expansions of the integrand and carrying out the integration we find only the tangential velocity component to be nonzero

$$u = w = 0 ,$$

$$v = 4a(L - 2) - \cos\psi[2a\epsilon(L - 3) - \frac{2\delta}{r_1}] + O(\epsilon^2 \ln\epsilon) .$$

The boundary condition is satisfied with

$$a = \frac{\Omega a}{4(\ln\frac{8}{\epsilon} - 2)} ,$$

$$\delta = \epsilon b(3\ln\frac{8}{\epsilon} - 7)a .$$

Calculating the stresses on $r_1 = b$ we find

$$\tau_{r_1 r_1} = \tau_{r_1 \psi} = 0 ,$$

$$\tau_{r_1 \theta} = -2\mu\{\frac{2a}{b} + \cos\psi[\frac{\delta}{b^2} + \frac{a}{b}\epsilon(3L - 8)] + O(\frac{\epsilon \ln\epsilon}{a})\} .$$

From (2. 1. 29) and (2. 1. 30)

$$f_r = f_z = 0 \quad ,$$

$$f_\theta = -8\pi\mu a \quad ,$$

$$M_r = M_\theta = 0 \quad ,$$

$$M_z = -2\pi\mu b[\frac{\delta}{b} + 3a\epsilon(L - 2)] \quad .$$

In this solution it is of interest to note that the contribution to M_z from the rotlet distribution and Stokeslet distribution are of the same order of magnitude. The total torque exerted on the fluid about the torus center, i. e., r = 0, z = 0, is

$$\underline{T} = -\int \underline{x} \times \underline{t}\, dS \quad ,$$

$$\underline{x} = r\,\underline{e}_r + b \sin\psi\, \underline{e}_z \quad .$$

On the torus surface,

$$\underline{t} = \tau_{r_1\theta}\,\underline{e}_\theta \qquad \text{(since } \tau_{r_1 r_1} = \tau_{r_1\psi} = 0\text{)}$$

and therefore

$$\underline{T} = \int_0^{2\pi}\int_0^{2\pi} [b\sin\psi\, \tau_{r_1\theta}\underline{e}_r - a(1 + \epsilon\cos\psi)\tau_{r_1\theta}\underline{e}_z]$$

$$ab(1 + \epsilon\cos\psi)d\psi\, d\theta$$

$$= 2\pi a(8\pi\mu a a - M_z)\underline{e}_z \quad .$$

The total rotlet strength times $8\pi\mu$ does not equal, as we might have expected, $2\pi a M_z$. This discrepancy is because the Stokeslet velocity

field generates stresses that contribute to the term M_z and thus to the total torque.

In figure (2. 4. 1) we have a comparison of the tangential drag coefficients for a torus and straight slender spheroid which shows dramatically how the actual body shape and motion interact to produce significant departures from the result of a straight body. The alteration of the result is due to the two quite different far-fields involved in the two situations. On physical grounds, we see that for a torus spinning about its longitudinal axis, a material point on the body centerline is dragging fluid with it, effectively increasing the incident flow at a point across the torus aperture. Accordingly, we find increased drag coefficients. This is very similar to the discussion in section 2. 3 for on-edge rotation. For a straight body moving tangentially each point of the body helps to reduce the oncoming velocity seen at any other point, thus resulting in a rather different situation. The tangential drag coefficient, C_s, for the torus defined by

$$f_\theta = -8\pi\mu a = -\mu C_s U ,$$

where

$$U = \Omega a$$

$$C_s = \frac{2\pi}{\ln \frac{8}{\epsilon} - 2}$$

is seen to have deviations as large as 25% to 50% even for small values of $\epsilon (< 0.2)$ where the theory is accurate.

2.5 Torus in radial flow

In this final section our torus is allowed to expand (or contract) radially so long as it remains circular and slender, i.e., $b/a \ll 1$. The major radius is assumed to be changing with velocity U, such that

$$a = a_o + Ut \quad , \qquad a_o = \text{constant} \quad .$$

The no-slip boundary condition now requires

$$\underline{u} = \frac{da}{dt}\,\underline{e}_r = U\,\underline{e}_r, \quad \text{on} \quad r_1 = b \quad .$$

At the end of this section we will extend the solution to the case of a torus with an infinite line source along its longitudinal axis.

The velocity field is given by a Stokeslet, doublet, source, stresslet, and quadrupole distribution with only the Stokeslet contributing a velocity term of order ϵa (or less) from the outer region, i.e., for $\gamma \leqslant \varphi \leqslant 2\pi - \gamma$. We have then

$$\underline{u} = \int_{\gamma}^{2\pi-\gamma} \underline{U}_S^{(o)}(\underline{R};\underline{a})\,ad\varphi + \int_{-\gamma}^{\gamma} \{\underline{U}_S^{(i)}(\underline{R};\underline{a}) + \underline{U}_D^{(i)}(\underline{R};\underline{\beta}) + \underline{U}_m^{(i)}(\underline{R};m)$$

$$+ A\underline{U}_{SS}^{(i)}(\underline{R};\underline{e}_r,\underline{e}_r) + B\underline{U}_Q^{(i)}(\underline{R};\underline{e}_z,\underline{e}_z)\}\,ad\varphi \quad .$$

The general expressions for the Stokeslet, doublet, source, and stresslet may be found in sections 2.1 and 2.2, however the quadrupole is most easily calculated from

$$\underline{u}_Q = B\frac{\partial}{\partial z}\,\underline{u}_D(\underline{e}_z) \quad .$$

The Stokeslet and doublet strengths/length are from the flow symmetry assumed constant and in the radial direction ($\underline{e}_r$).

Expansion of the integrands and integration gives the velocity field in the body vicinity, neglecting terms of $O(\epsilon^2 \ln\epsilon)$, as

$$u = 2a(\ln\frac{8}{\tilde{\epsilon}} - 3) + \frac{2\beta}{r_1^2} + 2(a - \frac{2\beta}{r_1^2})\cos^2\psi + \cos\psi[-a\tilde{\epsilon}(\ln\frac{8}{\tilde{\epsilon}} - \frac{7}{2}) + \frac{2m}{r_1} + \frac{4B}{r_1^3} + \cos 2\psi(\frac{2A}{r_1} - \frac{8B}{r_1^3} + \tilde{\epsilon}\frac{\beta}{r_1^2} - \frac{\tilde{\epsilon}a}{2})] ,$$

$$v = 0 , \qquad (2.5.1)$$

$$w = 2\sin\psi\cos\psi(a - \frac{2\beta}{r_1^2}) + \sin\psi[-a\tilde{\epsilon}(\ln\frac{8}{\tilde{\epsilon}} - \frac{1}{2}) + \frac{2\tilde{\epsilon}\beta}{r_1^2} + \frac{2m}{r_1} - \frac{4B}{r_1^3} + \cos 2\psi(\frac{2A}{r_1} - \frac{8B}{r_1^3} + \frac{\tilde{\epsilon}\beta}{r_1^2} - \frac{\tilde{\epsilon}a}{2})] ,$$

where Stokeslet, doublet, source, stresslet and quadrupole strengths per unit length are given by $a, \beta, m, A,$ and B respectively.

The boundary condition is satisfied up to $O(\epsilon^2 \ln\epsilon)$ if

$$a = \frac{U}{2(\ln\frac{8}{\epsilon} - \frac{5}{2})} ,$$

$$\beta = \frac{ab^2}{2} ,$$

$$m = \frac{\epsilon ba}{2}(\ln\frac{8}{\epsilon} - \frac{5}{2}) = \frac{\epsilon bU}{4} , \qquad (2.5.2)$$

$$A = -\epsilon ba ,$$

$$B = \frac{Ab^2}{4} = -\frac{\epsilon b^3 a}{4} .$$

Once more the now familiar Stokeslet-doublet relationship is present. With a normal centerline motion present we again need a stresslet and quadrupole with the same relationship between them as found before. Also in this case, as in the case of translation of section 2.2, the centerline possesses a velocity component normal to itself in the plane of the torus, and we find in both cases that the stresslet strength equals ϵb times the total Stokeslet strength/length except for a sign change.

For this case the body is changing volume with respect to time and therefore the time rate of change of the body volume should equal the total mass flux from the sources. This is easily seen from first principles. The continuity equation in integral form for an incompressible fluid with distributed sources is

$$v(t) = v_o + \int_{\varrho}^{t} \int_{v(t')} 4\pi m dv dt' \ , \qquad (v(t) = \text{torus volume}) \ ,$$

where $v_o = v(t = o)$ and we note that the 4π enters from our choice of the form of the source velocity $\underline{U}_m$. Differentiating the above equation gives

$$\frac{dv(t)}{dt} = \int_{v(t)} 4\pi m dv = 4\pi m_{total} \ . \qquad (2.5.3)$$

In our case $v(t) = \pi b^2(2\pi a) = 2\pi^2 b^2(a_o + Ut)$ and so

$$\frac{dv}{dt} = 2\pi^2 b^2 U \ .$$

The net flux $= 4\pi m_{total} = 8\pi^2 am$, and substituting m from (2. 5. 2) yields the net flux $= 2\pi^2 b^2 U$. Thus (2. 5. 3) is indeed satisfied as expected.

The stresses on $r_1 = b$ are found, as before, neglecting terms of $O(\frac{\epsilon \ln\epsilon}{a})$ as

$$\tau_{r_1 r_1} = -4\mu\frac{a}{b}\left(\frac{\epsilon}{2}\left(\ln\frac{8}{\epsilon} - \frac{9}{2}\right) + \cos\psi - \frac{5}{4}\epsilon\cos\psi\right) ,$$

$$\tau_{r_1\psi} = 4\mu\frac{a}{b}\left(\sin\psi - \frac{5}{4}\epsilon\sin 2\psi\right) ,$$

$$\tau_{r_1\theta} = 0 .$$

And thus the result for the force/length and moment/length on the torus are found by using (2. 1. 29) and (2. 1. 30), with an error of $O(\epsilon^2 \ln\epsilon)$

$$f_r = -8\pi\mu a ,$$

$$f_\theta = f_z = 0 ,$$

$$M_r = M_\theta = M_z = 0 .$$

We define the normal force coefficient, C_n, in the usual manner

$$f_r = -\mu C_n U ,$$

$$C_n = \frac{4\pi}{L - \frac{5}{2}}$$

in order to make comparison against the straight slender body coefficients. Figure (2. 5. 1) shows the large deviations as can be expected by motions of this type since the points on the body center-line are moving everywhere in radial directions.

The alternate radial flow problem produced by a line source on the longitudinal axis has an undisturbed velocity field given by

$$\underline{u} = \frac{Q}{r} \underline{e}_r \sigma .$$

The boundary condition on the torus surface then becomes

$$\underline{u} = \frac{Q}{a(1 + \epsilon \cos \psi)} \underline{e}_r$$

$$= U_o(1 - \epsilon \cos \psi + O(\epsilon^2))\underline{e}_r , \qquad (2. 5. 4)$$

where

$$U_o = \frac{Q}{a} .$$

Here we certainly know that there can be no net source strength present in the solution, therefore we use the same velocity field (2. 5. 1) as before taking $m = 0$. The boundary condition is therefore satisfied, neglecting in this case the terms of $O(\epsilon^2)$, by taking

$$\alpha = \frac{U_o}{2(L - \frac{5}{2})} ,$$

$$\beta = \frac{1}{2} \alpha b^2$$

$$A = - \epsilon b(\frac{1}{2} U_o + \alpha) ,$$

$$B = \frac{Ab^2}{4} .$$

As expected, the Stokeslet strength to this order is unchanged, and the stresslet and quadrupole are altered by the slightly different flow field near the body surface.

2.6 Conclusion

We have presented the solution for Stokes flow past a slender torus. The accuracy of the solution demonstrates how effective the method of flow singularities could be for constructing solutions to Stokes flow involving slender bodies of arbitrary centerline configurations. Furthermore, by first considering a torus we begin to obtain a physical feel for what singularities are necessary for various types of body centerline motions. The fundamentals learned here will be of great assistance in developing the solutions for the more difficult problems of slender-body theory to follow. For the simple case of a torus we have found many new features not presently available in the literature.

The primary importance of this preliminary study is to serve as a guide for the general case. Therefore it is fitting that we conclude with some general observations. First of all, during this analysis we always found that the boundary condition can be satisfied to lowest order by including a near and far field Stokeslet and a near field doublet. In fact, the normal or tangential doublet strength is always equal to $\frac{1}{2}b^2$ times the Stokeslet strength in the same direction. This might be expected since only the near field doublet distribution contributes to the velocity and thus the straight body results are found to be correct to lowest order. Furthermore, for

satisfying the boundary condition up to the error term of $O(\epsilon^2 \ln\epsilon)$ we found that only the Stokeslet was required in the far field distribution, or in the outer region. The role of the higher order singularities is to correct for centerline curvature effects. We found that stresslets and quadrupoles are needed whenever the body centerline moves normal to itself. Also the quadrupole strength is always equal, except for a possible sign change, to $\frac{b^2}{4}$ times the stresslet strength, with the latter being proportional to ϵb. The motion of the body centerline in its osculating plane (i. e. the plane containing $\underline{e}_r$, $\underline{e}_\theta$), as in the case of translation discussed in section 2. 2 or spinning, invariably requires use of a rotlet distribution normal to that plane. For the motion of the torus normal to its plane our solution also requires a rotlet, except now its direction is tangential to the body centerline. The rotlet strengths are, in all cases, proportional to ϵb. We will see that many of the characteristics for flow past a torus found here will be of use in the more challenging problem to be discussed in the next chapter.

Considerable deviations between the drag coefficients of the torus and a straight body have been found, often for very small values of ϵ where it might not be expected. These deviations are particularly large when the motion is such that there are points on the centerline moving in opposition to one another. This long range effect in Stokes flow clearly indicates how important it is to develop a general uniformly valid theory for undulatory motions of a flagellum where points separated by half a wavelength are moving in opposite directions. One further, rather surprising, result is that it has been

possible to correct the boundary condition up to an error of $O(\epsilon^2 \ln\epsilon)$ without affecting the Stokeslet strength previously found by satisfying the boundary condition to the lowest order. Therefore, extending the theory to higher orders in ϵ has not changed the force/length, although it has given an improved error estimate of that result.

III. THE STOKES FLOW PAST A FLEXIBLE SLENDER BODY IN ARBITRARY MOTION

We now consider the case of arbitrary motion of a flexible slender body with circular cross section and length 2ℓ. The centerline configuration of the slender body motion can be generally prescribed in the parametric form

$$\underline{x} = \underline{x}_o(s,t) = (x_1(s,t),\ x_2(s,t),\ x_3(s,t)) \qquad (-\ell \leqslant s \leqslant \ell)\ ,$$

where s is the arc length along the centerline and t is the time. The parametric function $\underline{x}_o(s,t)$ is assumed at least twice differentiable in s and t. In the sequel, all quantities having the dimensions of length will be nondimensionalized by the body half length ℓ (unless otherwise stated).

3.1 The case of spheroidal cross section

In this case we restrict our attention to bodies with circular cross sections whose area satisfied the spheroidal distribution:

$$r_1 = \epsilon\eta(s) = \epsilon(1 - s^2)^{1/2} \qquad (-1 \leqslant s \leqslant 1)\ , \qquad (3.1.1)$$

where as already mentioned we have nondimensionalized by ℓ and here $\epsilon = \frac{b}{\ell} \ll 1$. The body is further assumed to be inextensible, i.e.,

$$\frac{\partial x_{oi}}{\partial s}\ \frac{\partial x_{oi}}{\partial s} = 1\ , \qquad (3.1.2)$$

where the summation convention (over the repeated indicies $i = 1, 2, 3$) is employed and (x_1, x_2, x_3) are used interchangeably with (x, y, z). Therefore, associated with the centerline the unit vectors in the tangential, normal, and binormal directions are given by (see figure 3.1.1)

$$\underline{e}_s = \underline{x}_{o,s} , \qquad \underline{e}_n = \frac{1}{\kappa} \underline{x}_{o,ss} , \qquad \underline{e}_b = \underline{e}_s \times \underline{e}_n , \tag{3.1.3}$$

where κ is the local nondimensional curvature of the body centerline, i.e.,

$$\kappa = (\underline{x}_{o,ss} \cdot \underline{x}_{o,ss})^{1/2} .$$

Here a subscript s refers to differentiation with respect to the arc length variable s.

The body centerline velocity is

$$\underline{V}(s,t) = \frac{d\underline{x}_o}{dt} = \dot{\underline{x}}_o(s,t) \qquad (-1 \leqslant s \leqslant 1) ,$$

where the velocity is nondimensionalized by some characteristic velocity U. The admissible motions will be limited to those in which the radius of curvature, κ^{-1}, is for all s and t large compared to the cross-sectional radius of the body. It is particularly convenient, as in the torus problem, to decompose the velocity into its components along the $(\underline{e}_s, \underline{e}_n, \underline{e}_b)$ directions,

$$\underline{V}(s,t) = V_s \underline{e}_s + V_n \underline{e}_n + V_b \underline{e}_b \ ,$$

where

$$V_s = \dot{\underline{x}}_o \cdot \underline{x}_{o,s}$$

$$V_n = \frac{1}{\kappa} \dot{\underline{x}}_o \cdot \underline{x}_{o,ss}$$

$$V_b = \frac{1}{\kappa} \dot{\underline{x}}_o \cdot (\underline{x}_{o,s} \times \underline{x}_{o,ss}) \ .$$

The motion of the body surface at any station s may be regarded as consisting of a translation of velocity $\underline{V}$ and a rotation about the point $\underline{x}_o(s,t)$ with angular velocity, nondimensionalized by U/ℓ,

$$\underline{\Omega}(s,t) = \Omega_s \underline{e}_s + \Omega_n \underline{e}_n + \Omega_b \underline{e}_b \ ,$$

where

$$\Omega_s = \dot{\underline{e}}_n \cdot \underline{e}_b \ , \quad \Omega_n = \dot{\underline{e}}_b \cdot \underline{e}_s \ , \quad \Omega_b = \dot{\underline{e}}_s \cdot \underline{e}_n \ ,$$

since in general, $\dfrac{d\underline{e}_\nu}{dt} = \dot{\underline{e}}_\nu = \underline{\Omega} \times \underline{e}_\nu$ $(\nu = n, s, b)$.

The no-slip boundary condition on the body surface is given by

$$\underline{u} = \underline{V} + \underline{\Omega} \times r_1 \underline{e}_{r_1} \qquad \text{on } r_1 = \epsilon\eta,$$

where

$$\underline{e}_{r_1} = \sin\psi \, \underline{e}_b - \cos\psi \, \underline{e}_n \ , \qquad (3.1.4)$$

with (r_1, ψ) denoting the familiar polar coordinates in the body cross-sectional plane. In terms of the unit vectors $\underline{e}_s$, $\underline{e}_n$, $\underline{e}_b$ we have

$$\underline{u} = U_s \underline{e}_s + U_n \underline{e}_n + U_b \underline{e}_b \qquad \text{on } r_1 = b \ , \qquad (3.1.5)$$

where

$$U_s = V_s + \epsilon\eta(\Omega_n \sin\psi + \Omega_b \cos\psi) \ ,$$

$$U_n = V_n - \epsilon\eta\Omega_s \sin\psi \ ,$$

$$U_b = V_b - \epsilon\eta\Omega_s \cos\psi \ .$$

Following the same method as developed earlier for the torus problem, we assume that the velocity field is given to the first approximation by a line distribution of Stokeslets and doublets along the body centerline. The extent of the distribution, guided by the exact solution for straight prolate spheroid (Chwang & Wu, 1975), is taken to lie between the generalized foci of the body, i. e., the foci of the stretched straight body

$$s_1 = (1 - \epsilon^2)^{1/2} = e \ . \qquad (3.1.6)$$

where e is the generalized eccentricity.

The velocity field is therefore given by

$$\underline{u}(s, r_1, \psi) = \int_{-s_1}^{s_1} (\underline{U}_S(\underline{R};\alpha) + \underline{U}_D(\underline{R};\underline{\beta}))ds' \ , \qquad (3.1.7)$$

where $\underline{U}_S$ and $\underline{U}_D$ are the nondimensionalized forms of the equations given in (2.1.1). Here the Stokeslet and doublet strengths are functions of s and t and are nondimensionalized by U and $U\ell^2$ respectively. Also we have (see figure 3.1.1)

$$\underline{R} = \underline{R}_o + r_1 \underline{e}_{r_1}(s,t) \quad ,$$

$$\underline{R}_o = \underline{x}_o(s,t) - \underline{x}_o(s',t) \quad ,$$

$$R = |\underline{R}| = [R_o^2 + r_1^2 + 2r_1 \underline{e}_{r_1} \cdot \underline{R}_o]^{1/2} \quad , \qquad (3.1.8)$$

$$R_o = |\underline{R}_o| \quad .$$

Since evaluating the integrals by applying the simplified procedure used for the torus encounters difficulty near the body ends, we resort to the construction of uniformly valid expansions near the body surface as discussed in Chapter II.

In the vicinity of the body we let $r_1 = \epsilon\eta$ where $\eta = O(1)$ and write

$$R = (R_o^2 + \epsilon^2\eta^2 + 2\epsilon\eta \underline{e}_{r_1} \cdot \underline{R}_o)^{1/2} \quad . \qquad (3.1.9)$$

We further limit our analysis to the consideration of bodies for which

$$R_o > O(\epsilon) \quad , \qquad \text{for all } (s' - s) > O(\epsilon) \quad ,$$

i.e., we exclude from our study slender bodies in which the centerline reapproaches itself. In particular, the distance between the centerline must be greater than order ϵ for any two points on the centerline which are separated by a distance along the arc length greater than $O(\epsilon)$, for example, we must omit a helix of high pitch or a nearly closed partial torus. With this restriction the outer expansion of R^{-1} which is valid in the neighborhood of the body,

excluding the inner region centered at the point s at which section the boundary condition is to be applied, is

$$\frac{1}{R} \simeq \frac{1}{R_o}\left(1 - \frac{\epsilon\eta \underline{e}_{r_1} \cdot \underline{R}_o}{R_o^2} + O(\epsilon^2)\right) \qquad (3.1.10)$$

for $(s' - s) > O(\epsilon)$. Writing $\underline{R}_o$ in terms of the unit vectors $\underline{e}_s$, $\underline{e}_n$, $\underline{e}_b$ at s, i.e.,

$$\underline{R}_o = R_{os}\underline{e}_s + R_{on}\underline{e}_n + R_{ob}\underline{e}_b ,$$

we have upon using (3.1.4)

$$\frac{1}{R} \simeq \frac{1}{R_o}\left\{1 + \frac{\epsilon\eta}{R_o^2}\left[R_{on}\cos\psi - R_{ob}\sin\psi\right] + O(\epsilon^2)\right\} . \qquad (3.1.11)$$

For the inner expansion we will make use of the inner or stretched variable introduced in Chapter II. Here it is given by

$$\sigma = \frac{s' - s}{\epsilon} . \qquad (3.1.12)$$

We expand R_o^2 and $\underline{R}$ for σ fixed and $\epsilon \to 0$, or equivalently in a Taylor series about $s' = s$, giving

$$R_o^2 \simeq \epsilon\sigma^2 - \frac{1}{12}\epsilon^4\sigma^4\kappa^2 + O(\epsilon^5) , \qquad (3.1.13)$$

$$\underline{R} \simeq (\epsilon\sigma r_s^{(1)} + \epsilon^3\sigma^3 r_s^{(3)})\underline{e}_s + (\epsilon r_n^{(1)} + \epsilon^2\sigma^2 r_n^{(2)} + \epsilon^3\sigma^3 r_n^{(3)})\underline{e}_n$$
$$+ (\epsilon r_b^{(1)} + \epsilon^3\sigma^3 r_b^{(3)})\underline{e}_b + O(\epsilon^4) , \qquad (3.1.14)$$

where

$$r_s^{(1)} = -1, \quad r_s^{(3)} = \frac{1}{6}\kappa^2 ,$$

$$r_n^{(1)} = -\eta \cos\psi, \quad r_n^{(2)} = -\frac{1}{2}\kappa, \quad r_n^{(3)} = -\frac{1}{6}\kappa_{,s} ,$$

$$r_b^{(1)} = -\eta \sin\psi, \quad r_b^{(3)} = -\frac{1}{6}\kappa\tau ,$$

with τ being the torsion, i.e., the measure of the rate at which the curve $\underline{x}_o(s,t)$ twists out of the osculating plane. In equation (3.1.14) the base vectors $\underline{e}_s, \underline{e}_n, \underline{e}_b$ assume their values at s.

Using (3.1.13), (3.1.14) and (3.1.8) we find the inner expansion of R^{-1} as

$$\frac{1}{R^{(i)}} \tilde{=} \frac{1}{\epsilon\Delta}\{1 + \frac{\epsilon\sigma^2}{\Delta^2} R_1 + \frac{\epsilon^2}{\Delta^2}(\sigma^4 R_2 + \sigma^3 R_3) + O(\epsilon^3)\} , \tag{3.1.15}$$

where

$$R_1 = -\frac{1}{2}\eta\kappa \cos\psi ,$$

$$R_2 = \frac{\kappa^2}{24}\left(1 + \frac{9\eta^2\cos^2\psi}{\Delta^2}\right),$$

$$R_3 = -\frac{1}{6}\eta(\kappa_{,s}\cos\psi + \kappa\tau \sin\psi) ,$$

$$\Delta = (\sigma^2 + \eta^2)^{1/2} .$$

The Stokeslet strength, $\underline{a}$, which is to be determined as a function of s and t, has the inner expansion about $s' = s$,

$$\underline{a}^{(i)}(s',t) \tilde{=} \underline{a}^{(o)} + \epsilon\sigma\underline{a}^{(1)} + \epsilon^2\sigma^2\underline{a}^{(2)} + O(\epsilon^3) , \tag{3.1.16}$$

where

$$\underline{a}^{(o)} = \underline{a}(s,t) \ ,$$

$$\underline{a}^{(1)} = (\underline{a}'_s - \kappa a_n)\underline{e}_s + (a'_n + \kappa a_s + \tau a_b)\underline{e}_n + (a'_b - \tau a_n)\underline{e}_b \ ,$$

$$2\underline{a}^{(2)} = (a''_s - 2\kappa a'_n - \kappa' a_n - \kappa^2 a_s - \kappa\tau a_b)\underline{e}_s \qquad (3.1.17)$$

$$+(a''_n + \kappa' a_s + \tau' a_b + 2\kappa a'_s + 2\tau a'_b - \kappa^2 a_n - \tau^2 a_n)\underline{e}_n$$

$$+(a''_b - 2\tau a'_n - \tau' a_n - \kappa\tau a_s - \tau^2 a_b)\underline{e}_b \ .$$

In the above expressions the primes denote differentiation with respect to s, $(\underline{e}_s, \underline{e}_n, \underline{e}_b)$ are the unit vectors at s, and $a_\nu (\nu = n, s, b)$ are the components of $\underline{a}$ at s in terms of these unit vectors.

The doublet distribution may also be similarly expanded as a function of s, however, that particular choice makes the analysis unnecessarily complicated. By making use of the previous results for the torus and straight slender spheroids, namely, that the doublet strength is always proportional to the cross-sectional radius squared, we are led to take

$$\underline{\beta}(s,t) = \underline{B}(s,t,)(s_1^2 - s^2) \qquad (3.1.18)$$

This doublet strength, $\underline{\beta}$, can then be expanded in the inner region about $s' = s$ as,

$$\underline{\beta}^{(i)}(s',t) \tilde{=} \underline{\beta}^{(o)} + \epsilon\sigma\underline{\beta}^{(1)} + \epsilon^2\sigma^2\underline{\beta}^{(2)} + O(\epsilon^3) \ ,$$

where

$$\underline{\beta}^{(o)} = \underline{B}(s,t)(s_1^2 - s'^2) \quad ,$$

$$\underline{\beta}^{(1)} = \underline{B}^{(1)}(s,t)(s_1^2 - s'^2) \quad ,$$

$$\underline{\beta}^{(2)} = \underline{B}^{(2)}(s,t)(s_1^2 - s'^2) \quad ,$$

with $\underline{B}^{(1)}$ and $\underline{B}^{(2)}$ given by equation (3. 1. 17) if all the a_ν are replaced by B_ν. What we have done here is to expand the $\underline{B}$ about $s' = s$ while leaving the parabolic modulation intact, and by so doing we have generated a series in which the ordering of the terms is explicit, since all of the terms tend to zero at the same rate near $s' = \pm s_1$. Had we expanded $\underline{\beta}(s')$, as was done for $\underline{a}(s')$, without making use of the form (3. 1. 18), we would have constructed an expansion in which the first term, $B_\nu(s,t)(s_1^2 - s^2)$, was not always of the leading order, i. e., it would tend to zero near the ends whereas some of the higher order terms in the Taylor series would not. This procedure is in direct analogy with the two-timing or two-variable expansion method found in perturbation theory, in which we have a fast and slow variable (Van Dyke, 1975).

For satisfying the boundary conditions we will, in general, be considering the velocity components in the $\underline{e}_n, \underline{e}_s, \underline{e}_b$ directions at s, denoted respectively by (u, v, w). First, the inner expansion for the normal velocity component due to the Stokeslet distribution is given using (3. 1. 14) and (3. 1. 16) by,

$$u_S^{(i)} \simeq (a_n^{(o)} + \epsilon\sigma a_n^{(1)} + \epsilon^2\sigma^2 a_n^{(2)}) \frac{1}{R^{(i)}} + (\underline{a} \cdot \underline{R})^{(i)}(\epsilon r_n^{(1)} + \epsilon^2\sigma^2 r_n^{(2)} + \epsilon^3\sigma^3 r_n^{(3)}) \frac{1}{R^{(i)3}} + O(\epsilon^2) \quad , \qquad (3.1.19)$$

where $R^{(i)}$ is given in (3. 1. 15) and

$$(\underline{a} \cdot \underline{R})^{(i)} = \epsilon(\sigma C_{11} + C_{10}) + \epsilon^2(\sigma^2 C_{22} + \sigma C_{21}) + \epsilon^3(\sigma^3 C_{33} + \sigma^2 C_{32}) + O(\epsilon^4) \quad , \tag{3. 1. 20}$$

$$C_{11} = a_s^{(o)} r_s^{(1)} \quad ,$$

$$C_{10} = a_n^{(o)} r_n^{(1)} + a_b^{(o)} r_b^{(1)} \quad ,$$

$$C_{22} = a_s^{(1)} r_s^{(1)} + a_n^{(o)} r_n^{(2)} \quad ,$$

$$C_{21} = a_n^{(1)} r_n^{(1)} + a_b^{(1)} r_b^{(1)} \quad ,$$

$$C_{33} = a_s^{(2)} r_s^{(1)} + a_n^{(1)} r_n^{(2)} + a_s^{(o)} r_s^{(3)} + a_n^{(o)} r_n^{(3)} + a_b^{(o)} r_n^{(3)} \quad ,$$

$$C_{32} = a_n^{(2)} r_n^{(1)} + a_b^{(2)} r_b^{(1)} \quad .$$

The outer expansion of the normal velocity component due to the Stokeslet, by using (3. 1. 8) and (3. 1. 11), is

$$u_S^{(o)} \simeq \frac{a_n(s')}{R^{(o)}} + (\underline{a} \cdot \underline{R})^{(o)} \frac{R_{on} - \epsilon\eta\cos\psi}{R^{(o)3}} \quad , \tag{3. 1. 21}$$

where

$$(\underline{a} \cdot \underline{R})^{(o)} = \underline{a} \cdot \underline{R}_o - a_n \epsilon\eta\cos\psi + a_b \epsilon\eta\sin\psi \quad ,$$

$$\frac{1}{R^{(o)}} = \frac{1}{R_o}\left\{1 + \frac{\epsilon\eta}{R_o^2}(R_{on}\cos\psi - R_{ob}\sin\psi) + O(\epsilon^2)\right\} \quad .$$

In the above, the vector components are expressed in terms of the unit vectors at s. The common part expansion is most easily obtained by taking the inner limit of the outer expansion. This

amounts to substituting into equation (3. 1. 21) the inner expansion for $\underline{a}$ and

$$\frac{1}{R_o^{(i)}} \simeq \frac{1}{|\epsilon\sigma|}\left(1 + \frac{\epsilon^2\sigma^2\kappa^2}{24} + O(\epsilon^3)\right) ,$$

$$R_{os}^{(i)} \simeq \epsilon\sigma r_s^{(1)} + \epsilon^3\sigma^3 r_s^{(3)} + O(\epsilon^4) , \qquad (3.1.22)$$

$$R_{on}^{(i)} \simeq \epsilon^2\sigma^2 r_n^{(2)} + \epsilon^3\sigma^3 r_n^{(3)} + O(\epsilon^4) ,$$

$$R_{ob}^{(i)} \simeq \epsilon^3\sigma^3 r_b^{(3)} + O(\epsilon^4) .$$

The inner expansion for the tangential velocity component, v , is readily obtained from (3. 1. 19) by replacing $a_n^{(k)}, r_n^{(1)}, r_n^{(2)}, r_n^{(3)}$ by $a_s^{(k)}, \sigma r_s^{(1)}, 0, r_s^{(3)}$ respectively and using (3. 1. 20). Similarly, the outer expansion is obtained from (3. 1. 21) by replacing a_n, R_{on} by a_s and R_{os} and omitting the term $\epsilon\eta\cos\psi$. The common part expansion is constructed in precisely the same manner using (3. 1. 22). Likewise, the inner and outer expansions for the binormal velocity component, w, are given by replacing $a_n^{(k)}, r_n^{(1)}, r_n^{(2)}, r_n^{(3)}$ in (3. 1. 19) by $a_b^{(k)}, r_b^{(1)}, 0, r_b^{(3)}$ respectively, and $a_n, R_{on} - \epsilon\eta\cos\psi$ in (3. 1. 21) by a_b and $R_{ob} + \epsilon\eta\sin\psi$, with the common part given by the inner limit of the outer expansion, using (3. 1. 22).

The uniformly valid integrand of the velocity is, as discussed in section 2. 1, given by

$$\underline{u}_S^{(c)} \simeq \underline{u}_S^{(i)} + \underline{u}_S^{(o)} - \underline{u}_S^{(oi)}$$

where $\underline{u}_S^{(oi)}$ represents the common part expansion. The actual expression for the above will not be presented here since it is rather lengthy and of no particular interest.

For the doublet distribution we observe that the outer expansion is of order β/R_o^3 where β is the nondimensional strength and $R_o = O(1)$ for the outer region, since we require that the centerline does not reapproach itself. Assuming a priori, as for the torus, that $O(\beta) = O(\epsilon^2 a)$ we can conclude that the contribution to the velocity field from the far field doublet distribution is of higher order and can be neglected. This assumption on the order of the doublet strength will of course be verified later. Furthermore the common part expansion is readily obtained from the inner limit of the outer expansion and is therefore also of order $\epsilon^2 a$. This can be checked by considering the outer limit of the inner expansion which is a more formidable task. Therefore we need only calculate the inner expansion of the doublet distribution. This is easily obtained by replacing $a_\nu^{(k)} (\nu = n, s, b)$, $\frac{1}{R^{(i)}}$ and $\frac{1}{R^{(i)3}}$ by $\beta_\nu^{(k)}$, $\frac{1}{R^{(i)3}}$ and $\frac{-3}{R^{(i)5}}$ respectively in the inner expansion of the Stokeslet distribution.

Our first approximation to the velocity field thus becomes,

$$\underline{u}(s, r_1, \psi) \tilde{=} \int_{-\sigma_1}^{\sigma_2} (\underline{U}_S^{(i)} + \underline{U}_D^{(i)}) \epsilon \, d\sigma + \int_{-s_1}^{s_1} (\underline{U}_S^{(o)} - \underline{U}_S^{(oi)}) ds' + O(\epsilon^2 a) ,$$

where

$$\sigma_1 = \frac{s_1 + s}{\epsilon} ,$$

$$\sigma_2 = \frac{s_1 - s}{\epsilon} .$$

Integrating the uniformly valid expansion and evaluating the resulting velocity on the body surface gives, using the integrals in Appendix B and neglecting terms of $O(\epsilon^2 \ln \epsilon a)$

$$u \tilde{=} 2(a_n^{(o)} L + \frac{B_n^{(o)}}{\epsilon^2}) - h_1(s)\cos\psi G(a_s, B_s) + h_2(s)\cos\psi F(\psi; a_n, a_b, B_n, B_b)$$

$$+ u_n^{(o)} + \epsilon\eta\cos\psi u^{(1)} + \epsilon\eta\sin\psi u^{(2)} , \qquad (3.1.23)$$

$$v \tilde{=} 4(a_s^{(o)} L - \frac{B_s^{(o)}}{\epsilon^2}) - h_2(s)G(a_s, B_s) - h_1(s)F(\psi; a_n, a_b, B_n, B_b)$$

$$+ u_s^{(o)} + \epsilon\eta\cos\psi v^{(1)} + \epsilon\eta\sin\psi v^{(2)}, \qquad (3.1.24)$$

$$w \tilde{=} 2(a_b^{(o)} L + \frac{B_b^{(o)}}{\epsilon^2}) + h_1(s)\sin\psi G(a_s, B_s) - h_2(s)\sin\psi F(\psi; a_n, a_b, B_n B_b)$$

$$+ u_b^{(o)} + \epsilon\eta\cos\psi w^{(1)} + \epsilon\eta\sin\psi w^{(2)} , \qquad (3.1.25)$$

where

$$L = \ln\frac{2}{\epsilon} ,$$

$$h_1(s) = 2\epsilon\eta \frac{s}{1-e^2 s^2} ,$$

$$h_2(s) = 2\frac{1-s^2}{1-e^2 s^2} ,$$

$$G(a_\nu, B_\nu) = a_\nu^{(o)} - \frac{2B_\nu^{(o)}}{\epsilon^2} \qquad (\nu = n, s, b) ,$$

$$F(\psi; a_n, a_b, B_n, B_b) = \cos\psi G(a_n, B_n) - \sin\psi G(a_b, B_b) .$$

The velocity terms $u_\nu^{(o)}$ $(\nu = n, s, b)$, $u^{(k)}, v^{(k)}$ and $w^{(k)}$ $(k = 1, 2)$ are given by

$$u_\nu^{(o)} = \int_{-s_1}^{s_1} K_\nu(\underline{R}_o; \underline{\alpha})ds' \quad , \qquad (\nu = n, s, b) \quad ,$$

$$u^{(1)} = (2\alpha_s^{(1)} + \kappa\,\alpha_n^{(o)})(L-1) - \frac{3B_n^{(o)}\kappa}{\epsilon^2} - \frac{2B_s^{(1)}}{\epsilon^2} - \cos^2\psi\kappa\, G(\alpha_n, B_n)$$

$$+ \int_{-s_1}^{s_1} K_n^{(1)}(\underline{R}_o;\underline{\alpha})ds' \quad ,$$

$$u^{(2)} = \alpha_b^{(o)}\kappa(1-L) + \frac{\kappa B_b^{(o)}}{\epsilon^2} + \cos^2\psi\,\kappa G(\alpha_b, B_b) + \int_{-s_1}^{s_1} K_{nb}^{(2)}(\underline{R}_o; \underline{\alpha})ds',$$

$$v^{(1)} = \alpha_s^{(o)}\kappa(5-4L) + 2\alpha_n^{(1)}(L-1) + \frac{2\kappa B_s^{(o)}}{\epsilon^2} - \frac{2B_n^{(1)}}{\epsilon^2} - \int_{-s_1}^{s_1} K_{sn}^{(2)}(\underline{R}_o;\underline{\alpha})ds',$$

$$v^{(2)} = 2\alpha_b^{(1)}(1-L) + \frac{2B_b^{(1)}}{\epsilon^2} + \int_{-s_1}^{s_1} K_{sb}^{(2)}(\underline{R}_o; \underline{\alpha})ds' \quad ,$$

$$w^{(1)} = \alpha_b^{(o)}\kappa(1-L) - \frac{\kappa B_b^{(o)}}{\epsilon^2} + \kappa\sin\psi F(\psi;\alpha_n, \alpha_b, B_n, B_b)$$

$$- \int_{-s_1}^{s_1} K_{bn}^{(2)}(\underline{R}_o;\underline{\alpha})ds' \quad ,$$

$$w^{(2)} = (2\alpha_s^{(1)} + \kappa\alpha_n^{(o)})(1-L) + \frac{2B_s^{(1)}}{\epsilon^2} + \frac{\kappa B_n^{(o)}}{\epsilon^2} + \int_{-s_1}^{s_1} K_b^{(1)}ds' \quad ,$$

where

$$K_\nu(\underline{R}_o;\underline{a}) = \frac{a_\nu(s',t)}{R_o} + \frac{(\underline{a}(s',t)\cdot\underline{R}_o)R_{o\nu}}{R_o^3} - \frac{D_\nu a_\nu(s,t)}{|s-s'|}$$

(ν = n, s, b , no sum on the subscript ν) (3. 1. 26)

$$D_n = D_b = 1 , \qquad D_s = 2,$$

$$K_\nu^{(1)} = \frac{\underline{a}\cdot\underline{R}_o}{R_o^3}\left(1 - \frac{3R_{o\nu}^2}{R_o^2}\right) + \frac{\xi}{|\xi|^3}\left[a_s^{(o)} + \xi\left(a_s^{(1)} + \frac{\kappa}{2}\, a_n^{(o)}\right)\right]$$

(ν = n, s, b)

$$K_{mp}^{(2)} = \frac{1}{R_o^3}\left(a_p R_{om} - R_{op}a_m - 3\frac{\underline{a}\cdot\underline{R}_o}{R_o^2}R_{op}R_{om}\right) + k_{mp}$$

(m, p = n, s, b) ,

$$k_{nb} = -k_{bn} = \frac{\kappa a_b^{(o)}}{2|s-s'|} ,$$

$$k_{sn} = -\frac{3\kappa a_s^{(o)}}{2|\xi|} + \frac{\xi}{|\xi|^3}\left[a_n^{(o)} + \xi\left(a_n^{(1)} - \frac{\kappa}{2}\, a_s^{(o)}\right)\right] ,$$

$$k_{sb} = \frac{\xi}{|\xi|^3}\left(a_b^{(o)} + \xi a_b^{(1)}\right) ,$$

$$\xi = s - s' .$$

The vector components in the above kernels are referred to the base vectors $\underline{e}_s$, $\underline{e}_n$, $\underline{e}_b$ at s where the boundary condition is to be satisfied.

We observe that equations (3. 1. 23), (3. 1. 24) and (3. 1. 25) are capable of satisfying the boundary conditions (equations 3. 1. 5) to the

lowest order, with an error of $O(a\epsilon \ln\epsilon)$, provided the nondimensionalized rotation, $\underline{\Omega}$, is of $O(1)$ or less. With this restriction the terms involving $\underline{\Omega}$ in the boundary condition become of order ϵ or smaller, and we take for all s

$$B_\nu^{(o)} = \frac{1}{2}\epsilon^2 a_\nu^{(o)} \qquad (\nu = n, s, b), \tag{3.1.27}$$

in order to eliminate the terms which depend on the angle ψ. We are then left with the following integral equation for $\underline{a}$, neglecting terms of $O(a\epsilon \ln\epsilon)$

$$V_\nu(s,t) = a_\nu(s,t)L_\nu + \int_{-s_1}^{s_1} K_\nu(\underline{R}_o;\underline{a})ds' \qquad (\nu = s, n, b) \tag{3.1.28}$$

(no sum over subscript ν) ,

where

$$L_s = 2(2L-1) \quad , \qquad L_n = L_b = 2L + 1$$

and

$K_\nu(\underline{R}_o;\underline{a})$ is given by (3.1.26).

A similar integral equation is found by Keller and Rubinow (1976) by using the method of matched asymptotic expansions. Further discussion of this equation will be given later.

We now proceed to satisfy the boundary condition to higher orders in ϵ. Following the procedure used in the torus solution we define the remaining terms in the boundary condition after neglecting the terms of $O(\epsilon^2 \ln\epsilon\, a)$ as

$$\hat{u} = \epsilon\eta[\cos\psi\ u^{(1)} + \sin\psi(u^{(2)} + \Omega_s)] \quad ,$$

$$\hat{u} = \epsilon\eta[\cos\psi\ (v^{(1)} - \Omega_b) + \sin\psi(v^{(2)} - \Omega_n)] \quad ,$$

$$\hat{w} = \epsilon\eta[\cos\psi\ (w^{(1)} + \Omega_s) + \sin\psi\ w^{(2)}] \quad ,$$

where $(\hat{u}, \hat{v}, \hat{w})$ are the velocity components in the direction of $(\underline{e}_n, \underline{e}_s, \underline{e}_b)$. Higher order singularities will be required to cancel the above residual velocities on the body surface so that the boundary condition is satisfied to a higher order.

We begin by considering the velocity components in the n-b or cross section plane of the body, i. e., $\hat{u}$ and $\hat{w}$. The components can be rewritten as

$$\hat{u} = \epsilon\eta[(-a+b)\cos\psi + (-c+d)\sin\psi] \quad ,$$

$$\hat{w} = \epsilon\eta[(a+b)\sin\psi + (c+d)\cos\psi] \quad ,$$

where

$$a = \frac{1}{2}(w^{(2)} - u^{(1)}) \quad ,$$

$$b = \frac{1}{2}(w^{(2)} + u^{(1)}) \quad ,$$

$$c = \frac{1}{2}(w^{(1)} - u^{(2)}) \quad ,$$

$$d = \frac{1}{2}(w^{(1)} + u^{(2)} + 2\Omega_s) \quad .$$

The terms are easily identified by combining velocities $\hat{u}$ and $\hat{w}$ and converting the base vectors from the $(\underline{e}_n, \underline{e}_b)$ system to the $(\underline{e}_{r_1}, \underline{e}_\psi)$ system. Thus we find

$$\hat{u}\underline{e}_n + \hat{w}\underline{e}_b = a\underline{e}_{r_1} - b(\cos 2\psi\, \underline{e}_{r_1} - \sin 2\psi\, \underline{e}_\psi)$$

$$+c(\sin 2\psi\, \underline{e}_{r_1} + \cos 2\psi\, \underline{e}_\psi) + d\underline{e}_\psi \qquad (3.1.29)$$

in which we have used

$$\underline{e}_n = -\cos\psi\, \underline{e}_{r_1} + \sin\psi\, \underline{e}_\psi$$

$$\underline{e}_b = \sin\psi\, \underline{e}_{r_1} + \cos\psi\, \underline{e}_\psi \ .$$

We now recognize the familiar terms that were encountered for the torus. The first term with coefficient a is a "radial-like" flow and can be corrected for by a source distribution. The last term in (3.1.29) is a "rotational-like" flow about the body centerline which will be eliminated by admitting a tangential rotlet distribution. The remaining two terms represent two separate "extensional-like" flows, with their principal axes subtending an angle of $\frac{\pi}{4}$. Each of these will be canceled by an appropriate stresslet-quadrupole pair.

The higher order tangential velocity term, $\hat{v}$, represents two "shear-like" flows in the $\underline{e}_s$ direction and can be adjusted to satisfy the boundary condition by introducing a rotlet oriented in the $\underline{e}_n$ and $\underline{e}_b$ direction.

We further note that if we only desire to satisfy the boundary conditions up to terms of $O(a\epsilon \ln\epsilon)$, with an error of $O(a\epsilon)$, then only a rotlet and source distribution is needed, since to this order, we have, by using (3.1.27),

$$u^{(1)} = -w^{(2)} = (2a_s' - \kappa a_n)\ln\frac{2}{\epsilon}$$

$$u^{(2)} = w^{(1)} = -a_b \kappa \ln\frac{2}{\epsilon}$$

and therefore $b = c = 0$. In practice, to satisfy the boundary condition to this order is a much easier task since the integrals in the terms $u^{(k)}$, $v^{(k)}$, and $w^{(k)}$ $(k = 1, 2)$ may be neglected.

The velocity field induced by the rotlet is given by

$$\underline{u}_R = \int_{-s_1}^{s_1} \underline{U}_R(\underline{R};\underline{\delta})ds$$

where $\underline{U}_R$ is given in (2. 1. 20) and the rotlet strength here is non-dimensionalized by $U\ell$. Based on the fact that for the torus the dimensional rotlet strength was found to be always proportional to $\frac{b^2}{a}$, where a was the torus radius, we shall assume that the rotlet strength here is given by

$$\underline{\delta}(s,t) = \epsilon^2(\delta_n(s,t)\underline{e}_n + \delta_s(s,t)\underline{e}_s + \delta_b(s,t)\underline{e}_b)(s_1^2 - s^2)$$

As will be verified later, $\delta_\nu(\nu = n, s, b)$ is of $O(a\ln\epsilon)$ and hence the outer and common part expansions will be of $O(a\epsilon^2\ln\epsilon)$ to leading order and can therefore be neglected. Thus the uniformly valid expansion consists, to the order retained here, of only the inner expansion. Substituting (3. 1. 14), (3. 1. 15) and the expansion for $\underline{\delta}(s', t)$ about $s'=s$ in the integral representation of $\underline{u}_R$ we find after integration and neglecting terms of $O(\delta\epsilon^2\ln\epsilon)$

$$u_R \tilde{=} -2\epsilon\eta \sin\psi\, \delta_s \ ,$$

$$v_R \tilde{=} 2\epsilon\eta(\cos\psi\delta_b + \sin\psi\, \delta_n) \ ,$$

$$w_R \tilde{=} -2\epsilon\eta \cos\psi\delta_s \ .$$

Thus we see that by incorporating the rotlet distribution into our solution the terms $\hat{v}$ and de_{ψ} are canceled by taking

$$\delta_s = \frac{1}{2} d = \frac{1}{4}(w^{(1)} + u^{(2)} + 2\Omega_s) \ ,$$

$$\delta_b = \frac{1}{2}(\Omega_b - v^{(1)}) \ , \qquad (3.1.30)$$

$$\delta_n = \frac{1}{2}(\Omega_n - v^{(2)}) \ .$$

In the case when the boundary condition is satisfied up to $O(a\epsilon \ln\epsilon)$ these results reduce to

$$\delta_s = \frac{1}{2}(\Omega_s - a_b \kappa \ln\frac{2}{\epsilon}) \ ,$$

$$\delta_b = \frac{1}{2}\Omega_b + (\kappa a_s - \tau a_b - a'_n)\ln\frac{2}{\epsilon} \ ,$$

$$\delta_n = \frac{1}{2}\Omega_n + (a'_b - \tau a_n)\ln\frac{2}{\epsilon} \ .$$

we further note that the assumption on the outer expansion is also verified since $\delta_\nu = O(a\ln\epsilon)$, $\nu = n, s, b$.

In precisely the same manner as was done for the rotlet, we conclude that the source strength is of the form

$$\hat{m} = m(s,t)\epsilon^2(s_1^2 - s^2) \ .$$

The contribution from this source distribution to the velocity field is due to the inner expansion of the integrand, since the outer and common part expansions are of higher order than retained here. Therefore after integration we find

$$\underline{u}_m \tilde{=} -2\epsilon\eta m(\cos\psi\,\underline{e}_n - \sin\psi\,\underline{e}_b) + O(m\epsilon^2 \ln\epsilon).$$

Accordingly, the radial-like flow term is canceled by taking

$$m = -\frac{1}{2}a = \frac{1}{4}(u^{(1)} - w^{(2)}) \quad . \tag{3.1.31}$$

The leading order term of this source strength is given by

$$m = \frac{1}{2}(2a'_s - \kappa a_n)\ln\frac{2}{\epsilon} \quad .$$

It remains only to eliminate the extensional-like flow terms. This can be accomplished by introducing two stresslet-quadrupole pairs with characteristic directions $(\underline{e}_n, \underline{e}_n)$ and $(\underline{e}_n, \underline{e}_b)$. Based on the torus solution, in which we found the stresslet strength to be proportional to $\frac{b^2}{a}$ and the quadrupole strength proportional to $\frac{b^4}{a}$, we assume the required strengths to be of the form

$$\hat{A}_k = A_k(s,t)\epsilon^2(s_1^2 - s^2) \quad ,$$

$$\hat{B}_k = B_k(s,t)\epsilon^4(s_1^2 - s^2)^2 \qquad (k = 1, 2) \quad ,$$

where $k = 1$ and 2, respectively for the characteristic directions $(\underline{e}_n, \underline{e}_n)$ and $(\underline{e}_n, \underline{e}_b)$. As has been explained, we neglect the outer and common part expansions of these two distributions since the

contributions to the velocity field will be of $O(a\epsilon^2)$ and $O(a\epsilon^4)$ for the stresslet and quadrupole, respectively.

The inner expansions of the integrands can be constructed as before making use of the expansions of the base vectors $\underline{e}_n(s')$ and $\underline{e}_b(s')$ about $s' = s$, which are

$$\underline{e}'_n = \underline{e}_n - \epsilon\sigma(\kappa \underline{e}_s + \tau \underline{e}_b) + O(\epsilon^2)$$

$$\underline{e}'_b = \underline{e}_b + \epsilon\sigma\tau \underline{e}_n + O(\epsilon^2)$$

where the primes indicate the unit vectors at s'. Upon integration you find, neglecting the term of $O(a\epsilon^2 \ln\epsilon)$,

$$u_{SS}(\underline{e}_n, \underline{e}_n) + u_Q(\underline{e}_n, \underline{e}_n) \tilde{=} -2\epsilon\eta\cos\psi[2B_1 + \cos 2\psi(A_1 - 4B_1)] ,$$

$$v_{SS}(\underline{e}_n, \underline{e}_n) + v_Q(\underline{e}_n, \underline{e}_n) \tilde{=} 0 ,$$

$$w_{SS}(\underline{e}_n, \underline{e}_n) + w_Q(\underline{e}_n, \underline{e}_n) \tilde{=} -2\epsilon\eta \sin\psi[2B_1 - \cos 2\psi(A_1 - 4B_1)] ,$$

and

$$u_{SS}(\underline{e}_n, \underline{e}_b) + u_Q(\underline{e}_n, \underline{e}_b) \tilde{=} 2\epsilon\eta \sin\psi[A_2 - 2B_2 + \cos 2\psi(A_2 - 4B_2)] ,$$

$$v_{SS}(\underline{e}_n, \underline{e}_b) + v_Q(\underline{e}_n, \underline{e}_b) \tilde{=} 0 ,$$

$$w_{SS}(\underline{e}_n, \underline{e}_b) + w_Q(\underline{e}_n, \underline{e}_b) \tilde{=} -2\epsilon\eta\cos\psi[A_2 - 2B_2 - \cos 2\psi(A_2 - 4B_2)].$$

Those two remaining terms in the boundary condition are now eliminated by taking

$$A_1 = b = \frac{1}{2}(w^{(2)} + u^{(1)}) \quad ,$$

$$A_2 = c = \frac{1}{2}(w^{(1)} - u^{(2)}) \quad , \qquad (3.1.32)$$

$$B_1 = \frac{1}{4} A_1 \quad ,$$

$$B_2 = \frac{1}{4} A_2 \quad .$$

As was anticipated in the torus case we see that the quadrupole strength is $\frac{1}{4}$ the stresslet strength. If we satisfy the boundary conditions only up to order $O(a\epsilon \ln\epsilon)$, we have

$$A_1 = A_2 = B_1 = B_2 = 0 \quad ,$$

i.e., no stresslet or quadrupole is needed as mentioned earlier.

3.2 Slender bodies with arbitrary circular cross sections

We now extend the previous analysis to the more general case for slender bodies having circular cross sections with arbitrary but slowly varying distribution of cross-sectional area

$$r_1 = \epsilon\eta(s) \quad , \qquad -1 \leqslant s \leqslant 1 \quad , \tag{3.2.1}$$

except we still require that the body has spheroidal ends, namely we require $\eta^2(s) \sim (1 - s^2)(1 + O(\epsilon^2))$ as $s \to \pm 1$. For this case, we construct separate expansions for the velocity field, one being valid for the center region away from the body ends (at $s = \pm 1$) and the other for the end regions with $s \sim \pm 1$. The Stokeslet strength assumes the same functional form as in the preceeding case, with its inner expansion given by (3.1.16). For the doublet distribution, however, we assume

$$\underline{\beta}(s,t) = \begin{cases} \underline{B}(s,t)\eta^2(s) & \text{(center region)} \\ \\ \underline{B}(s,t)(s_1^2 - s^2) & \text{(end regions)} \end{cases} \tag{3.2.2}$$

The inner expansion of the doublet strength is given by

$$\underline{\beta}(s',t) \sim \begin{cases} \underline{\beta}^{(o)} + \epsilon\sigma\underline{\beta}^{(1)} + O(\epsilon^2) & \text{(center region)} \\ \\ (\underline{B}^{(o)} + \epsilon\sigma\underline{B}^{(1)} + O(\epsilon^2))(s_1^2 - s'^2) & \text{(end regions)} \quad , \end{cases} \tag{3.2.3}$$

where in the end regions we find it convenient to use a two-variable expansion to account for the quadratic modulation, while in the center region this is unnecessary so we simply use a one-variable Taylor

series expansion. The explicit expressions for $\underline{\beta}^{(k)}$ and $\underline{B}^{(k)}$ $(k = 0, 1, 2)$ can be obtained directly from equation (3. 1. 17) by replacing $a_\nu(\nu = n, s, b)$ by $B_\nu \eta^2$ or by B_ν for the respective regions. In the end regions the inner and outer expansions for the Stokeslet and doublet distributions are therefore identical to those of section 3. 1, since the expansions of the strengths and cross-sectional shapes are the same. Consequently, we see that the velocity field in the neighborhood of each body end will be given by (3. 1. 23), (3. 1. 24) and (3. 1. 25). The boundary conditions in the end regions, by virtue of the spheroidal shape of the body ends, are therefore again given by equations (3. 1. 26) and (3. 1. 27) and hence are satisfied just as before. The expansions of the velocity field integrands in the center region are also similar to those of section 3. 1 except that $\underline{B}(s,t)(s_1^2 - s^2)$ must be replaced by $\underline{B}(s,t)\,\eta^2(s)$; with this change the integrands there will generally yield different results.

If we now use the integral table given in Appendix C for the present general case we find that the expansions for the velocity field valid in the center region are given by equations (3. 1. 23), (3. 1. 24) and (3. 1. 25) with the following changes

$$h_2(s) \to 2 \ ,$$

$$L \to \ln \frac{2(1-s^2)^{1/2}}{\epsilon \eta(s)} \ ,$$

$$h_1(s)\left(a_\nu^{(o)} - \frac{2B_\nu^{(o)}}{\epsilon^2}\right) \to 2\epsilon\eta(s)\left(\frac{s}{1-s^2}\, a_\nu^{(o)} + \frac{2B_\nu^{(o)}}{\epsilon^2}\, \frac{1}{\eta}\, \frac{\partial \eta}{\partial s}\right) \ ,$$

$$(\nu = n, s, b) \ . \qquad (3.2.4)$$

From this result we see that for the center region, after substituting the changes (3. 2. 4) in (3. 1. 23), (3. 1. 24) and (3. 1. 25), the boundary condition is satisfied, neglecting terms of $O(a\epsilon \ln\epsilon)$, by

$$B_\nu^{(o)} = \frac{1}{2}\epsilon^2 a_\nu^{(o)} \qquad (\nu = n, b) \ , \qquad (3.2.5)$$

and the solution for $\underline{a}$ from the integral equation (3. 1. 27) where L assumes the new expression given in (3. 2. 4). We note that in the center region the tangential doublet strength cannot be fully determined as yet. This term will be determined from the matching condition between the expansions of the velocities in the center and end regions. Namely, we must require the end limit of the center velocity expansion to equal the center limit of the end velocity expansion. In the end limit of the center expansion we have

$$\eta(s) \sim (1-s^2)^{1/2}\,(1 + O(\epsilon^2))$$

and therefore

$$\begin{aligned} &\frac{2(1-s^2)^{1/2}}{\eta(s)} \sim 2 + O(\epsilon^2) \ , \\ &\ln\frac{2(1-s^2)^{1/2}}{\epsilon\,\eta(s)} \sim \ln\frac{2}{\epsilon} + O(\epsilon^2) \ , \qquad (3.2.6) \\ &\frac{1}{\eta}\frac{\partial\eta}{\partial s} \sim \frac{-s}{1-s^2} + O(\epsilon^2) \ . \end{aligned}$$

From these expressions (equations 3. 2. 6) and the relations for the doublet strengths (3. 1. 27) and (3. 2. 5) we find that the leading order term and the terms $v^{(1)}, v^{(2)}, u^{(2)}, w^{(1)}$ of the center and end velocity expansions match completely. Matching of the remaining terms

namely $u^{(1)}$ and $w^{(2)}$, requires that

$$-\frac{\partial}{\partial s}\left(a_s - \frac{2B_s}{\epsilon^2}\right) + \frac{2s}{1-s^2}\left(1 + O(\epsilon^2)\right)\left(a_s - \frac{2B_s}{\epsilon^2}\right) = 0$$

and

$$\frac{2s}{1-s^2}\left(1 + O(\epsilon^2)\right)\left(a_s - \frac{2B_s}{\epsilon^2}\right) = 0 \ .$$

which are satisfied, as expected, by

$$B_s = \frac{1}{2}\epsilon^2 a_s \ .$$

The uniformly valid expansion of the velocity field near the body surface is

$$\underline{u} \sim \underline{u}_C + \underline{u}_E - (\underline{u}_C)_E \ ,$$

where $\underline{u}_C$, $\underline{u}_E$ and $(\underline{u}_C)_E$ represent, respectively, the center expansion, end expansion, and common part or end limit of the center expansion. Thus on the body surface $r_1 = \epsilon\eta(s)$ we have

$$u_\nu \tilde{=} a_\nu L_\nu + \int_{-s_1}^{s_1} K_\nu(\underline{R}_o;\underline{a})ds' + \epsilon\eta\cos\psi\, u_\nu^{(1)} + \epsilon\eta\sin\psi\, u_\nu^{(2)} \qquad (\nu = n, s, b) \qquad (3.2.7)$$

where $L_\nu (\nu = n, s, b)$ is given in equation (3.1.28) except now

$$L = \ln\frac{2(1-s^2)^{1/2}}{\epsilon\eta} \ ,$$

and

$$
\begin{aligned}
u_n^{(1)} &= a_s'(2L-3)-\kappa a_n(L-\tfrac{1}{2}) - 2a_s f(s) - \tilde{u}_n^{(1)} \quad , \\
u_n^{(2)} &= \kappa a_b(\tfrac{3}{2} - L) + \tilde{u}_n^{(2)} \quad , \\
u_s^{(1)} &= (a'_n - \kappa a_s + \tau a_b)(2L-3)-2a_n f(s) + \tilde{u}_s^{(1)} \quad , \\
u_s^{(2)} &= (a'_b - \tau a_n)(3-2L) + 2a_b f(s) - \tilde{u}_s^{(2)} \quad , \\
u_b^{(1)} &= \kappa a_b(\tfrac{1}{2} -L) + \tilde{u}_b^{(1)} \quad , \\
u_b^{(2)} &= (a'_s - \tfrac{\kappa}{2} a_n)(3-2L) + 2a_s f(s) + \tilde{u}_b^{(2)} \quad .
\end{aligned}
\tag{3.2.8}
$$

The terms $\tilde{u}_\nu^{(k)}$ ($\nu = n, s, b$; $k = 1, 2$) refer to the integral terms found in $u^{(k)}$, $v^{(k)}$, and $w^{(k)}$ of section 3.1 (see equations 3.1.23 - 3.1.25) and

$$
f(s) = \frac{s}{1-s^2} + \frac{1}{\eta}\frac{\partial \eta}{\partial s} \quad .
$$

These equations clearly reduce to those found for a body of spheroidal cross section when $\eta = (1-s^2)^{1/2}$.

We may further extend the solution to satisfy the boundary condition to higher orders in ϵ by including the near field distributions of the same higher order singularities as used before. Their strengths are given respectively for the center and end regions by

$$\hat{\delta}_\nu(s,t) = \begin{cases} \delta_\nu(s,t)\epsilon^2\eta^2(s) \\ \\ \delta_\nu(s,t)\epsilon^2(s_1^2 - s^2) \qquad (\nu = n, s, b) \end{cases},$$

$$\hat{m}(s,t) = \begin{cases} m(s,t)\epsilon^2\eta^2(s) \\ \\ m(s,t)\epsilon^2(s_1^2 - s^2) \end{cases},$$

$$\hat{A}_k(s,t) = \begin{cases} A_k(s,t)\epsilon^2\eta^2(s) \\ \\ A_k(s,t)\epsilon^2(s_1^2 - s^2) \qquad (k = 1, 2) \end{cases},$$

$$\hat{B}_k(s,t) = \begin{cases} B_k(s,t)\epsilon^4\eta^4 \\ \\ B_k(s,t)\epsilon^4(s_1^2 - s^2)^2 \qquad (k = 1, 2) \end{cases}.$$

The expansions of the velocity field, which are uniformly valid for all s, induced by these singularity distributions can be constructed here as in the previous case, yielding the same expressions for the velocity field near the body surface as were found for the higher order singularities in section 3.1, except here $\eta(s)$ need not be $(1-s^2)^{1/2}$. This should be expected since it is only the leading order term of these higher order singularities which generally contributes to the velocity field at the order required here. Therefore the results for the strengths $\delta_\nu(\nu = n, s, b), m, A_k$ and $B_k(k = 1, 2)$ are the same as given in section 3.1 by equations (3.1.30), (3.1.31) and (3.1.32)

except with $u^{(k)}$, $v^{(k)}, w^{(k)}$ $(k = 1, 2)$ respectively replaced by $u_n^{(k)}, u_s^{(k)}, u_b^{(k)}$ which are given in (3. 2. 8).

In summary, we have satisfied the boundary condition up to an error term of $O(\epsilon^2 \ln\epsilon)$ for the case of a body having an arbitrary distribution of circular cross sections over most of its length except for its spheroidal ends. The remaining task is to solve the set of simultaneous integral equations (3. 1. 27) for the Stokeslet strength and its counterpart for the more general case in which we have to replace $\ln \frac{2}{\epsilon}$ by $\ln[2(1-s^2)^{1/2}/\epsilon\eta]$ in (3. 1. 27). Once the Stokeslet strength is known we have also obtained the higher-order singularity strengths, since they are given in terms of the Stokeslet strength and its first derivative with respect to arc length.

We now conclude this section with a verification that the force/length exerted on the body is in fact $-8\pi\mu\underline{a}$. As was already mentioned in Chapter II, this result does not follow immediately from the method of singularities and therefore we include this calculation. In general, the total force is given by

$$\underline{F} = \int_{S_b} (-p\underline{n} + \tau\underline{n})dS \ ,$$

where $\underline{n}$ is the outward unit normal to the body surface S_b. For incompressible flows this may be written in terms of the vorticity $\underline{\omega}$ as

$$\underline{F} = \int_{S_b} (-p\underline{n} + \mu\underline{\omega} \times \underline{n})dS \ .$$

For bodies with circular cross sections considered here we have

$$\underline{n} = \frac{1}{(1+\epsilon^2\eta'^2)^{1/2}}(\underline{e}_{r_1} - \epsilon\eta'\,\underline{e}_s)$$

and

$$dS = b\ell\eta(1+\epsilon^2\eta'^2)^{1/2}\,(1+\epsilon\eta\kappa\cos\psi)d\psi\,ds\ ,$$

where

$$\eta' = \frac{\partial\eta}{\partial s}\ .$$

Defining the force/length, $\underline{f}$, as $\underline{F}/\ell ds$ (note s is dimensionless), we then have

$$\underline{f} = \int_0^{2\pi}(-p\underline{N} + \mu\underline{\omega}\times\underline{N})\,b(1+\epsilon\eta\kappa\cos\psi)d\psi\ , \qquad (3.2.9)$$

where

$$\underline{N} = \underline{n}\eta(1+\epsilon^2\eta'^2)^{1/2} = \eta\,\underline{e}_{r_1} - \epsilon\eta\eta'\,\underline{e}_s\ .$$

The pressure due to the various singularities was given in Chapter II, while the vorticity, after being nondimensionalized by U/ℓ, is

$$\underline{\omega}_S = \int_{-s_1}^{s_1}\frac{2\underline{a}\times\underline{R}}{R^3}\,ds'\ ,$$

$$\underline{\omega}_R = \int_{-s_1}^{s_1}\left(-\frac{\underline{\delta}}{R^3} + \frac{3(\underline{\delta}\cdot\underline{R})\underline{R}}{R^5}\right)ds'\ ,$$

$$\underline{\omega}_{SS} = \int_{-s_1}^{s_1}\frac{3[(\underline{\rho}_1\cdot\underline{R})\underline{\rho}_2 + (\underline{\rho}_2\cdot\underline{R})\underline{\rho}_1]\times\underline{R}}{R^5}\,ds'\ ,$$

$$\underline{\omega}_m = \underline{\omega}_D = \underline{\omega}_Q = 0.$$

We represent the total pressure and vorticity by

$$p = p_S + p_{SS} = \int_{-s_1}^{s_1} P\,ds' \quad ,$$

$$\underline{\omega} = \underline{\omega}_S + \underline{\omega}_R + \underline{\omega}_{SS} = \int_{-s_1}^{s_1} \underline{\zeta}\,ds' \quad .$$

The analysis is conveniently carried out by substituting the above expressions into (3. 2. 9) and then interchanging the order of integration to take advantage of the fact that many of the terms dependent on ψ will integrate to zero. We will calculate $\underline{f}$, neglecting terms of order ϵ^2, by constructing the uniformly valid expansions for P and $\underline{\zeta}$ precisely as has been done before for the velocity fields. As already explained, to the order of accuracy desired here, only the Stokeslet pressure and vorticity has an outer expansion which must be retained. The outer expansions, now given in dimensional form up to an error term of $O(a\epsilon^2)$, are found as

$$\hat{\underline{P}}_S^{(o)} \tilde{=} 2\mu U \epsilon \eta \frac{\underline{a} \cdot \underline{R}_o}{R_o^3} (\sin\psi\, \underline{e}_b - \cos\psi\, \underline{e}_n) \quad ,$$

$$\hat{\underline{\zeta}}_S^{(o)} \tilde{=} 2\mu U \epsilon \eta \frac{\underline{a} \times \underline{R}_o}{R_o^3} \times (\sin\psi\, \underline{e}_b - \cos\psi\, \underline{e}_n) \quad ,$$

where

$$\hat{\underline{P}} = UP\underline{N}\epsilon(1 + \epsilon\eta\kappa\cos\psi) \quad ,$$

$$\hat{\underline{\zeta}} = \mu U \underline{\zeta} \times \underline{N}\epsilon(1 + \epsilon\eta\kappa\cos\psi) \quad .$$

We also note that the common-part expansions, which are given by the inner limit of the outer expansion, will have the same ψ dependence. It is thus clear that upon integration with respect to ψ these terms will vanish. Thus it remains only to examine the contribution of the inner expansion. The inner expansions of the pressure and vorticity due to the Stokeslet distribution are, leaving out an error of $O(a\epsilon^2)$,

$$\hat{P}_S^{(i)} \simeq 2\mu U\epsilon\eta \frac{(\underline{a}\cdot\underline{R})^{(i)}}{R^{(i)3}}(1+\epsilon\eta\kappa\cos\psi)(\sin\psi\,\underline{e}_b - \cos\psi\,\underline{e}_n - \epsilon\eta'\underline{e}_s) ,$$

$$\hat{\underline{\zeta}}_S^{(i)} \simeq 2\mu U\epsilon\eta\{(a_bR_n - a_nR_b)(\cos\psi\,\underline{e}_b + \sin\psi\,\underline{e}_n) +$$

$$+ (a_bR_s - a_sR_b)(\sin\psi\,\underline{e}_s + \epsilon\eta'\underline{e}_b) + (a_sR_n - a_nR_s)(\cos\psi\,\underline{e}_s$$

$$- \epsilon\eta'\underline{e}_n)\}\frac{1+\epsilon\eta\kappa\cos\psi}{R^{(i)3}} ,$$

where

$$a_pR_m - a_mR_p \simeq \epsilon(a_p^{(o)}\hat{r}_m^{(1)} - a_m^{(o)}\hat{r}_p^{(1)}) + \epsilon^2(a_p^{(1)}\hat{r}_m^{(1)}\sigma - a_m^{(1)}\hat{r}_p^{(1)}\sigma$$

$$+ a_p^{(o)}\hat{r}_m^{(2)} - a_m^{(o)}\hat{r}_p^{(2)}) + \epsilon^3(a_p^{(2)}\hat{r}_m^{(1)}\sigma^2 - a_m^{(2)}\hat{r}_p^{(1)}\sigma^2$$

$$+ a_p^{(1)}\hat{r}_m^{(2)}\sigma - a_m^{(1)}\hat{r}_p^{(2)}\sigma + a_p^{(o)}\hat{r}_m^{(3)} - a_m^{(o)}\hat{r}_p^{(3)}) + O(\epsilon^4) ,$$

$$(p = n, s, b;\ m = n, s, b;\ p \neq m)$$

and

$$\hat{r}_s^{(1)} = \sigma r_s^{(1)}, \quad \hat{r}_\nu^{(1)} = r_\nu^{(1)} \qquad (\nu = n, b) \quad ,$$

$$\hat{r}_n^{(2)} = \sigma^2 r_n^{(2)}, \quad \hat{r}_\nu^{(2)} = 0 \qquad (\nu = s, b) \quad ,$$

$$\hat{r}_\nu^{(3)} = \sigma^3 r_\nu^{(3)} \qquad (\nu = n, s, b) \quad .$$

Integrating these two inner expansions with respect to ψ and then with respect to s' gives the expected result,

$$\underline{f}_S = -8\pi\mu\underline{a} \quad . \tag{3.2.10}$$

where here $\underline{a}$ is taken as the dimensional Stokeslet strength. This will be the total force/length within an error of $O(\epsilon^2)$ provided the higher order singularities have no contribution up to this order.

The contribution from the rotlet distribution is due to its vorticity which has an inner expansion

$$\hat{\underline{\zeta}}_R^{(i)} \simeq \epsilon^3 \mu U g(s) \left[-(\underline{\delta} \times \underline{N}) + \frac{3(\underline{\delta} \cdot \underline{R})(\underline{R} \times \underline{N})}{R^2} \right]^{(i)} \frac{1 + \epsilon\eta\kappa\cos\psi}{R^{(i)3}} \quad ,$$

where the rotlet strength is given by $\epsilon^2 \delta g(s)$, $g(s)$ being $\eta^2(s)$ or $(s_1^2 - s^2)$ as is appropriate for the center or end regions, and $(\underline{\delta} \cdot \underline{R})^{(i)}$ is given in (3.1.20) with $a_\nu^{(k)}$ replaced by $\delta_\nu^{(k)}$. We also have

$$\underline{G} \times \underline{N} = \eta\{(G_n \sin\psi + G_b \cos\psi)\underline{e}_s - (G_s \sin\psi + \epsilon\eta' G_b)\underline{e}_n$$

$$-(G_s \cos\psi - \epsilon\eta' G_n)\underline{e}_b\} \quad ,$$

$\underline{G}$ being $\underline{\delta}^{(i)}$ or $\underline{R}^{(i)}$ as the case may be. Integrating the expression for $\hat{\underline{\zeta}}_R^{(i)}$ with respect to ψ gives a nonzero result, however, the

subsequent integration over s' gives zero, after neglecting terms of $O(\epsilon^2)$. Therefore the contribution to the force/length by the rotlet distribution, at the order of interest here, is zero.

Similarly, by constructing the expressions for the pressure and vorticity due to the stresslets with characteristic directions $(\underline{e}_n, \underline{e}_n)$ and $(\underline{e}_n, \underline{e}_b)$ and then integrating those expressions with respect to ψ and s', we find no contribution from them to the same order of approximation as specified. The details of this calculation will be curtailed here since they are quite lengthy and identical to what we have done above. Therefore we have, in fact, verified that equation (3. 2. 10) is the force/length if we neglect the terms of $O(\epsilon^2)$.

3. 3 Application to the partial torus

In order to elucidate the combined effects of centerline curvature and the body ends we shall seek in this section the solution of the integral equations for $\underline{a}$ for a partial torus, that is a segment of a torus. The equation for this case, to be repeated here for convenience, is given by

$$V_\nu(s,t) = a_\nu(s,t)L_\nu + \int_{-s_1}^{s_1} K_\nu(\underline{R}_o;\underline{a})ds' \qquad (\nu = s,n,b) \ , \tag{3. 3. 1}$$

where

$$L_s = 2(2L - 1) \ , \qquad L_n = L_b = 2L + 1 \ ,$$

$$L = \ln\frac{2(1 - s^2)^{1/2}}{\epsilon\eta} \ ,$$

$$K_\nu(\underline{R}_o;\underline{a}) = \frac{a_\nu(s',t)}{R_o} + \frac{\underline{a}(s',t)\cdot\underline{R}_o)R_{o\nu}}{R_o^3} - \frac{D_\nu a_\nu(s,t)}{|s-s'|} \quad ,$$

$$\underline{R}_o = \underline{x}_o(s,t) - \underline{x}_o(s',t) = R_{os}\underline{e}_s + R_{on}\underline{e}_n + R_{ob}\underline{e}_b \quad ,$$

$$\underline{a}(s',t) = a_s\underline{e}_s + a_n\underline{e}_n + a_b\underline{e}_b \quad .$$

Here we recall that the base vectors $\underline{e}_s, \underline{e}_n, \underline{e}_b$ in the above expression assume their values at s where $V_\nu(s,t)$ is specified.

Some general observations can be made concerning these equations. For bodies with a planar centerline, i.e., bodies for which $\underline{e}_n, \underline{e}_s$ lie in the same plane for all s and $\tau = 0$, we see that $R_{ob} = 0$ and thus the integral equation for a_b separates from the equations for a_s and a_n. Thus, if $V_b = 0$ we have the trivial solution $a_b = 0$, and we are left with two coupled integral equations for a_n, and a_s. Furthermore, if $V_n = V_s = 0$ but $V_b \neq 0$, we have the trivial solution $a_n = a_s = 0$ and have simply one integral equation for a_b. For the torus problem of Chapter II the integral equation (3.3.1) holds valid if s_1 is taken to be π, s replaced by θ, and $L = \ln\frac{2}{\epsilon}$. In that particular case we have, in fact, solved analytically the integral equation. When examining bodies of other shapes and with ends, it is generally necessary to resort to approximate numerical techniques.

One rather obvious procedure is to use the iteration scheme defined by

$$a_\nu^{(k+1)}(s,t) = \frac{1}{L_\nu}\{V_\nu(s,t) - \int_{-s_1}^{s_1} K_\nu(\underline{R}_o; a^{(k)}(s',t))ds'\}$$

$$(k = 0, 1, 2, \ldots) \quad , \qquad (3.3.2)$$

where $\underline{a}^{(k)}$ is the kth iterate of $\underline{a}$. With the initial guess $\underline{a}^{(o)} = 0$ we see that $\underline{a}^{(1)}$ gives the familiar result for a straight, slender spheroid. We may thus expect that in higher-order iterations the integral in (3.3.2) will provide increasingly improved corrections to the solution sought for the actual body shape and motion. This iteration scheme generates an expansion for a_ν in a series of $(\frac{1}{L_\nu})^n$, with an error in the kth iterate being of order $(\frac{1}{L_\nu})^{k+1}$. The expansion here is of a somewhat more general nature than the expansions in terms of $(\frac{1}{\ln\epsilon})^n$ given by Cox (1970) and a similar iteration procedure proposed by Keller & Rubinow (1976). In fact, if we have the same number of terms in the two expansions we must neglect certain terms in the expansion found from (3.3.2) to obtain the expansion in terms of $(\frac{1}{\ln\epsilon})^n$. This suggests that the expansions in terms of $(\frac{1}{L_\nu})^n$ may be more accurate than those introduced by Cox or Keller & Rubinow. We will illustrate this point shortly when we examine some simple examples.

Although the iteration method given by (3.3.2) seems reasonable, the kth iterate has an error of $O(\frac{1}{L_\nu})^{k+1}$ and therefore the sequence is slowly convergent. Accordingly, many iterates may often be needed to obtain accurate results. Also we see that it is impossible with this method to take full advantage of the true accuracy of $\underline{a}$

inherent in the original integral equation, which theoretically determines $\underline{a}$ up to an error of $O(\epsilon^2)$. For this reason we introduce what will be referred to as the direct computation method to be used here and in the following chapter. This procedure involves replacing the integrals in equation (3. 3. 1) by a sum, using a convenient quadrature formula, thus giving a set of linear equations. Here a quadratic quadrature fomula has been employed to approximate the integral in equation (3. 3. 1) and from the many direct and indirect methods available for solving linear systems we have chosen to use the Gaussian elimination procedure with iterative improvement as discussed by Isaacson & Keller (1966). We should note that the original integral equation which results from the singularity method is a Fredholm equation of the first kind and as such is generally quite difficult to solve numerically, however, the expansions performed on the integrands have allowed us to single out part of the integral, i. e., the term $a_\nu L_\nu$, and we find that this modified Fredholm integral equation of the first kind is successfully solved by the above mentioned procedure.

A useful example to clarify the iteration procedure prescribed by (3. 3. 2) is to consider the translation of a closed torus along its longitudinal axis. As already mentioned (3. 3. 1) also holds for the closed torus provided we take the integration limits to be $-\pi$ and π. For this case $V_n = V_s = O$, $V_b = 1$, and therefore $a_n = a_s = O$. We then have,

$$a_b^{(1)} = \frac{1}{L_b} ,$$

$$a_b^{(2)} = a_b^{(1)} - \frac{1}{L_b^2} \int_{-\pi}^{\pi} \{ \frac{1}{|2 \sin \frac{\varphi}{2}|} - \frac{1}{|\varphi|} \} d\varphi$$

$$= a_b^{(1)} + \frac{2 \ln \pi/4}{L_b^2} ,$$

and similarly for the higher-order iterates. Therefore it is easy to see that the kth iterate is given by

$$a_b^{(k)} = \frac{1}{L_b} \sum_{n=o}^{k} (\frac{2\ln \pi/4}{L_b})^n .$$

Now recalling the exact solution found in section 2. 1, we have

$$\frac{a}{U} = \frac{1}{2(\ln 8 \frac{a}{b} + \frac{1}{2})} = \frac{1}{L_b(1 - \frac{2\ln \pi/4}{L_b})} = \frac{1}{L_b} \sum_{n=o}^{\infty} (\frac{2\ln \pi/4}{L_b})^n ,$$

which is precisely the limit of infinite iterations using the previous approximate solution technique.

We can also easily obtain the second iterate for the similar translation of a partial spheroidal torus, i. e., a body with a spheroidal cross section and a centerline given in polar corrdinates by r = a. For this case

$$a_b^{(2)} = \frac{1}{L_b} \{1 - \frac{1}{L_b} \int_{-(\theta_1+\theta)}^{\theta_1-\theta} [\frac{1}{|2 \sin \frac{\varphi}{2}|} - \frac{1}{|\varphi|}] d\varphi \} ,$$

where $\theta_1 = e\theta_o$, $\theta_o a$ being the body half length ℓ. Upon integration,

$$a_b^{(2)} = \frac{1}{L_b} - \frac{F_2}{L_b^2} + O(\frac{1}{L_b})^3 \quad , \qquad (3.3.3)$$

where

$$F_2 = \ln\left(\frac{16}{\varphi_1\varphi_2} \tan\frac{\varphi_1}{4} \tan\frac{\varphi_2}{4}\right) \quad ,$$

$$\varphi_1 = \theta_1 + \theta \quad ,$$

$$\varphi_2 = \theta_1 - \theta \quad .$$

The equivalent expansion in terms of $(\frac{1}{\ln\epsilon})^3$ is

$$a_b \sim \frac{-1}{2\ln\epsilon} - \frac{2\ln 2 + 1 + F_2}{(2\ln\epsilon)^2} + O(\frac{1}{\ln\epsilon})^3 \qquad (3.3.4)$$

A comparison of the results from (3.3.3) and (3.3.4) given in figure (3.3.2) for two typical cases shows that they differ by approximately 40%. However, if we compare the result from the expansion in terms of $(\frac{1}{L_b})^n$ (equation 3.3.3) with the solution obtained from the direct numerical solution method, we find that they differ by less than 1% and are essentially indistinguishable in figure (3.3.2). Apparently the terms $\frac{1}{L_b}$ have summed an infinite number of terms, in a way similar to that found for Padé approximants, to produce a result more accurate than is indicated by the error term. For this simple case the accuracy is rather dramatic and we should note that for more complex body centerlines and motions we find that it is overly optimistic to expect this method to have such a high degree of accuracy with so few iterates.

An example which will allow us to compare the present theory with that of Cox's, in which the end effects are neglected, is the translation of a partial spheroidal torus in its own plane. The no-slip boundary condition in dimensional form, namely $\underline{u} = U\underline{e}_x$ on $r_1 = \eta$, gives

$$V_n = d_1 \sin\theta - d_2 \cos\theta \quad ,$$

$$V_s = -d_1 \cos\theta - d_2 \sin\theta \quad ,$$

$$V_b = 0,$$

where $d_1 = \sin\theta_i$, $d_2 = \cos\theta_i$, θ_i being the angle between $\underline{e}_x$ and the unit radial vector at the midpoint of the body, i.e., $\theta = 0$ (see figure 3.3.1). Here, $\underline{e}_r = -\underline{e}_n$ since we have taken the curvature, κ, to be positive. As discussed earlier, we have $a_b = 0$ and the first iterates for a_n and a_s become

$$a_n^{(1)}(\theta') = (V_n(\theta)\cos\varphi - V_s(\theta)\sin\varphi)\frac{1}{L_n} \quad ,$$

$$a_s^{(1)}(\theta') = (V_s(\theta)\cos\varphi + V_n(\theta)\sin\varphi)\frac{1}{L_s} \quad ,$$

$$\varphi = \theta' - \theta \quad .$$

The second iterates are given by

$$a_n^{(2)}(\theta) = \frac{V_n(\theta)}{L_n} - \frac{F_n(\theta)}{L_n^2} + O(\frac{1}{L_n})^3 \quad ,$$

$$a_s^{(2)}(\theta) = \frac{V_s(\theta)}{L_s} - \frac{F_s(\theta)}{L_s^2} + O(\frac{1}{L_s})^3 \quad , \qquad (3.3.5)$$

where

$$F_n(\theta) = \int_{-\varphi_1}^{\varphi_2} \{L_n[\alpha_n^{(1)}(\theta')(3\cos\varphi - 1) + 3\alpha_s^{(1)}(\theta')\sin\varphi] \frac{1}{|4\sin\frac{\varphi}{2}|} - \frac{V_n(\theta)}{|\varphi|}\} d\varphi,$$

$$F_s(\theta) = \int_{-\varphi_1}^{\varphi_2} \{L_s[\alpha_s^{(1)}(\theta')(3\cos\varphi + 1) - 3\alpha_n^{(1)}(\theta')\sin\varphi] \frac{1}{|4\sin\frac{\varphi}{2}|} - \frac{2V_s}{|\varphi|}\} d\varphi,$$

$$\varphi_1 = \theta_1 + \theta, \quad \varphi_2 = \theta_1 - \theta.$$

Carrying out the integrals for F_n and F_s yield

$$F_n(\theta) = V_n(\theta)k_1(\theta) - V_s(\theta)k_2(\theta),$$

$$F_s(\theta) = V_n(\theta)k_3(\theta) + V_s(\theta)k_4(\theta),$$

where

$$k_1(\theta) = A + a(1 - 3\mathcal{L}) + c(1 - \mathcal{L}) - 2(1 - 2\mathcal{L}),$$

$$k_2(\theta) = b(1 - 3\mathcal{L}) + d(1 - \mathcal{L}),$$

$$k_3(\theta) = b(5 - \mathcal{L}^{-1}) + d(1 - \mathcal{L}^{-1}),$$

$$k_4(\theta) = 2A + a(5 - 3\mathcal{L}^{-1}) + c(1 - \mathcal{L}^{-1}) - 2(3 - 2\mathcal{L}^{-1}),$$

and

$$\mathcal{L} = \frac{L_n}{L_s},$$

$$a = \cos\frac{\theta_1}{2}\cos\frac{\theta}{2},$$

$$b = -\cos\frac{\theta_1}{2}\sin\frac{\theta}{2},$$

$$c = \cos\frac{3\theta_1}{2}\cos\frac{3\theta}{2},$$

$$d = -\cos^2\frac{3\theta_1}{2}\sin\frac{3\theta}{2} ,$$

$$A = \ln\left(\frac{16}{\varphi_1\varphi_2}\tan\frac{\varphi_1}{4}\tan\frac{\varphi_2}{4}\right) .$$

In order to compare the present result with that of Cox for the force/length in the x-direction we again need to further approximate expression (3. 3. 5) by neglecting the terms of $O(\frac{1}{\ln\epsilon})^3$, giving

$$a_n^{(2)} \sim -\frac{V_n}{2\ln\epsilon} - \frac{1}{(2\ln\epsilon)^2}(V_n g_1 - V_s g_2) ,$$

$$a_s^{(2)} \sim -\frac{V_s}{2\ln\epsilon} - \frac{1}{(4\ln\epsilon)^2}(V_n g_3 + V_s g_4) ,$$

$$g_1 = A + 2\ln 2 + 1 + \frac{1}{2}(c-a) ,$$

$$g_2 = \frac{1}{2}(d-b) , \qquad (3. 3. 6)$$

$$g_3 = -b-d ,$$

$$g_4 = 2A + 4\ln 2 - a - c .$$

In figure (3. 3. 3) we compare the Stokeslet strengths given by the two expansions (3. 3. 5) and (3. 3. 6) with the results computed by the direct numerical method for a hemi-torus with $\theta_o = \pi/2$, $\theta_i = 0$, $\epsilon = 0.1$. As we have already noted, the generalized expansion in terms of $(\frac{1}{L_\nu})^n$, $\nu = n, s$, yields results in closer agreement with those found by the direct numerical method. We note, however, that the difference

between the results of the two expansions here is not nearly as large as we found in the previous case (figure 3. 3. 2).

The present result for a_x to be compared with that of Cox (1970) is given by

$$a_x = -a_n \cos(\theta + \theta_i) - a_s \sin(\theta + \theta_i) \ .$$

Substituting (3. 3. 6) into the above expression gives

$$a_x = \frac{1}{4\ln\epsilon}(\sin^2\bar{\theta}-2) - \frac{1}{4\ln^2\epsilon}\{(1 - \frac{1}{2}\sin^2\bar{\theta})[A+2\ln 2+1 - \frac{1}{2}(a-c)]$$

$$- \frac{1}{4}\cos\bar{\theta}\sin\bar{\theta}(3d-b) - \frac{1}{2}\sin^2\bar{\theta}(1+c)\} \ , \qquad (3.3.7)$$

where $\bar{\theta} = \theta + \theta_i$.

The expression (3. 3. 7) is found to agree with that given by Cox if we further expand the present (uniformly valid) solution for points away from the body ends. This amounts to substituting the following approximation for A into (3. 3. 7),

$$A = \ln(16 \tan\frac{\varphi_1}{4}\tan\frac{\varphi_2}{4}) - \ln(\theta_1^2 - \theta^2)$$

$$= \ln(16 \tan\frac{\varphi_1}{4}\tan\frac{\varphi_2}{4}) - \ln(\theta_o^2 - \theta^2)(1 - \frac{\epsilon^2\theta_o^2}{\theta_o^2-\theta^2})$$

$$\sim \ln(16 \tan\frac{\varphi_1}{4}\tan\frac{\varphi_2}{4}) - \ln\eta^2 + O(\frac{\epsilon^2}{\theta_o^2-\theta^2}) \ .$$

Thus we see that the error given by Cox as being of $O(\frac{1}{\ln\epsilon})^3$ is not uniformly valid since at the ends it is actually of $O(\frac{1}{\ln\epsilon})^2$. Although the region over which this error exists is small, it is necessary to

take an accurate account of it as has been done here, in order to satisfy the boundary condition to higher orders in ϵ.

It is instructive to examine the solution for the planar translation of a partial torus obtained by using the accurate direct numerical method. In figures (3. 3. 4 - 3. 3. 8) some typical results for the force/length in the radial and tangential directions of several representative cases are compared with the classical resistive force theory which is based on the following (generally approximate) relations,

$$f_r = \mu C_n V_n, \qquad f_\theta = \mu C_s V_s \tag{3. 3. 8}$$

where

$$C_n = -\frac{8\pi}{L_n}, \qquad C_s = \frac{8\pi}{L_s},$$

C_n and C_s being the coefficients for a straight slender spheroid. As may be expected, for very small ϵ the results are reasonably good while for moderately small values the error becomes significant. We also see that the error is often largest near the body ends. From these examples it might appear that (3. 3. 8) would be a good approximation to the force/length for slender bodies in general, however, for bodies with more complex centerline motions, as in the case of finite-amplitude flagellar undulations, equations (3. 3. 8) are rather poor approximations even for very small values of ϵ, as we shall see later.

Figures (3. 3. 9) and (3. 3. 10) give an indication of the long range effect present in low-Reynolds-number flows. In these figures

we have a comparison of the force/length for a half torus (extending from $\theta = -\pi/2$ to $\pi/2$) with that of a quarter torus which has its centerline coinciding with the half torus for $\theta = 0$ to $\pi/2$. Although the qualitative behavior of the solution does not change, we see that neglecting the contribution from the far-field distribution can result in a considerable error. This suggests that if results of high accuracy are required, it would be insufficient to approximate a given slender body by superposing segments of bodies of specified local shape, since the present results have shown that the force densities at the corresponding points on these body segments are appreciably different from those in the actual case. Therefore the class of hydromechanical models of flagellum based on representing a finite flagellum by a segment of an infinitely long flagellum in determining the hydromechanical forces and moments, such as that adopted by Shen, J. S., et al, (1975), should be examined with scrutiny.

IV. FLAGELLAR HYDRODYNAMICS

4.1 Finite amplitude planar motion of a flagellum

We now apply the theory developed in the previous chapters to the finite-amplitude motion of a flagellum. The undulatory motion of a flagellum is modeled by a slender spheroidal body whose centerline is in a coordinate frame translating with the propulsive velocity of the organism $-U\underline{e}_x$, given in dimensional form by

$$\underline{x}_o = (x(s,t), -a\cos(ks - f(t)), 0) \qquad -\ell \leqslant s \leqslant \ell \ , \tag{4.1.1}$$

where k is the wave number $2\pi/\Lambda$, Λ being the wave length measured along the centerline and $f(t)$ is at this point an arbitrary function of time. The coordinate frame is chosen so that $x(-\ell, t) = 0$. This particular description, i.e., (4.1.1), is chosen since it is a fairly good representation of the observed waveforms of many spermatozoa and its parametric form is particularly convenient for calculating the positions and velocities of material points on the body centerline. The inextensibility condition (3.1.2) can be written as

$$\frac{\partial x}{\partial s} = \sqrt{1 - a^2k^2\sin^2(ks - f(t))} \ , \tag{4.1.2}$$

and therefore

$$x(s,t) = \int_{-k\ell - f}^{ks - f} \frac{1}{k}\sqrt{1 - a^2k^2\sin^2\zeta}\ d\zeta \ ,$$

$$kx(s,t) = E(ks - f/a^2k^2) + E(k\ell + f/a^2k^2) \ , \tag{4.1.3}$$

where E represents an elliptic integral of the second kind.

The velocity of a material point on the body centerline with respect to the laboratory or absolute frame is

$$\underline{V} = (-U + \frac{dx}{dt})\,\underline{e}_x + \frac{dy}{dt}\,\underline{e}_y \quad ,$$

where $y = -a\cos(ks - f(t))$. We note that a more general description of an actual micro-organism motion might include an additional y component of velocity and a pitching of the x axis. For rectilinear locomotion of a self-propelling flagellate, however, both the above motions are expected to be small.

The dimensional centerline velocity can be written in terms of the base vectors $\underline{e}_s, \underline{e}_n, \underline{e}_b$ as

$$\begin{aligned} V_s &= (C-U)x_{,s} - c \\ V_n &= (U-C)y_{,s} \\ V_b &= 0 \end{aligned} \qquad (4.1.4)$$

where we have taken $\underline{e}_n = (-y_{,s},\ x_{,s},\ 0)$, and we have

$$\begin{aligned} C &= c(t)\ \sqrt{1 - a^2k^2\sin^2(k\ell + f)} \\ c(t) &= \dot{f}(t)/k \\ y_{,s} &= \partial y/\partial s = ak\sin(ks - f) \end{aligned} \qquad (4.1.5)$$

with $x_{,s} = \partial x/\partial s$ given by (4.1.2) and $\dot{f} = \frac{df}{dt}$. Recalling the original definition of $\underline{e}_n$ (equation 3.1.3), we see that taking $\underline{e}_n$ as given above requires κ to be positive or negative according as y is negative or positive. We note that C is the wave speed in the x-direction with respect to the translating x, y frame, while c is

the velocity with which the wave propagates along the arc length. For the purpose of comparison between various theories we require C to be constant. Therefore we take

$$\frac{df}{dt} = \frac{Ck}{\sqrt{1-a^2k^2\sin^2(k\ell + f)}} \qquad (4.1.6)$$

and for convenience $f(0) = 0$. This equation is easily solved for $f(t)$ with given data by using any of the numerical schemes available, such as the method of Runge-Kutta. For a few of the special cases to follow we also briefly considered $f(t) = \omega t$, i.e., c = constant and C = C(t), and found that the qualitative behavior of the solutions for the force/length is similar to the behavior of those solutions corresponding to (4.1.6). The accuracy of the data available at present actually precludes a definite conclusion as to which of the above choices for C is more accurate and therefore we make use of the more common choice, namely C = constant.

One restriction on our geometry arises from condition (4.1.2) which requires that $ak \leqslant 1$. Now integrating (4.1.2) from $x = 0$ to λ, where λ is the wavelength measured along the x-axis, we obtain for $t = 0$

$$\lambda = \int_{-\ell}^{-\ell+\Lambda} \sqrt{1 - y^2_{,s}}\, ds$$

$$= \frac{1}{k}\{E(k(\Lambda-\ell)/a^2k^2) + E(k\ell/a^2k^2)\}$$

$$= \frac{1}{k} E(2\pi/a^2k^2) = \frac{4}{k}\tilde{E}(a^2k^2) , \qquad (4.1.7)$$

where $\tilde{E}(a^2k^2)$ denotes the complete elliptic integral of the second kind. From (4. 1. 7) it follows that

$$\frac{a}{\lambda} = \frac{ak}{4\tilde{E}(a^2k^2)} \leqslant \frac{1}{4} \quad . \tag{4. 1. 8}$$

This limitation is not particularly troublesome, however, since the amplitude-to-wavelength ratio of many spermatozoa fall within this range (see Brennen & Winet, 1977).

The terms in dimensional form needed for use in the integral equation (3. 3. 1) are

$$\underline{R}_o = X\,\underline{e}_x + Y\,\underline{e}_y \quad ,$$

$$R_o = |\underline{R}_o| \quad ,$$

$$X = \frac{1}{k}\{E(ks-f(t))/a^2k^2) - E(ks'-f(t))/a^2k^2)\} \quad ,$$

$$Y = -a\{\cos(ks-f(t)) - \cos(ks'-f(t))\} \quad ,$$

$$R_{on} = \underline{R}_o \cdot \underline{e}_n(s) = -X\nu_2(s) + Y\nu_1(s) \quad ,$$

$$R_{os} = \underline{R}_o \cdot \underline{e}_s(s) = X\nu_1(s) + Y\nu_2(s) \quad ,$$

$$a_n(s') = \underline{a}(s') \cdot \underline{e}_n(s) = a'_n\,\xi_1 + a'_s\xi_2 \quad ,$$

$$a_s(s') = \underline{a}(s') \cdot \underline{e}_s(s) = a'_s\,\xi_1 - a'_n\,\xi_2 \quad ,$$

where a'_ν refers to the components ($\nu = n, s$) of the vector $\underline{a}(s')$ corresponding to the unit vectors $\underline{e}_n$ and $\underline{e}_s$ at the point s', and

$$\xi_1 = \underline{e}_s(s') \cdot \underline{e}_s(s) , \qquad \xi_2 = \underline{e}_s(s') \cdot \underline{e}_n(s) ,$$

$$\nu_1 = \frac{\partial x}{\partial s} , \qquad \nu_2 = \frac{\partial y}{\partial s} .$$

We now apply our model to the spermatozoa of oyster and the spermatozoa Chaetopterus variopedatus, using the data of Denehy (1975) and Brokaw (1965). From these data we can specify for our numerical scheme, the number of waves along the flagellum n, the amplitude-to-wavelength ratio a/λ, the slenderness parameter ϵ, the nondimensional wave speed C/U, and the frequency of the oscillatory motion. The data taken from the above papers are given in table (4. 1. 1). A sketch of a typical waveform for Chaetopterus calculated from equation (4. 1. 1) with the given data is shown for a few time intervals in figure (4. 1. 1). Satisfactory agreement over most of the flagellum length is found between the waveform calculated from equation (4. 1. 1) and the photographs given by Brokaw (1965). In particular, we note that equation (4. 1. 1) describes the curved regions well and simulates the waveform used by Brokaw (1965) which consisted of circular arcs joined by straight segments. We should note, however, that the waveform observed on the proximal part of the flagellum, i. e., that part nearest the point of attachment to the cell body, is not in general accurately described by equation (4. 1. 1). Nevertheless, we apply equation (4. 1. 1) since the region of the flagellum that is inadequately described by (4. 1. 1) is rather small.

We proceed to make comparisons between the results of the existing theories and those obtained by using the methods developed

here. First, we remark here that numerical experiments on the direct computation method for both the partial torus and the undulating slender body were carried out by varying the number of intervals used in the quadrature formula in computing the integral in equation (3. 3. 1). The results indicated that one can generally determine the Stokeslet strength to an accuracy of 3 or 4 significant figures with only 20 divisions per wave length. This accuracy is quite sufficient for practical application and therefore the results to be presented in the sequel are obtained from computations with at least 20 divisions per wavelength. With respect to the time the motion was divided into 20 intervals per cycle, while at each of these instants the integral equations (3. 3. 1) were solved for $\underline{a}$.

In figures (4. 1. 2) and (4. 1. 3) we present a comparison of the average thrust per cycle versus C/U for Chaetopterus and oyster, calculated separately by the present method, the resistive-force theory, and the methods developed by Lighthill (1975b). For the resistive-force theory we make use of the force/length in the normal and tangential directions given by Gray & Hancock (1955), i. e. ,

$$f_n = \mu C_n V_n, \qquad f_s = \mu C_s V_s \tag{4. 1. 9}$$

where

$$C_n = \frac{4\pi}{\ln \frac{2\lambda}{b} - \frac{1}{2}} , \qquad C_s = 0.5\, C_n .$$

From the figures (4. 1. 2) and (4. 1. 3) we see that the Gray & Hancock resistance coefficients consistently overestimate the thrust. This is partly because the second equation in (4. 1. 9) often underestimates

the tangential force/length, which is always contributing to the drag, by as much as 30%. A more accurate estimate of the zero thrust point is obtained by increasing the ratio of C_s/C_n used in equation (4. 1. 9), see figure (4. 1. 8), however, variation of C_s/C_n alone can not produce uniform agreement with the present results over the entire range of C/U. The normal force/length found using Gray & Hancock theory is not altered by the above changes in C_s/C_n and often underestimates the correct result by 20% or more as indicated in figure (4. 1. 9) for a typical case.

In a recent study Denehy (1975) found the theoretical propulsive velocity of oyster spermatozoa to be 239 μm/sec by using the Gray & Hancock coefficients while her observed value was 163. 8 μm/sec. This finding also supports the contention that the classical formulas (4. 1. 9) overestimate the thrust of a flagellum. We also note that corresponding to the error in the force/length calculated by equations (4. 1. 9), we see in figures (4. 1. 4) and (4. 1. 5) that the mean energy expenditure, given as a first approximation by the time average of

$$E = \int_{-\ell}^{\ell} \underline{f} \cdot \underline{V} \, ds \quad ,$$

is also underestimated, by a large amount (approximately 30%), by the Gray & Hancock theory. Using the present theory it is now possible to accurately calculate the energy expenditure of a finite amplitude flagellar motion.

The force coefficients given by Lighthill (1975b) for a flagellum which is not generating any thrust, i. e., a self propelling

flagellum which has no cell body drag to overcome, are

$$C_n = \frac{4\pi}{\ln \frac{2q}{b} + \frac{1}{2}} \quad , \qquad C_s = \frac{2\pi}{\ln(\frac{2q}{b})} \quad , \tag{4.1.10}$$

with $q = 0.09\Lambda$. These expressions are shown by Lighthill to be a suboptimal representation of the resistance coefficients for spiral or planar motions of small amplitude, neglecting end effects. As shown in figures (4.1.2) and (4.1.3) pertaining to finite-amplitude planar motions, it is remarkable how well Lighthill's coefficients predict the zero thrust point, i.e., the intercept of the thrust curve with the C/U axis. Also plotted in figures (4.1.2) and (4.1.3) is the thrust resulting from the approximate expression for the thrust/length,

$$\text{thrust/length} = \mu C_x (U_o - U) \quad ,$$

$$C_x = \frac{2\pi}{\ln \frac{2q}{b}} \quad ,$$

given by Lighthill (1975b) for a flagellum which is producing a non-zero thrust. For an extended application of the above expressions Lighthill argues that a reasonable choice of q is $\frac{1}{6}\, n\lambda$ if U is the actual propulsive velocity and U_o is the zero-thrust swimming speed given for planar undulations by Lighthill (1975a) as

$$U_o = \frac{(1-\beta)(1-\gamma)}{(1-\beta+\gamma\beta)} \quad , \qquad \gamma = C_s/C_n \quad ,$$

β being the mean square cosine of the angle between the flagellar tangent and the swimming direction. Using the above approximation to the thrust we see from figures (4.1.2) and (4.1.3) that it generally

underestimates the mean force on the flagellum. Furthermore, we should note that these non-zero thrust results given by Lighthill are obtained by assuming a constant mean thrust/length along the flagellum. For this reason, we may expect that accurate instantaneous results for the force/length acting on the flagellum which is important for the study of internal flagellar mechanics, can not be obtained from this approximate method. However, solving the integral equation presented by Lighthill (1975b) more precisely is expected to produce more accurate results for the instantaneous force/length.

In figure (4. 1. 6) we plot the average thrust generated by the flagellum of Chaetopterus versus number of waves along the flagellum as the flagellum is hypothetically being lengthened, other factors being equal. We note that Chaetopterus, which has an observed value of $n = 1.25$, operates in one of the 'favorable' regions with respect to the variable n. In searching for further evidence of the significance that this behavior for the thrust versus number of waves may exist in general for other spermatozoa, we note that many spermatozoa have been observed to have a value of n between 1. 25 and 1. 5 (Brokaw, 1965; Brennen & Winet, 1977). Plotting the thrust and energy expenditure versus ak, or a/λ using equation 4. 1. 8, (figure 4. 1. 7) we see that the thrust and energy expenditure is monotonically increasing over the entire range $0 \leqslant a/\lambda \leqslant \frac{1}{4}$. Unfortunately, our kinematical description, which is particularly convenient for the desired type of waveforms, requires major modification for examining the rather interesting cases in which $\frac{\partial x}{\partial s}$ can be negative, i. e., waveforms that bend back over themselves, as observed by Brokaw

(1965) for Chaetopterus in solutions of high viscosity. Further research along these lines should yield interesting information on the behavior of the solution for very large values of a/λ.

From the present numerical results we further note that due to the velocity field induced by the moving flagellum, the local differential forces generally do not vanish with the local velocity of the centerline. Therefore the resistive-force theory in which the force is assumed to be proportional to the centerline velocity is not entirely correct. However, if we define C_n and C_s, excluding points on the body centerline with very small local velocities, the numerical results show that the values of C_n and C_s will often vary, with respect to position along the flagellum and time, by 20% as should be expected for planar waves, with the maximum differences in time or space being much larger. Therefore the classical resistance coefficients which are independent of s and t, such as equations (4. 1. 9) and (4. 1. 10), require major modification in order to be used to accurately calculate the instantaneous force/length acting on the body. Furthermore, the numerical solutions indicate that assigning an appropriate empirical expression, which would properly account for the above mentioned variations with respect to s and t, is a rather difficult problem. If it is still desirable to use the classical resistive-force theory, we might mention that the coefficients given by Lighthill (equation 4. 1. 10), offer a more reasonable approximation to the force/length than does the Gray & Hancock coefficients, as is suggested by the figures. Although constant resistive force coefficients are fairly accurate when calculating time-average values of the

thrust, there is no better way at present to evaluate instantaneous forces acting on a slender body than to solve integral equation (3. 3. 1), which is easily accomplished numerically, as has been demonstrated here.

4. 2 An approximate solution for the interaction between a spherical cell body and its flagellum

We now wish to examine the behavior of the solution when we include the interaction between a cell body and its flagellum. The cell body of the spermatozoa is assumed to be a spherical surface of radius d centered at a distance d in the negative x-direction from the end of our flagellum, $s = -\ell$. Using the method introduced by Burgers (1938) we approximately satisfy the no-slip boundary condition on the sphere surface by placing a Stokeslet at the sphere center with its strength chosen such that the surface mean value of the velocity on the sphere induced by the flagellum plus this Stokeslet equals the velocity of the cell body. We then include the velocity induced along the length of the flagellum by this cell-body Stokeslet into our integral equation (3. 3. 1), thereby acquiring an approximate account of the flagellar-cell body interactions. Very little work has been done on this interaction problem, although Lighthill (1975b) has proposed an approximate method of solution in which he essentially places a Stokeslet in the center of a cell body with a strength chosen such that the total force on the flagellum plus cell body equals zero. No attempt, however, is made to satisfy a no-slip boundary condition on the cell body. Here we expect to more accurately account for the

presence of a cell body by approximately satisfying the boundary condition on the spherical surface. This boundary condition based on the surface mean velocity is given by

$$-U\,\underline{e}_x + \frac{dy(-\ell,t)}{dt}\,\underline{e}_y = \frac{1}{4\pi d^2}\int_{\text{sphere}} (\underline{u}_f + \underline{U}_S(\underline{x};\underline{a}^h))dS \qquad (4.2.1)$$

where $\underline{u}_f$ and $\underline{U}_S$ are the velocities induced by the flagellum and cell body (or head), respectively. We approximate the velocity induced by the flagellum on the spherical surface by the contribution of only its Stokeslet distribution because the contribution from the higher order singularities is negligible as we have repeatedly noted in our previous discussion. The velocities $\underline{u}_f$ and $\underline{U}_S(\underline{x};\underline{a}^h)$ are given by

$$\underline{u}_f = \int_{-s_1}^{s_1} \underline{U}_S(\underline{R};\underline{a})ds' \quad ,$$

$$\underline{U}_S(\underline{x};\underline{a}^h) = \frac{\underline{a}^h}{r} + \frac{(\underline{a}^h \cdot \underline{x})\underline{x}}{r^3} \quad ,$$

where $\underline{R}$ is the position vector from a point s' on the flagellum centerline to a field point and $\underline{x}$ is the position vector from the sphere center to a field point with $r = |\underline{x}|$.

The integral equation (3.3.1) becomes, after including the Stokeslet that represents the cell body,

$$V_\nu(s,t) - \underline{e}_\nu(s,t)\cdot\underline{U}_S(\underline{R}_h;\underline{a}^h) = a_\nu L_\nu + \int_{-s_1}^{s_1} K_\nu(\underline{R}_o;\underline{a})ds'$$

$$(\nu = n, s, b) \quad , \qquad (4.2.2)$$

where $\underline{R}_h$ is the position vector from the sphere center to the point s on the flagellum centerline. Equations (4. 2. 1) and (4. 2. 2) are then four scalar equations for the four unknown components of $\underline{a}^h$ and $\underline{a}$.

The numerical calculation is reduced immensely by an analytical evaluation of the integral in the boundary condition (4. 2. 1). First, the term involving $\underline{U}_S(\underline{x};\underline{a}^h)$ is easily evaluated by choosing the base vectors $\underline{e}_1, \underline{e}_2, \underline{e}_3$ such that $\underline{a}^h = a^h \underline{e}_1$ and using the spherical coordinates such that

$$\underline{e}_r = \cos\theta\, \underline{e}_1 + \sin\theta \cos\varphi\, \underline{e}_2 + \sin\theta \sin\varphi\, \underline{e}_3 .$$

we then have

$$\frac{1}{4\pi d^2} \int_{\text{sphere}} \underline{U}_S(\underline{x};\underline{a}^h) dS = \frac{1}{4\pi d} \int_0^{2\pi} \int_0^{\pi} (a^h \underline{e}_1 + a^h \cos\theta\, \underline{e}_r) \sin\theta\, d\theta\, d\varphi$$

$$= \frac{4}{3} \frac{\underline{a}^h}{d} . \qquad (4.2.3)$$

The other integral term in (4. 2. 1) can be written as,

$$\underline{u}_f = \int_{-s_1}^{s_1} \{ \frac{2\underline{a}}{R} - \nabla(\frac{\underline{a} \cdot \underline{R}}{R}) \}\, ds'$$

where $\underline{R} = \underline{x} - \underline{x}'$, $\underline{x}'$ being the position vector from the sphere center to a point s' on the flagellum and $\nabla = \underline{e}_i \frac{\partial}{\partial x_i}$. This may be written

$$\underline{u}_f = \int_{-s_1}^{s_1} \{ \frac{2\underline{a}}{R} + \nabla' (\frac{\underline{a} \cdot \underline{R}}{R}) \}\, ds'$$

where $\nabla' = \underline{e}_i \frac{\partial}{\partial x'_i}$. Now we take the surface integral and change the order of integration, giving

$$\int_{\text{sphere}} \underline{u}_f \, dS = \int_{-s_1}^{s_1} \int_{\text{sphere}} \{\frac{2\underline{a}}{R} + \nabla' (\frac{\underline{a} \cdot \underline{R}}{R})\} \, dS \, ds'$$

where the integration over the sphere is with respect to the variable $\underline{x}$. Noting that $\frac{2\underline{a}}{R}$ is a harmonic function, we use the mean value theorem to find

$$\frac{1}{4\pi d^2} \int_{\text{sphere}} \frac{2\underline{a}}{R} \, dS = \frac{2\underline{a}}{|\underline{x}'|} \quad . \tag{4.2.4}$$

For the second term we may interchange the gradient operator and the integration since the gradient is with respect to $\underline{x}'$, i.e., we have

$$\nabla' \int_{\text{sphere}} (\frac{\underline{a} \cdot \underline{R}}{R}) \, dS \quad .$$

On the sphere we have $\underline{R} = d\underline{e}_r - \underline{x}'$ where $\underline{e}_r$ is the radial unit vector of a polar coordinate system with its origin at the sphere center. The above expression therefore may be written as

$$\nabla' \{ \int_{\text{sphere}} \frac{(\underline{a} \cdot \underline{e}_r)d - \underline{a} \cdot \underline{x}'}{R} \, dS \} \quad .$$

We see that the second term above is also a harmonic function, therefore by the mean value theorem,

$$\frac{1}{4\pi d^2} \int_{\text{sphere}} \frac{\underline{a} \cdot \underline{x}'}{R} \, dS = \frac{\underline{a} \cdot \underline{x}'}{|\underline{x}'|} \quad . \tag{4.2.5}$$

Thus it only remains to evaluate

$$\frac{1}{4\pi d} \int_{\text{sphere}} \frac{\underline{a} \cdot \underline{e}_r}{R} \, dS \quad . \tag{4. 2. 6}$$

This is done by making use of the $\underline{e}_\eta, \underline{e}_\xi, \underline{e}_\zeta$ coordinate system shown in figure (4. 2. 1), chosen such that

$$\underline{a} = a_\eta \underline{e}_\eta + a_\xi \underline{e}_\xi \quad ,$$

$$\underline{e}_r = \cos\theta \, \underline{e}_\eta + \sin\theta \cos\varphi \, \underline{e}_\xi + \sin\theta \sin\varphi \, \underline{e}_\zeta \quad .$$

We now substitute in (4. 2. 6) the result for $\underline{a} \cdot \underline{e}_r$ and the well-known Legendre polynomial expansion for R^{-1}, which for $|\underline{x}| = d$ is

$$\frac{1}{R} = \sum_{\ell=0}^{\infty} \frac{1}{|x'|} \left(\frac{1}{|\underline{x}'|}\right)^\ell P_\ell(\cos\theta) \quad .$$

After integrating the resulting expression for (4. 2. 6) with respect to φ we find,

$$\frac{d}{2} a_\eta \sum_{\ell=0}^{\infty} \frac{1}{|\underline{x}'|} \left(\frac{d}{|\underline{x}'|}\right)^\ell \int_0^\pi -\cos\theta \, P_\ell(\cos\theta) d(\cos\theta) \quad .$$

From the orthogonality relations for the Legendre polynomials we have

$$= \frac{1}{3} \frac{d^2}{|x'|^2} a_\eta \quad . \tag{4. 2. 7}$$

Therefore from equations (4. 2. 4), (4. 2. 5) and (4. 2. 7), using $a_\eta = \dfrac{\underline{a} \cdot \underline{x}'}{|\underline{x}'|}$, we have

$$\frac{1}{4\pi d^2}\int_{\text{sphere}} \underline{u}_f dS = \int_{-s_1}^{s_1} \left\{ \frac{2\underline{a}}{|\underline{x}'|} - \nabla'\left(\frac{\underline{a}\cdot\underline{x}'}{|\underline{x}'|}\right) + \frac{d^2}{3}\nabla'\left(\frac{\underline{a}\cdot\underline{x}'}{|\underline{x}'|^3}\right)\right\} ds'$$

$$= \int_{-s_1}^{s_1} \{\underline{U}_S(\underline{x}';\underline{a}) + \frac{d^2}{3}\underline{U}_D(\underline{x}';\underline{a})\} ds' \quad .$$

We have found that the mean velocity, averaged over a sphere, of a Stokeslet of strength $\underline{a}$ located at $\underline{x}'$ outside the sphere is equal to the velocity field evaluated at the sphere center due to the same Stokeslet plus a doublet of strength $\frac{d^2}{3}\underline{a}$ also located at $\underline{x}'$. This is, in some sense, a mean value theorem for the Stokes equations.

From equation (4. 2. 1) and (4. 2. 3) we then find that the Stokeslet strength $\underline{a}^h$ is given by

$$\underline{a}^h = \frac{3}{4} d \left\{-U \underline{e}_x + \frac{dy(-\ell, t)}{dt}\underline{e}_y - \int_{-s_1}^{s_1} \underline{H}(\underline{x}';\underline{a}) ds'\right\} \quad ,$$

where

$$\underline{H}(\underline{x}';\underline{a}) = \underline{U}_S(\underline{x}';\underline{a}) + \frac{d^2}{3}\underline{U}_D(\underline{x}';\underline{a}) \quad .$$

We now substitute $\underline{a}^h$ given above into equation (4. 2. 2) and solve the resulting equation, precisely as before, for the Stokeslet strength distributed along the flagellum centerline, $\underline{a}$.

The spermatozoa of oyster were particularly well suited for applying the present analysis since they have a very nearly spherical cell body with $\frac{d}{\ell} = 0.057$ whereas the cell bodies of Chaetopterus have a length-to-width ratio of 2. For Chaetopterus we approximate the head radius-to-flagellar length ratio by assuming the sphere

radius to be the mean of the actual dimensions, thus giving $\frac{d}{\ell} = 0.080$; we also reduced this value by 20% to ascertain the trend of the effect of head size on the results.

In figures (4. 2. 2), (4. 2. 3) and (4. 2. 4) we repeat the thrust curves for the headless spermatozoa and compare them to the thrust generated by the equivalent flagellum possessing a cell body. In all the cases examined we note that the presence of a head enhances the thrust generation by the flagellum. The physical reason for this is that the large cell body is dragging fluid with it thereby increasing the velocity component in the negative $\underline{e}_x$ direction incident on the traveling flagellar wave. This then increases the thrust in regions between the wave peaks and decreases the drag everywhere by decreasing the force/length in the tangential direction. Also shown in these figures is a comparison of the total force on the head and flagellar system with the thrust of the headless case minus the Stokes drag on a sphere of the same radius. This comparison provides an estimate of the interaction effect since it is absent in the latter case. The difference in the value of C/U at the zero total thrust point is in all cases slightly less than 15%. The result shows that the effects of cell-body and flagellar interactions will always increase the swimming speed for a fixed wave speed. We also note that decreasing the head size of Chaetopterus by 20% (see figure 4. 2. 4) only decreases slightly the thrust of the flagellum while the drag on the head is decreased by about 25%, thus resulting in a decrease of C/U at the zero total thrust point by approximately 10%. It was also found that

the energy expenditure of the flagellum when the head was present was decreased, from the case without a head, by about 5%.

It should be pointed out that in both cases the observed values for C/U, 4. 9 and 6. 7 respectively for Chaetopterus and oyster, do not agree very well with the zero thrust point in figures (4. 2. 2) and (4. 2. 3). However, the data were collected from and averaged over many organisms; consequently we should perhaps examine the range in which the data fall. Denehy (1975) has furnished a standard deviation for the measured swimming velocity U to be about 20% of the mean value, with similarly large deviations in the measured wave speed C. Although Brokaw (1965) has not included such information we might suspect similar deviations from one specimen to another within a species. Under this qualification, the zero thrust point certainly falls within the observed limits. With variations in the data of this sort it makes it difficult to assess the accuracy of the present results. It is of great importance to obtain accurate data on one organism and then to model carefully the waveform based on the observations in order to closely examine the theoretical results. One further comment concerning the data is in order at this point. It is very clear how important the long range effect is in low-Reynolds-number flows, as we saw for the torus which for various modes of motion experiences drags considerably different from those of a corresponding straight slender body. Therefore, as has often been pointed out, the effect of neighboring boundaries on bodies in the Stokes flow regime is significant. Since the data are taken for spermatoza swimming in a proximity to either a glass or air surface,

the problem of boundary effect on slender bodies performing finite-amplitude motions warrants further study. It is well known that for straight slender bodies the ratio of axial to normal force coefficients decreases when it comes closer to a rigid boundary. This would suggest an increased or more effective thrust production by a flagellum and therefore increased swimming speed. However, we also note that for a sphere moving parallel to a rigid boundary the drag increases with decreasing distance to the wall, this suggests that in the above analysis the strength of the Stokeslet located in the cell body, $\underline{a}^h$, will increase when coming closer to a rigid boundary. The result of this will have an effect similar to that due to an increase in head size and thus, as we saw for a variation in head size of Chaetopterus, the zero-thrust value of C/U will increase with increasing head size, or equivalently the swimming speed decreases for fixed wave speed. We therefore have two conflicting mechanisms, one suggesting an increase while the other is implying a decrease in propulsive velocity. The figures (4. 2. 2) and (4. 2. 3) do not help to clarify as to which is the more dominating since we have seen the present calculation overestimate the zero-thrust value of C/U for Chaetopterus and underestimate it for oyster spermatozoa. We also note that data indicating the distance the organism was from a boundary when the measurements were taken is not available.

In figure (4. 2. 5) we have a comparison of the instantaneous thrust forces for the flagellum of Chaetopterus with and without a cell body. In this typical case we have plotted the thrust/length for $-\ell \leqslant s \leqslant -\ell/2$, i. e., the proximal or first part of the flagellum

connected to the cell body, the result being given at five instants (in equal time progression) during half a cycle. We observe that the presence of the cell body results in enhancing the thrust production of the flagellum, since the value of f_x is greatly increased within the first stretch of flagellum close to the cell body. Generally when the cell body is present the thrust and drag in the range $-\ell \leqslant s \leqslant -0.6\ell$ are respectively increased and decreased by 10% or more from the values found for the headless case. After the point $s = -0.6\ell$ the cell body interaction effect becomes rather small, giving only a slightly increased thrust. Similar behavior has been found for oyster spermatozoa. Since the flow around a cell body has a long range effect, it will have a significant effect on normal and tangential force components such that the forward thrust is enhanced. We note that our model does not accurately describe a flagellum when it bends only slightly near the cell body, however, large reductions in the tangential force can always be expected.

4.3 A note on possible drag reduction by prolate spheroidal cell bodies

Spermatozoa have been observed to possess cell bodies which not only have a component of velocity in the direction of propulsion but also perform periodic motions with respect to the transverse direction and angle of attack to the direction of swimming. A particularly good example of the motion of this type is shown by Yanagimachi (1970) for the capacitated spermatozoa of the golden hamster. One can visualize the type of motion of the cell body to be discussed here

by considering the similar motion of a small segment of the flagellum. Here we consider the possibility of non-spherical cell bodies reducing their drag, as a result of this motion coupled with the fluid flow induced by the flagellar undulations. We consider a prolate spheroid with an angle of attack, i. e., the angle between the major axis and the direction of propulsive velocity U, given by

$$\theta = \theta_o \cos \omega t$$

(see figure (4. 3. 1)). The velocity of the fluid incident on the body is taken to be

$$\underline{V} = \underline{V}_T + \underline{V}_R$$

where

$$\underline{V}_T = U(\underline{e}_x - U_1 \cos(\omega t + \varphi)\underline{e}_y)$$

$$\underline{V}_R = - \underline{\Omega} \times \underline{x}'$$

$$\underline{\Omega} = \Omega \underline{e}_z = \frac{d\theta}{dt} \underline{e}_z = - \theta_o \omega \sin \omega t \, \underline{e}_z$$

and $\underline{x}'$ is the position vector of a point on the body surface in the body frame of reference. The velocity term U_1, which is nondimensionalized by U, includes the velocity of the head oscillations in the y-direction plus a contribution due to the motion of the flagellum which induces a flow near the cell body. We have also incorporated an arbitrary phase angle φ. It is a straightforward calculation to consider an additional oscillation of the same frequency in the x-direction; this term, however, has been found to make no contribution to the time average force in the x-direction although it does

produce a non-zero average transverse force. In order to curtail some of the details we will neglect this x-component oscillation since we are at present interested in drag reduction. The force on the cell body moving in the above prescribed manner is

$$\underline{F} = 2\mu L(C_s U_s \underline{e}_s + C_n U_n \underline{e}_n) \quad ,$$

where

$$U_s = U(\cos\theta + U_1 \cos(\omega t + \varphi)\sin\theta) \quad ,$$

$$U_n = U(\sin\theta - U_1 \cos(\omega t + \varphi)\cos\theta) \quad ,$$

L is the cell body half length, and C_s and C_n are given for a prolate spheroid by Chwang & Wu (1975). In terms of the x-y coordinates we have

$$\underline{F} = 2\mu C_s L \{(U_s \cos\theta + \gamma U_n \sin\theta)\underline{e}_x + (\gamma U_n \cos\theta - U_s \sin\theta)\underline{e}_y\},$$

where

$$\gamma = C_n/C_s \quad \text{and} \quad \theta = \theta_o \cos\omega t.$$

The average force over one period is therefore,

$$\overline{F}_x = \mu C_s L U \mathcal{F} \quad , \qquad (4.3.1)$$

$$\overline{F}_y = 0 \quad ,$$

where

$$\mathcal{F} = 1 + \gamma + (1 - \gamma)(J_o(2\theta_o) + U_1 \cos\varphi\, J_1(2\theta_o)) \qquad (4.3.2)$$

and $J_k(2\theta_o)$, $k = 0, 1$, represent Bessel functions of the first kind. The energy expended by such a motion is

$$E = 2\mu C_s L(U_s^2 + \gamma U_n^2) + M\Omega \quad ,$$

$$M = 8\pi\mu\Omega L c^2 C_{MR} \quad ,$$

where C_{MR} is given for a prolate spheroid by Chwang & Wu (1975). Upon calculating the time average we find

$$\bar{E} = \mu C_s L U^2 \mathcal{E} + 4\pi\mu(\theta_o\omega)^2 L c^2 C_{MR} \quad ,$$

where

$$\mathcal{E} = (1+\gamma)(1+\tfrac{1}{2}U_1^2) + (1-\gamma)[J_o(2\theta_o) + 2U_1 \cos\varphi J_1(2\theta_o)$$

$$- \tfrac{1}{2}U_1^2(J_o(2\theta_o) - \cos 2\varphi J_2(2\theta_o))] \quad .$$

In figure (4. 3. 2) we have plotted the force on the cell body with reference to the force on a stationary cell body, $\mu C_s 2LU$, of the same dimensions for the case $\varphi = 0$ which corresponds to observations. We first note that the maximum drag reductions for $U_1 = 1.0$, 2. 0 and 3. 0 occur respectively at $\theta_o \tilde{=} 25^o$, 34^o, and 45^o, which are within the range of observed head oscillations. We see in the figure that drag reductions of 10% or more are possible for values of $U_1 \geqslant 2.0$ when the cell body aspect ratio $c/L = 1/4$ and for $U_1 \geqslant 3.0$ when $c/L = 1/2$. Although data are not readily available, suppose we construct what might be a typical hypothetical case. We consider an organism with a swimming speed $U = 125$ μm/sec, a frequency of 30 hertz or 188 radians per second, a wave amplitude of the flagellum of 4. 5 μm and suppose the amplitude of the head motion

in the transverse direction is 1.5 μm, i.e., the ratio of head amplitude to flagellum amplitude has a moderate value of 1/3. For this organism we would have a transverse head velocity nondimensionalized by U of 2.26. This head velocity plus the fluid velocity induced by the flagellum near the head, which can be estimated from the numerical data for the spherical head case, gives a value for U_1 in the neighborhood of 2.75. Therefore depending on the aspect ratio of the cell body, c/L, it seems quite possible to obtain drag reductions of 10% or more. From the observations of Yanagimachi (1970) for capacitated spermatozoa we see that the ratio of head oscillation amplitude to flagellar amplitude can be considerably larger than 1/3 and therefore could result in a still larger drag reduction than found for our hypothetical organism.

These force considerations on a cell body can be extended slightly based on some observations made on the numerical results for flagellar undulations. It was regularly found that maximum thrust was generated by the flagellum when the point $s = -\ell$ was at a peak, i.e., $y = \pm a$, and minimum thrust was generated when $s = -\ell$ was at $y = 0$. This suggests for our present purposes that the maximum and minimum fluid velocities in the $\underline{e}_x$ direction near the cell body should occur when $y(-\ell, t) = \pm a$ and $y(-\ell, t) = 0$ respectively. Therefore in the previous analysis we include a second harmonic in the $\underline{e}_x$ velocity component, i.e., replace $U\underline{e}_x$ by $U(1 - U_2 \cos 2\omega t)\underline{e}_x$. Upon calculating the time average forces we find

$$\overline{F}_x = \mu C_s L U \hat{\mathcal{F}}$$

$$\overline{F}_y = 0$$

where

$$\hat{\mathcal{F}} = \mathcal{F} + (1 - \gamma)U_2 J_2(2\theta_o) \quad .$$

Therefore for positive U_2 the new term further enhances the drag reduction capability of the cell body. However, estimation of U_2 from the numerical results for spheroidal cell bodies indicates that a value of 0.6 is appropriate and therefore this new term gives only a few per cent additional drag reduction for $c/L = 1/2$ and $1/4$ at moderate angles of attack, θ_o. We will briefly mention that any of the oscillatory cell body motions discussed above generally produce a significant increase in energy expenditure over that found for the stationary case, as should be expected.

Although the preceding discussion has been of a very simplified nature it clearly presents an interesting concept to planar motion of flagellated micro-organisms, namely that the cell body may in some cases play an active part in propulsion. This area of research certainly deserves further study in which the cell body motions are accurately described with a proper account of the flagellar-cell body interactions for non-spherical bodies.

V. CONCLUSION

We have seen that by applying the method of singularities it has been possible to construct a solution, in a stepwise fashion, for the Stokes flow past slender bodies with finite centerline curvature. In fact, this procedure has enabled us to satisfy the no-slip boundary condition to a high degree of accuracy, designated by an error only of $O(\epsilon^2 \ln\epsilon)$, along the entire body length, including the ends. Accounting for the end effects and satisfying the boundary condition to such a high order in the slenderness parameter has not previously been accomplished for slender bodies having finite curvature. One of the principal results is that a set of simultaneous integral equations have been obtained for determining the Stokeslet strength with an error of $O(\epsilon^2)$. We note that this error in the Stokeslet strength is a considerable improvement over those results found by using the previous method of matched asymptotic expansions, which gives the same result in terms of the weak expansion in $(\frac{1}{\ln\epsilon})^n$. For the torus, the exact solution of these integral equations was found by assuming the appropriate functional form for the Stokeslet strength a priori. The torus solution exhibited many new features of the Stokes flow past slender bodies having finite centerline curvature, such as the higher order singularities which are required for improved accuracy and the large differences, found in certain classes of motion, between the actual force coefficients and those of classical resistive-force theory. The present theory was then applied to finite-amplitude planar motions of the flagellum of flagellated micro-organisms. Comparisons were made between both the classical theories and available data. We also

included, for the first time to this author's knowledge, the interaction between cell body and flagellum by approximately satisfying the no-slip boundary condition on the cell body. Significant differences between the results with and without the cell body-flagellar interactions were observed. A brief note was given to introduce the concept that the cell body may, in some cases, play a partially active role in propulsion.

It is now worthwhile to conclude with a brief comment on some of the remaining problems that need to be studied. First, in order to assess more carefully the accuracy of the theory developed here in application to micro-organism propulsion, it is becoming increasingly important to accurately model the observed waveforms of spermatozoa specimen. This is a rather formidable data collection task, since we require not only the positions but also the velocities of a set of material points on a flagellar centerline. Along these lines it is also a challenging problem to construct the motion of a freely swimming micro-organism from a theoretical model that makes use of the integral equation presented here for calculating the forces on the flagellum and accounts for the internal mechanics (or elastic response) of the flagellum. In such a model it would be necessary to require the total force and moment on the organism to vanish at each instant in time. With respect to cell body-flagellar interaction a further study is desirable to produce a solution that can accurately satisfy the no-slip boundary condition on the cell body, especially for non-spherical cell bodies. Another extremely important area of research is the problem of wall effects. This is important for comparing theoretical

results with experimental data where the organism is in close proximity to the air or glass interface of a microscope slide and for the study of spermatozoa swimming in tubes, such as the oviduct. One further problem of interest, to which the integral equations developed here can be easily adapted to handle, is the interaction between slender bodies that are separated by a distance large compared to their cross-sectional radius, b. A qualitative study of this problem has been carried out by Sir G. I. Taylor (1951). The list of new problems to consider is numerous, the few mentioned above are intended only to indicate the areas that should be of great importance. We believe that the present work forms the solid foundation needed for treating many of the remaining difficult and challenging problems.

REFERENCES

Batchelor, G.K. 1970 Slender-body theory for particles of arbitrary cross section in Stokes flow. J. Fluid Mech. 44, 419-440.

Brennen, C. and Winet, H. 1977 Fluid mechanics of propulsion by cilia and flagella. Ann. Rev. Fluid Mech. 9, 339-398.

Brokaw, C.J. 1965 Non-sinusoidal beanding waves of sperm flagella. J. Exp. Biol. 43, 155-169.

Burgers, J.M. 1938 On the motion of small particles of elongated form in a viscous liquid. Chap. III of Second Report on Viscosity and Plasticity. Kon. Ned. Akad. Wet., Verhand 16, 113-184.

Chwang, A.T. and Wu, T.Y. 1974 Hydromechanics of low-Reynolds-number flow, Part 1. Rotation of axisymmetric prolate bodies. J. Fluid Mech. 63, 607-622.

Chwang, A.T. and Wu, T.Y. 1975 Hydromechanics of low-Reynolds-number flow, Part 2. The singularity method for Stokes flows. J. Fluid Mech. 67, 787-815.

Cole, J.D. 1968 Perturbation Methods in Applied Mathematics. Blaisdell, Waltham, Mass.

Cox, R.G. 1970 The motion of long slender bodies in a viscous fluid, Part 1. General theory. J. Fluid Mech. 44, 791-810.

Denehy, M.A. 1975 The propulsion of nonrotating ram and oyster spermatozoa. Biol. of Reprod. 13, 17-29.

Gray, J. and Hancock, G.J. 1955 The propulsion of sea-urchin spermatozoa. J. Exp. Biol. 32, 802-814.

Handelsman, R. A. and Keller, J. B. 1967 Axially symmetric potential flow around a slender body. J. Fluid Mech. 28, 131-147.

Isaacson, E. and Keller, H. B. 1966 Analysis of Numerical Methods. John Wiley and Sons, Inc., New York.

Kaplun, S. 1967 Fluid Mechanics and Singular Perturbations. Academic Press, New York.

Keller, J. B. and Rubinow, S. I. 1976 Slender-body theory for slow viscous flow. J. Fluid Mech. 75, 705-714.

Lighthill, M. J. 1975a Mathematical Biofluiddynamics. SIAM, Philadelphia.

Lighthill, M. J. 1975b Flagellar hydrodynamics. The John von Neumann Lecture, SIAM Review 18, 161-230.

Shen, J. S., Tam, P. Y., Shack, W. J. and Lardner, T. J. 1975 Large amplitude motion of self-propelling slender filaments at low-Reynolds-numbers. J. Biomechanics 8, 229-236.

Taylor, G. I. 1951 Analysis of swimming of microscopic organisms. Proc. Roy. Soc. London A 209, 447-461.

Tillet, J. P. K. 1970 Axial and transverse Stokes flow past slender axisymmetric bodies. J. Fluid Mech. 44, 401-417.

Tuck, E. O. 1964 Some methods for flows past blunt slender bodies. J. Fluid Mech. 18, 619-635.

Van Dyke, M. 1975 Perturbation Methods in Fluid Mechanics. Parabolic Press, Stanford, California.

Wu, T. Y. and Yates, G. 1976 Finite-amplitude unsteady slender-body flow theory. Eleventh Symposium on Naval Hydrodynamics, University College London.

Yanagimachi, R. 1970 The movement of golden hamster spermatozoa before and after capacitation. J. Reprod. Fert. 23, 193-196.

APPENDIX A

1. Here we present the integrals used to compute the velocity field induced near the body surface by the near-field singularity distributions that arise from the various motions of a torus (Chapter II). We define

$$I_{mn} = \int_0^{\gamma} \frac{\varphi^n}{\Delta^m} \, d\varphi \quad ,$$

where

$$\Delta = \{(1 + \epsilon \cos\psi)\varphi^2 + \epsilon^2\}^{1/2} \quad .$$

Recall that γ is chosen to be $\epsilon \ll \gamma \ll \pi$. We have,

$$I_{10} = (1 - \tfrac{\epsilon}{2}\cos\psi)\ln\frac{2\gamma}{\epsilon} + \tfrac{\epsilon}{2}\cos\psi + O(\epsilon^2 \ln\epsilon, \tfrac{\epsilon^2}{\gamma^2}) \quad ,$$

$$I_{12} = \frac{\gamma^2}{2} + O(\epsilon\gamma^2, \epsilon^2 \ln\epsilon) \quad ,$$

$$I_{14} = O(\gamma^4) \quad ,$$

$$I_{30} = \frac{1}{\epsilon^2}\{1 - \tfrac{\epsilon}{2}\cos\psi - \tfrac{1}{2}(\tfrac{\epsilon}{\gamma})^2 + \tfrac{3}{8}\epsilon^2\cos^2\psi + O(\tfrac{\epsilon^3}{\gamma^2})\} \quad ,$$

$$I_{32} = (1 - \tfrac{3}{2}\epsilon\cos\psi)\ln\frac{2\gamma}{\epsilon} - 1 + 2\epsilon\cos\psi + O(\epsilon^2 \ln\epsilon) \quad ,$$

$$I_{34} = \frac{1}{2}\gamma^2 + O(\epsilon\gamma^2, \epsilon^2 \ln\epsilon) \quad ,$$

$$I_{36} = \frac{1}{4}\gamma^4 + O(\epsilon\gamma^4) \quad ,$$

$$I_{50} = \frac{1}{3\epsilon^4}(2 - \epsilon\cos\psi + O(\tfrac{\epsilon^2}{\gamma^2})) \quad ,$$

$$I_{52} = \frac{1}{3\epsilon^2}(1 - \tfrac{3}{2}\epsilon\cos\psi + O(\tfrac{\epsilon^2}{\gamma^2})) \quad ,$$

$$I_{54} = \ln \frac{2\gamma}{\epsilon} + O(1) ,$$

$$I_{56} = \frac{1}{2}\gamma^2 + O(\epsilon\gamma^2, \epsilon^2 \ln \epsilon) ,$$

$$I_{58} \leqslant \gamma^2 I_{56} ,$$

$$I_{70} = \frac{8}{15\epsilon^6}\left(1 - \frac{\epsilon}{2}\cos\psi + O\left(\frac{\epsilon^2}{\gamma^2}, \epsilon^2\right)\right) ,$$

$$I_{72} = O\left(\frac{1}{\epsilon^4}\right) , \quad I_{74} = O\left(\frac{1}{\epsilon^2}\right) , \quad I_{76} = O(\ln\epsilon) ,$$

$$I_{78} \leqslant \gamma^2 I_{76}$$

$$I_{94} = O\left(\frac{1}{\epsilon^4}\right) , \quad I_{96} = O\left(\frac{1}{\epsilon^2}\right) , \quad I_{98} = O(1) .$$

2. Integrals arising from the far-field or outer expansions for the motion of a torus are given below. We define

$$J_k = \int_{\gamma}^{\pi} \frac{d\varphi}{R^k} ,$$

where here

$$R = \sqrt{2}a(1 + \epsilon\cos\psi)^{1/2}(1 - \cos\varphi)^{1/2} .$$

We find,

$$J_1 = \frac{1}{a}\left\{(1 - \frac{\epsilon}{2}\cos\psi)\ln\frac{4}{\gamma} - \frac{\gamma^2}{48} + O(\gamma^4, \epsilon^2\ln\gamma)\right. ,$$

$$J_3 = O\left(\frac{1}{\gamma^2 a^3}\right) ,$$

$$J_5 = O\left(\frac{1}{\gamma^4 a^5}\right) .$$

We also define

$$C_{mn} = \int_{\gamma}^{\pi} \frac{\cos^n \varphi}{R^m}\, d\varphi \quad ; \qquad S_{mn} \int_{\gamma}^{\pi} \frac{\sin^n \varphi}{R^m}\, d\varphi \quad .$$

We have

$$C_{12} = \frac{1}{a}\{(1 - \frac{\epsilon}{2}\cos\psi)\ln\frac{4}{\gamma} - \frac{4}{3} + \frac{23}{48}\gamma^2 + \frac{2}{3}\epsilon\cos\psi + O(\epsilon\gamma^2, \epsilon^2\ln\epsilon)\} \ ,$$

$$S_{12} = \frac{4}{3a}(1 - \frac{3}{8}\gamma^2 - \frac{\epsilon}{2}\cos\psi + O(\gamma^4)) \ ,$$

$$C_{11} = \frac{1}{a}\{(1 - \frac{\epsilon}{2}\cos\psi)\ln\frac{4}{\gamma} - 2 + \frac{11}{48}\gamma^2 + \epsilon\cos\psi + O(\gamma^4, \epsilon^2\ln\epsilon)\} \ ,$$

$$C_{32} = O(\frac{1}{a^3\gamma^2}) \ ,$$

$$S_{32} = \frac{1}{a^3}\{(1 - \frac{3}{2}\epsilon\cos\psi)\ln\frac{4}{\gamma} - 1 + \frac{5}{48}\gamma^2 + \frac{3}{2}\epsilon\cos\psi + O(\gamma^4, \epsilon^2\ln\epsilon)\} \ ,$$

$$C_{31} = O(\frac{1}{a^3\gamma^2}) \ , \quad C_{52} = O(\frac{1}{a^5\gamma^4}) \ , \quad S_{52} = O(\frac{1}{a^3\gamma^2}) \ .$$

We also have

$$D_3 = \int_\gamma^\pi \frac{\sin^2\varphi \cos\varphi}{R^3}\, d\varphi = \frac{1}{a^3}\{\ln\frac{4}{\gamma} - \frac{5}{3} - \frac{3}{2}\epsilon\cos\psi \ln\frac{4}{\gamma}$$

$$+ \frac{17}{48}\gamma^2 + \frac{5}{2}\epsilon\cos\psi + O(\gamma^4)\} ,$$

$$D_5 = \int_\gamma^\pi \frac{\sin^2\varphi \cos\varphi}{R^5}\, d\varphi = O(\frac{1}{a^5\gamma^2}) ,$$

$$K_1 = \int_\gamma^\pi (1 - \cos\varphi)^{1/2}\, d\varphi = 2\sqrt{2}(1 - \frac{\gamma^2}{8} + O(\gamma^4)) .$$

APPENDIX B

In this appendix we present the integrals used in evaluating the velocity field on the surface of an arbitrary slender body having a spheroidal cross-section. We define

$$I_{mn} = \int_{-\varphi_1/\epsilon}^{\varphi_2/\epsilon} \frac{\sigma^n}{\Delta^m} \, d\sigma \ ,$$

where

$$\varphi_1 = s_1 + s \ , \qquad \varphi_2 = s_1 - s \ , \qquad s_1 = e \ ,$$

$$e = (1 - \epsilon^2)^{1/2} \ ,$$

$$\Delta = (\sigma^2 + \eta^2)^{1/2} \ ,$$

$$\sigma = \frac{s' - s}{\epsilon} \ ,$$

$$\eta^2 = 1 - s^2 \ .$$

For convenience we define

$$L_e = \ln \frac{1 + e}{1 - e} \ ,$$

$$g(s) = 1 - e^2 s^2 \ ,$$

$$h_2(s) = 2 \frac{1 - s^2}{1 - e^2 s^2} \ .$$

It is also useful to make use of the following recursion relations,

$$I_{k0} = \frac{1}{s}\left(\frac{1}{k-2} \frac{\partial I_{k-20}}{\partial s} - \frac{1}{\epsilon} I_{k1}\right) \ ,$$

$$I_{k2} = I_{k-20} - \eta^2 I_{k0}$$

The integrals evaluated on the body surface $\eta^2 = 1 - s^2$ are given by

$$I_{10} = \ln \frac{1+e}{1-e} \sim 2 \ln \frac{2}{\epsilon} + O(\epsilon^2) ,$$

$$I_{11} = - \frac{2es}{\epsilon} \sim - \frac{2s}{\epsilon} + O(\epsilon) ,$$

$$I_{12} = \frac{e}{\epsilon^2}(1 + s^2) - \frac{\eta^2}{2} L_e ,$$

$$I_{13} = \frac{2es}{\epsilon^3}(e^2 s^2 - s^2 - e^2) ,$$

$$I_{30} = 2e/g(s) ,$$

$$I_{31} = - 2e\epsilon s/g(s) ,$$

$$I_{32} = L_e - e h_2(s) ,$$

$$I_{33} = - \frac{2es}{\epsilon}(1 - \frac{\epsilon^2}{2} h_2(s)) ,$$

$$I_{34} = \frac{e}{\epsilon^2}\{e^2(1 + s^2) + \epsilon^2(3 - s^2 - \epsilon^2 h_2 s^2)\} - \frac{3}{2}\eta^2 L_e ,$$

$$I_{50} = \frac{2e(3 - e^2)}{3g^2} + \frac{8e^3(1-e^2)s^2}{3g^3} ,$$

$$I_{51} = - \frac{2es\epsilon^3}{g^2}(1 + \frac{4e^2 s^2}{3g}) ,$$

$$I_{52} = \frac{2e}{g}\{1 - \frac{1}{6} h_2(3 - e^2 + \frac{4e^2\epsilon^2 s^2}{g})\} ,$$

$$I_{53} = \frac{2es\epsilon}{g}(- 1 + \frac{\epsilon^2}{2} h_2 + \frac{2}{3}\epsilon^2 e^2 s^2 \frac{h_2}{g}) ,$$

$$I_{54} = -\frac{2}{3}e(1 + (1 + \frac{e^2}{2})h_2) + L_e + \frac{2e\epsilon^2 s^2}{g}[1$$

$$- \frac{\epsilon^2}{3g}(5 - 3s^2 + 2e^2 s^2 h_2)] \ ,$$

$$\epsilon^2 \eta I_{55} \sim -2\epsilon\eta s + O(\epsilon^3) \ ,$$

$$\epsilon^2 I_{56} \sim (1 + s^2) + O(\epsilon^2 \ln\epsilon) \ ,$$

$$I_{70} = \frac{8e^3(5 - 3e^2)}{15\, g^3} + \frac{48e^5\epsilon^2 s^2}{15\, g^4} + \frac{2\epsilon^4 e(5 + 10e^2 s^2 + e^4 s^4)}{5\, g^5} \ ,$$

$$I_{71} = -\frac{2\epsilon^5 es}{5\, g^5}(5 + 10e^2 s^2 + e^4 s^4) \ ,$$

$$\epsilon^2\eta^2 I_{74} \leqslant O(\epsilon^2 \ln\epsilon), \quad \epsilon^2\eta^3 I_{75} = O(\epsilon^2) \ , \quad \epsilon^2\eta^2 I_{76} = O(\epsilon^2).$$

We also define

$$J_{mn} = \int_{-\varphi_1/\epsilon}^{\varphi_2/\epsilon} \frac{(s_1^2 - s'^2)\sigma^n}{\Delta^m}\, d\sigma \ ,$$

and note the recursion relations

$$J_{k2} = \frac{\epsilon}{k-2}\frac{\partial J_{k-21}}{\partial s} + \frac{1}{k-2} J_{k-20} - \epsilon s J_{k1} \ ,$$

$$J_{kn} = (s_1^2 - s^2) I_{kn} - 2\epsilon s\, I_{kn+1} - \epsilon^2 I_{kn+2} \ ,$$

$$J_{k1} = \epsilon\left(\frac{1}{k-2}\frac{\partial J_{k-20}}{\partial s} - s J_{k0}\right) .$$

We find,

$$J_{10} = \left(\frac{e^2+1}{2} L_e - e\right) + s^2\left(\frac{e^2-3}{2} L_e + 3e\right) ,$$

$$J_{11} = -\frac{2es}{\epsilon}\left(1 - s^2 + \frac{2}{3} e^2 s^2\right) + \frac{s}{\epsilon}(1 - s^2)\epsilon^2 L_e ,$$

$$J_{30} = 2e - \epsilon^2 L_e ,$$

$$J_{31} = 2\epsilon s(2e - L_e) ,$$

$$J_{32} = \left(\frac{3-e^2}{2} L_e - 3e\right) + s^2\left(5e - \frac{5-3e^2}{2} L_e\right) ,$$

$$J_{50} = \frac{4e^3}{3g} ,$$

$$J_{51} = -\frac{4\epsilon e^3 s}{3g} ,$$

$$J_{52} = 2e - \frac{2e^3}{3} h_2 - \epsilon^2 L_e ,$$

$$J_{53} = 2\epsilon s\left(2e - L_e + \frac{e^3}{3} h_2\right) ,$$

$$\epsilon^2 J_{54} = O(\epsilon^2 \ln\epsilon) ,$$

$$J_{70} = \frac{4e^3}{15\, g^2}\left(5 - e^2 + \frac{4e^2\epsilon^2 s^2}{g}\right) ,$$

$$J_{71} = -\frac{4\epsilon e^3 s}{15\, g}\left(5 - 3e^2 + \frac{4e^2\epsilon^2 s^2}{g}\right) ,$$

$$J_{72} = \frac{4e^3}{15\, g}\left(e^2 + \frac{5\epsilon^4 s^2}{g} + \frac{4e^2\epsilon^4 s^4}{g^2}\right) ,$$

$$J_{73} = -\frac{4\epsilon e^3 s}{15\,g}\left(2 + e^2 - \frac{\epsilon^2}{g}(2 - 5\epsilon^2 s^2) + \frac{4e^2\epsilon^4 s^4}{g^2}\right) ,$$

$$J_{74} = 2e - \frac{e^3}{3} h_2 - \epsilon^2 L_e - \frac{2e^3 h_2}{15}\left(e^2 + \frac{5\epsilon^4 s^2}{g} + \frac{4e^2\epsilon^4 s^4}{g^2}\right) ,$$

$$J_{75} = O(\epsilon) , \qquad \epsilon^2 J_{76} = O(\epsilon^2) ,$$

$$\epsilon^2\eta^2 J_{94} \leqslant O(\epsilon^2) , \qquad \epsilon^2\eta^2 J_{95} \leqslant O(\epsilon^3) , \qquad \epsilon^2\eta^2 J_{96} \leqslant O(\epsilon^2) .$$

We further define

$$K_{mn} = \int_{-\varphi_1/\epsilon}^{\varphi_2/\epsilon} (s_1^2 - s'^2)^2 \frac{\sigma^n}{\Delta^m}\, d\sigma ,$$

and find

$$K_{50} = \frac{2e}{3}(5e^2 - 3) + \epsilon^4 L_e ,$$

$$K_{51} = -\frac{4}{3} s\epsilon(6e - 4e^3 - 3\epsilon^2 L_e) ,$$

$$K_{52} \leqslant O(1) ,$$

$$K_{70} = \frac{16e^5}{15\,g} ,$$

$$K_{71} = -\frac{16\epsilon s e^5}{15\,g} ,$$

$$K_{72} \leqslant s_1^2 J_{72} , \qquad K_{73} \leqslant s_1^2 J_{73} .$$

Integrals arising from the common part expansion are

$$C_0 = \int_{-\varphi_1}^{\varphi_2} \frac{\varphi}{|\varphi|}\, d\varphi = -2s \ ,$$

$$C_1 = \int_{-\varphi_1}^{\varphi_2} \frac{\varphi^2}{|\varphi|}\, d\varphi = s_1^2 + s^2 \sim 1 + s^2 + O(\epsilon^2) \ ,$$

$$C_2 = \int_{-\varphi_1}^{\varphi_2} \frac{\varphi^3}{|\varphi|^3}\, d\varphi = C_0 = -2s \ .$$

APPENDIX C

Here we present the center region approximation of the integrals that arise when considering slender bodies having arbitrary circular cross sections. The integrals, I_{mn}, are defined as in Appendix B and we find,

$$I_{10} \sim 2 \ln \frac{2(1 - s^2)^{1/2}}{\epsilon \eta} + O(\epsilon^2) ,$$

$$\epsilon I_{11} \sim -2s + O(\epsilon^2) ,$$

$$\epsilon^2 I_{12} \sim 1 + s^2 + O(\epsilon^2 \ln \epsilon) ,$$

$$\epsilon^3 I_{13} \sim -\frac{2}{3}(3s + s^3) - \epsilon^3 \eta^2 I_{11} ,$$

$$\eta^2 I_{30} \sim 2 + O(\epsilon^2) ,$$

$$I_{31} \sim -2\epsilon \frac{s}{1-s^2} + O(\epsilon^3) ,$$

$$I_{32} \sim 2 \ln \frac{2(1-s^2)^{1/2}}{\epsilon \eta} - 2 + O(\epsilon^2) ,$$

$$\epsilon I_{33} \sim -2s + O(\epsilon^2) ,$$

$$\epsilon^2 I_{34} \sim 1 + s^2 + O(\epsilon^2 \ln \epsilon) ,$$

$$\eta^4 I_{50} \sim \frac{4}{3} + O(\epsilon^2) ,$$

$$I_{51} \sim -\frac{2\epsilon^3 s(3 + s^2)}{3(1 - s^2)^3} + O(\epsilon^5) ,$$

$$\eta^2 I_{52} \sim \frac{2}{3} + O(\epsilon^2) ,$$

$$\epsilon\eta^2 I_{53} \sim O(\epsilon^2) ,$$

$$\epsilon\eta I_{54} \sim 2\epsilon\eta(\ln \frac{2(1-s^2)^{1/2}}{\epsilon\eta} - \frac{4}{3}) + O(\epsilon^3) ,$$

$$\epsilon^2 \eta I_{55} \sim -2\epsilon\eta s + O(\epsilon^3) ,$$

$$\epsilon^2 I_{56} \sim 1 + s^2 + O(\epsilon^2 \ln\epsilon) ,$$

$$\eta^6 I_{70} \sim \frac{16}{15} + O(\epsilon^2) ,$$

$$\epsilon\eta^5 I_{72} \sim \frac{4}{15}\epsilon\eta + O(\epsilon^3) ,$$

$$\epsilon\eta^4 I_{73} \sim O(\epsilon^4) ,$$

$$\epsilon\eta^3 I_{74} \sim \frac{2}{5}\epsilon\eta + O(\epsilon^3) ,$$

$$\epsilon^2\eta^3 I_{75} \sim O(\epsilon^3) ,$$

$$\epsilon^2\eta^2 I_{76} \sim O(\epsilon^2 \ln\epsilon) ,$$

$$\eta^4 I_{94} \leqslant \eta^2 I_{74} ,$$

$$\eta^3 I_{95} \leqslant \eta I_{75} ,$$

$$\eta^2 I_{96} \leqslant I_{76} .$$

We note that in the end region where $\eta^2 \sim (1-s^2)(1+O(\epsilon^2))$ on the body surface we have

$$\frac{1}{(\sigma^2+\eta^2)^{1/2}} \sim \frac{1}{[\sigma^2+(1-s^2)(1+O(\epsilon^2))]^{1/2}} \sim \frac{1}{\Delta}(1+O(\epsilon^2)) ,$$

where

$$\Delta = (\sigma^2 + 1 - s^2)^{1/2} .$$

Therefore we see that to the order of terms retained here the end region integrals become the same as those given in Appendix B.

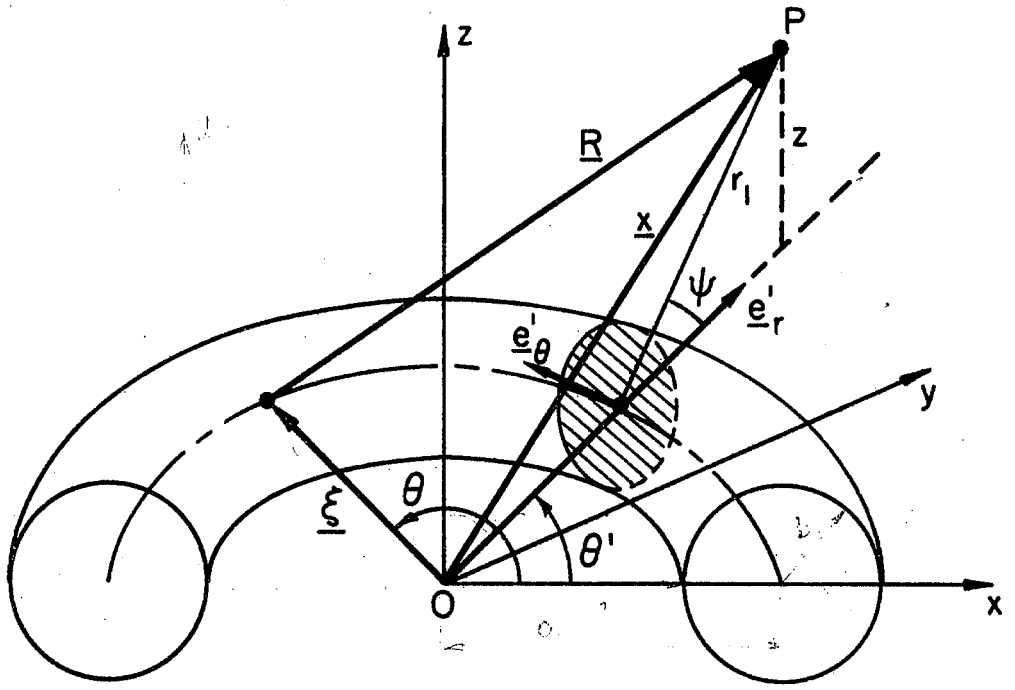

Figure 2. 1. 1 Torus and coordinates.

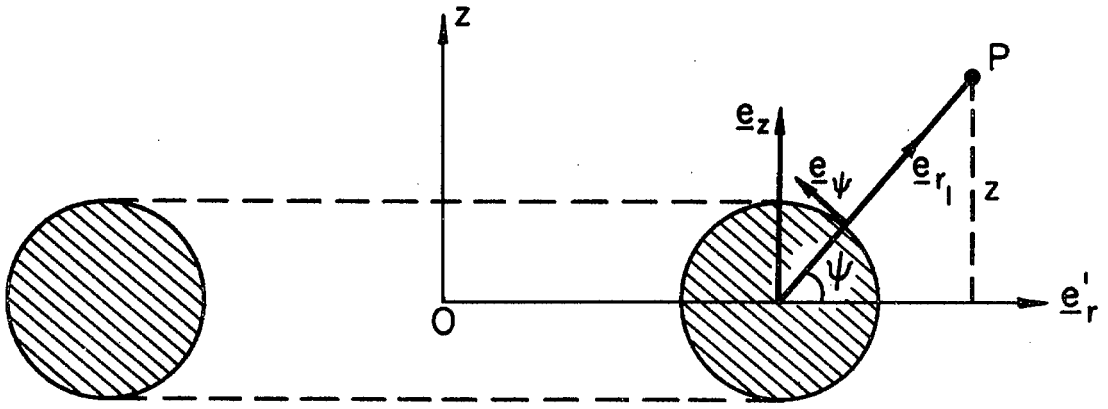

Figure 2. 1. 2 Sectional view of torus at θ' = constant.

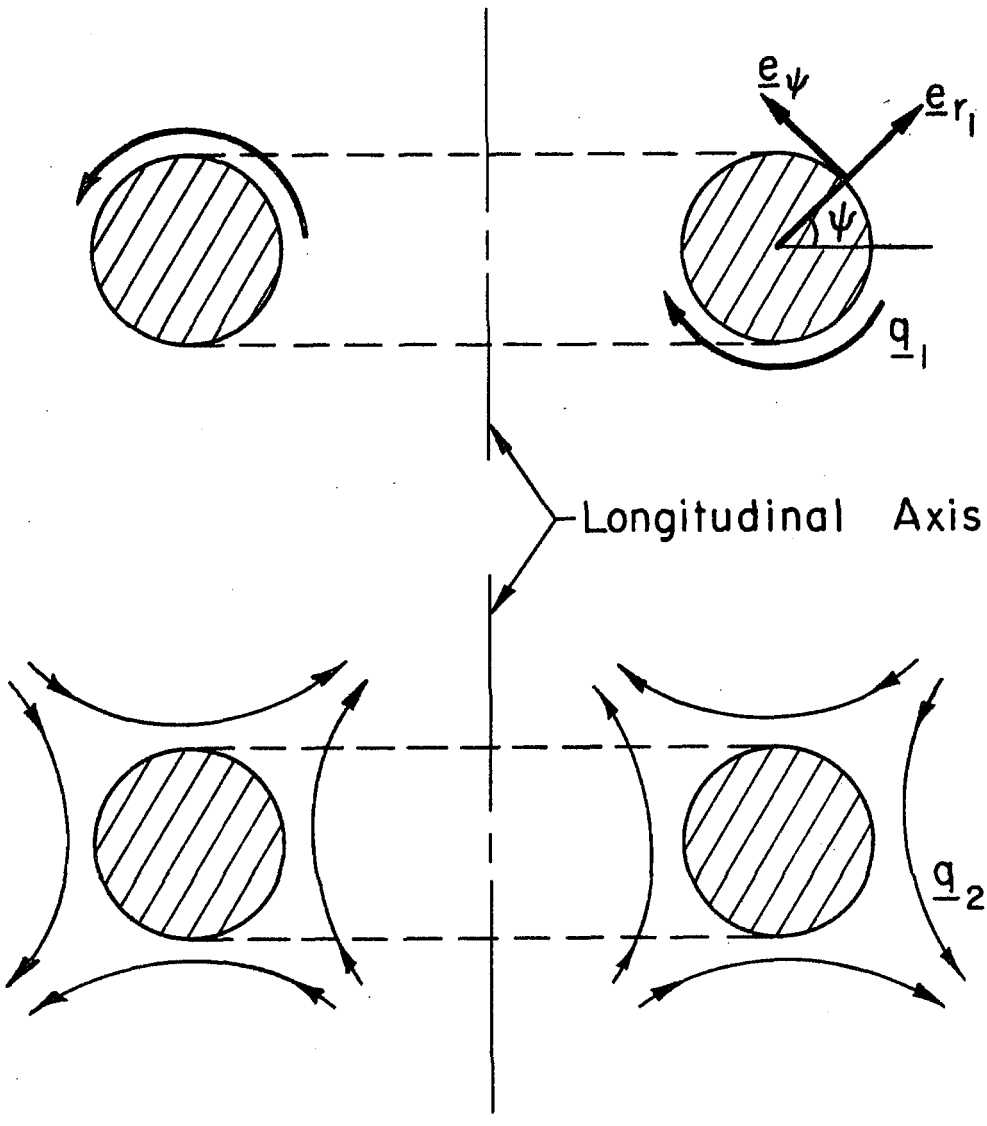

Figure 2. 1. 3 Rotational and extensional like velocity field induced near torus surface by Stokeslet and doublet distribution.

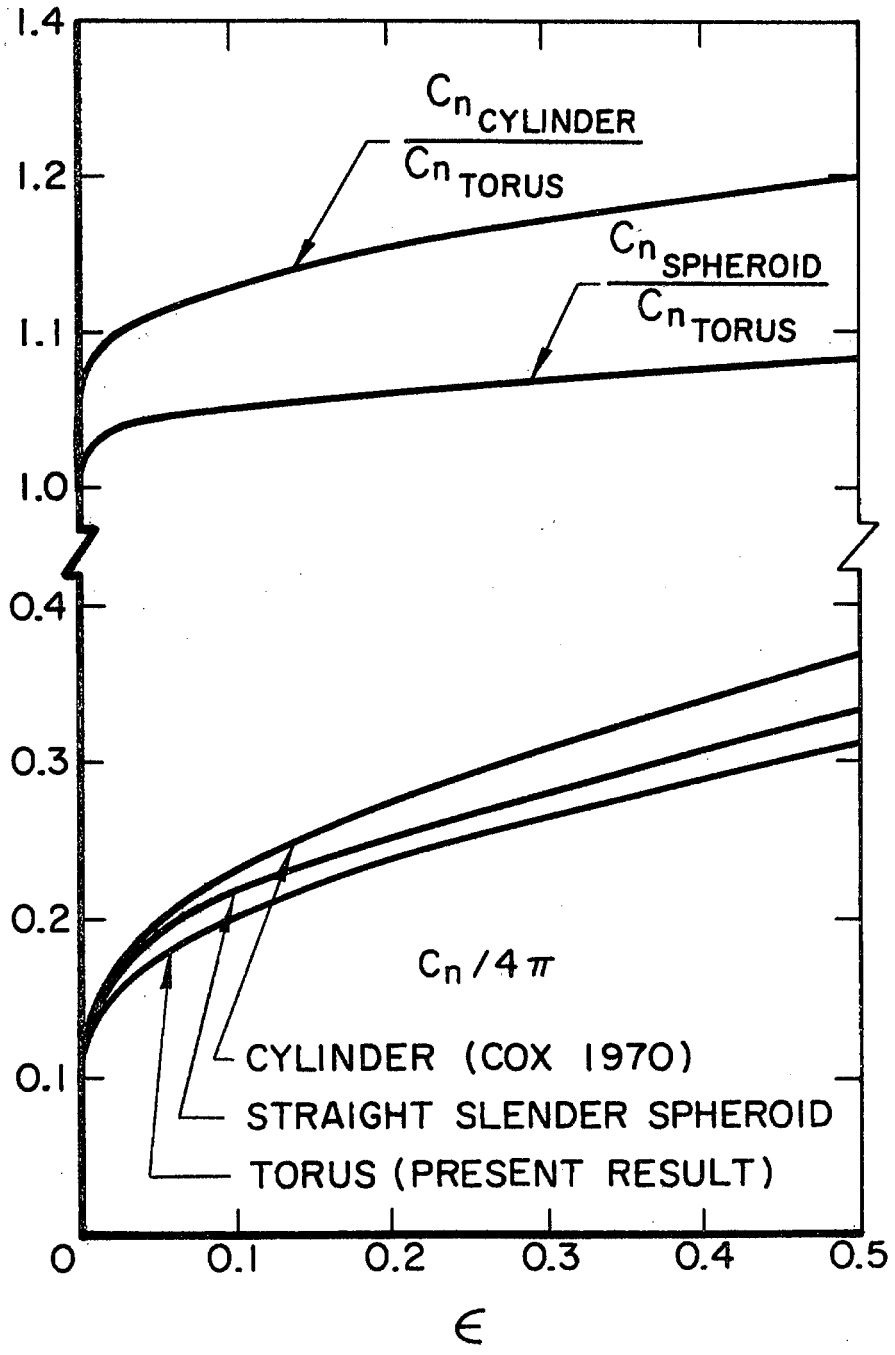

Figure 2. 1. 4 Drag coefficient comparisons for a torus translating along its longitudinal axis.

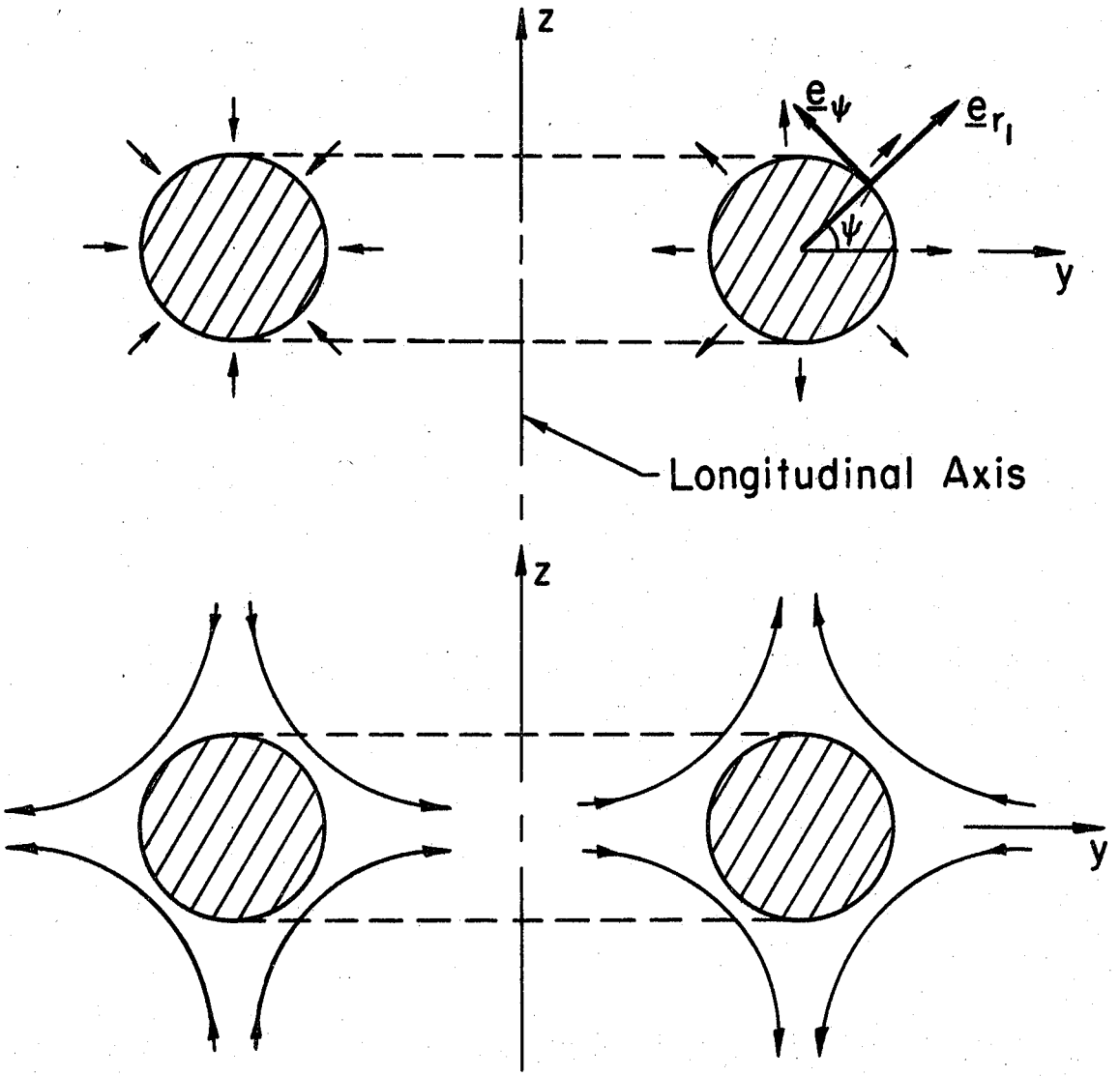

Figure 2. 2. 1 Radial and extensional like velocity field induced near torus surface by Stokeslet and doublet distribution.

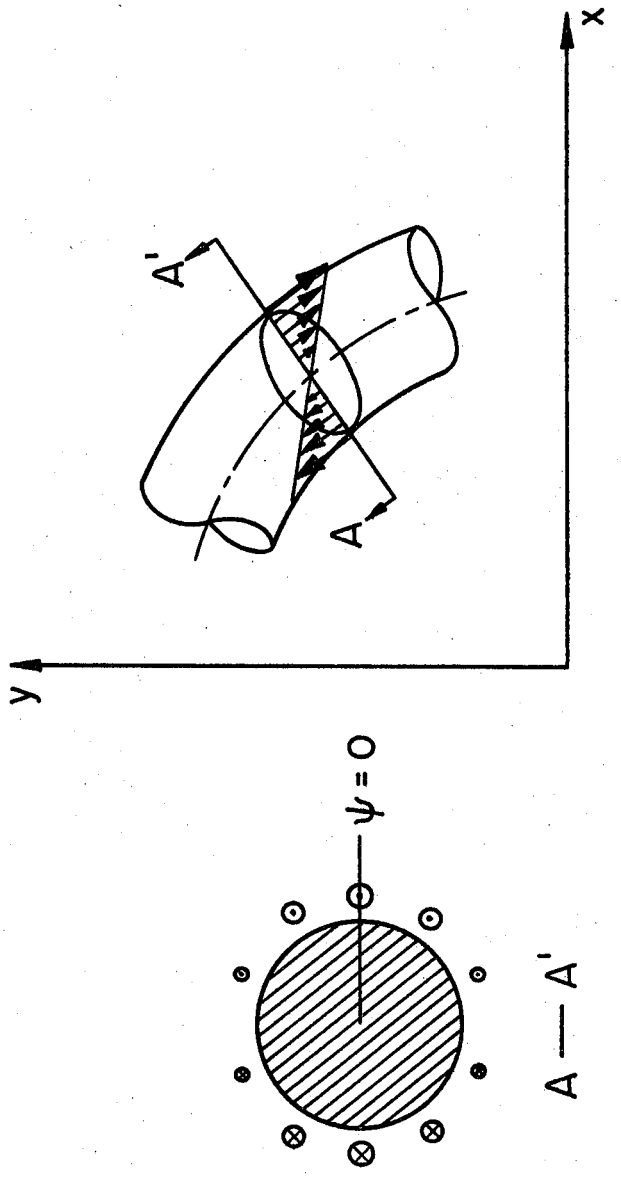

Figure 2. 2. 2 Shear like velocity field induced near torus surface by Stokeslet and doublet distribution.

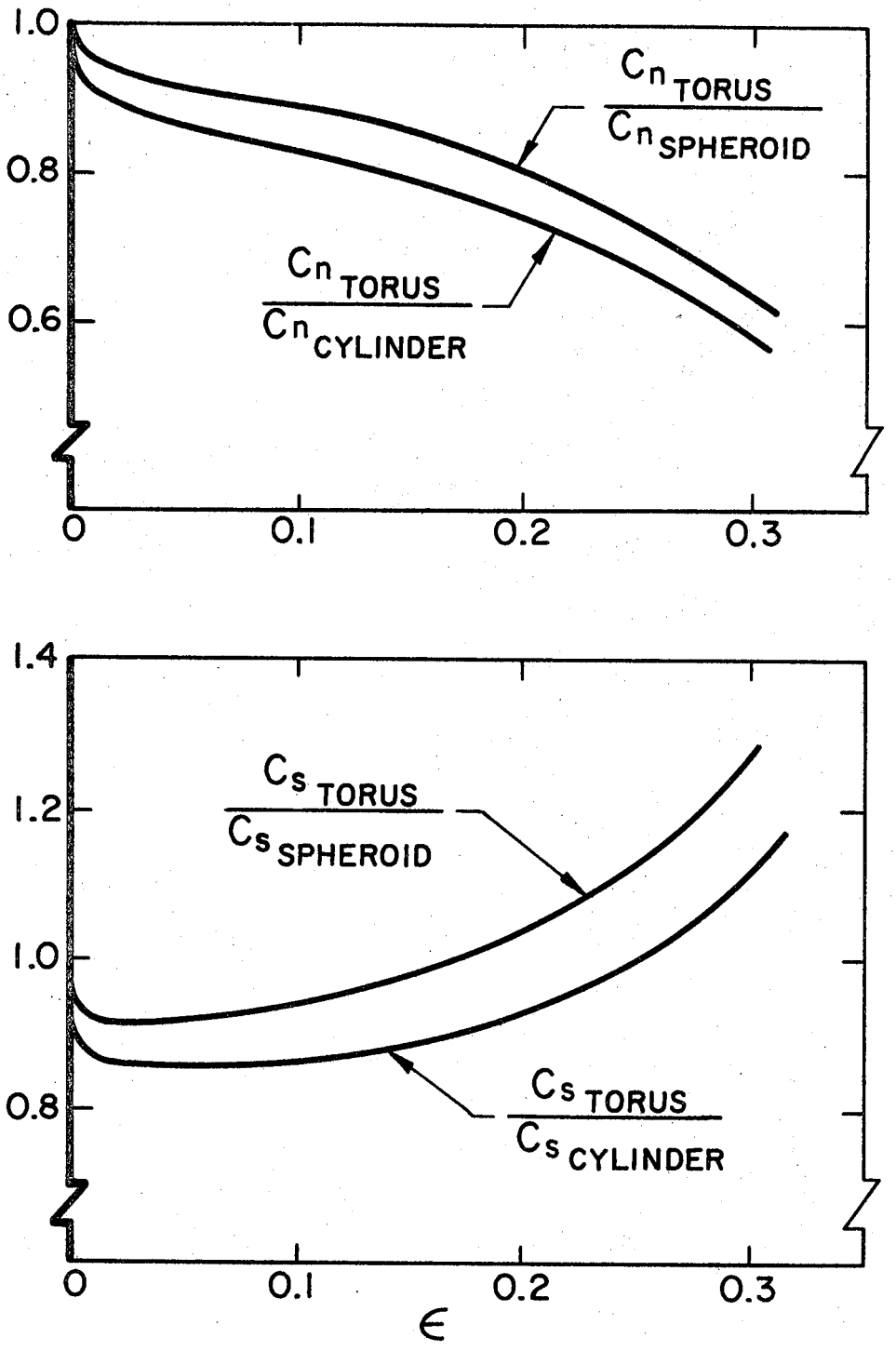

Figure 2. 2. 3 Drag coefficient comparisons for a torus translating in its own plane.

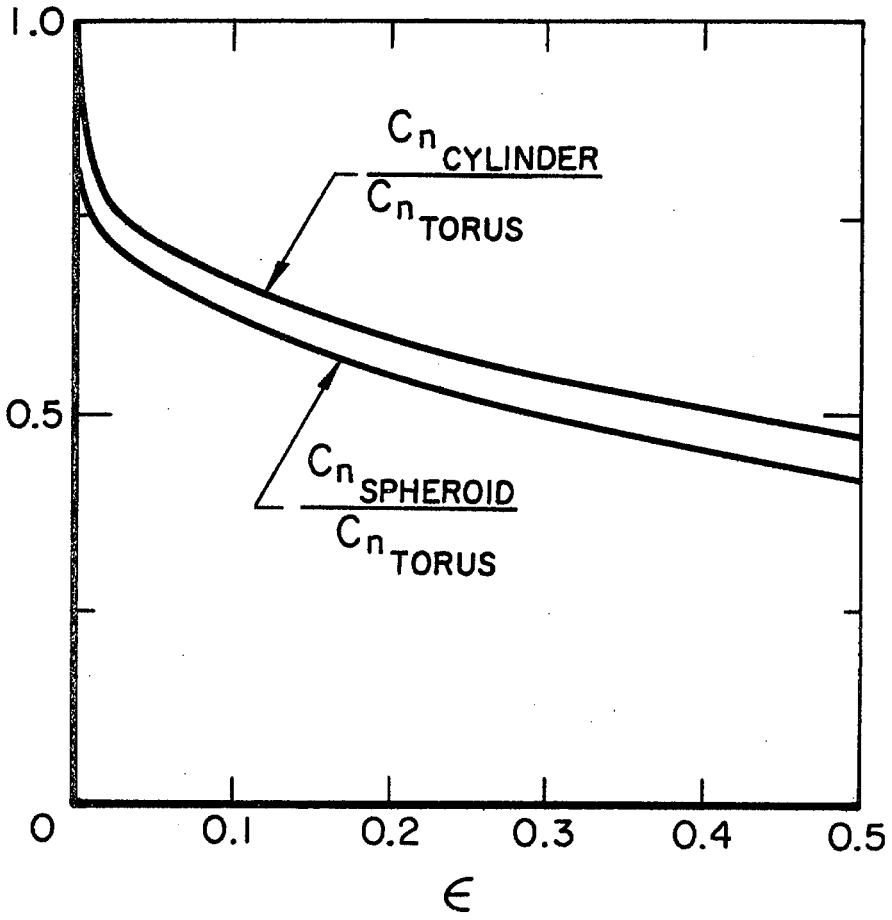

Figure 2. 3. 1 Drag coefficient comparisons for on-edge rotation of a torus.

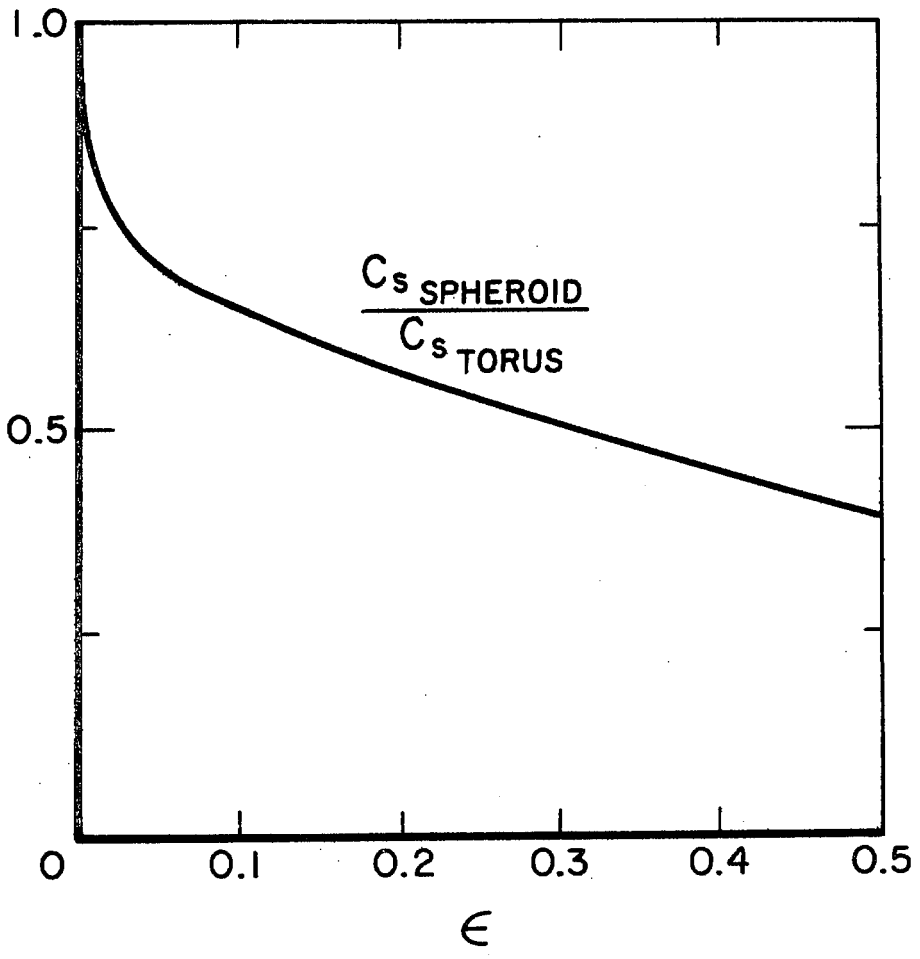

Figure 2. 4. 1 Drag coefficient comparison for a torus rotating in its plane (spinning).

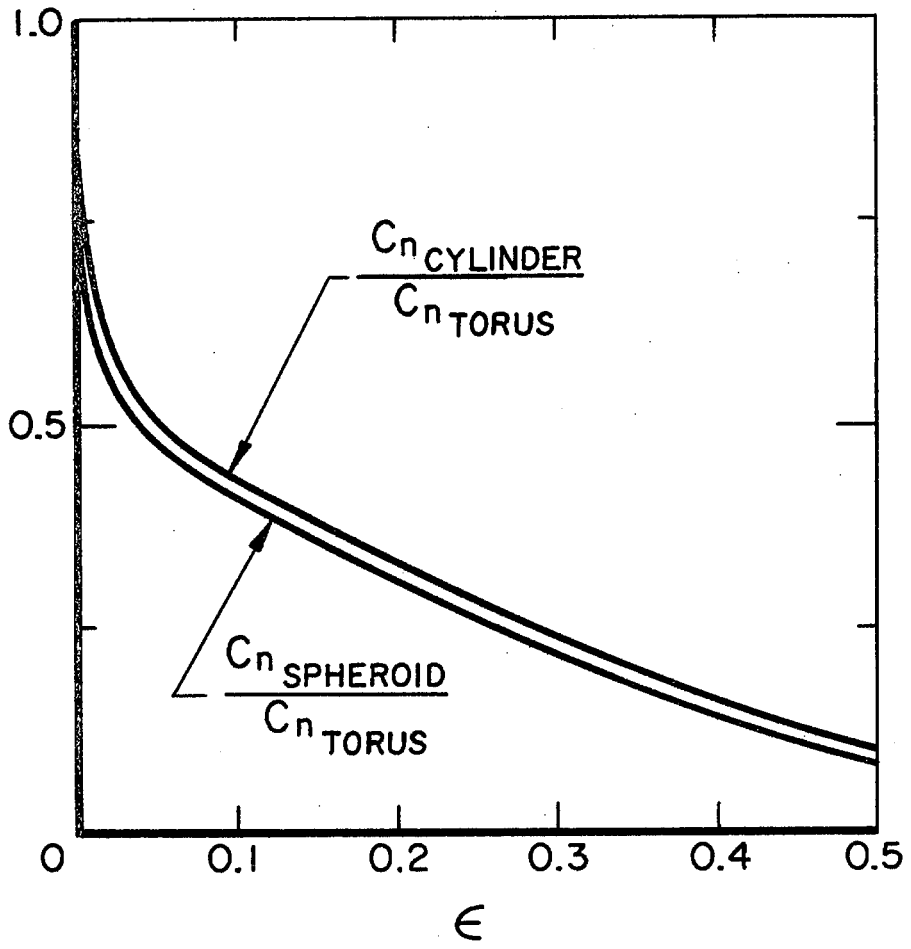

Figure 2. 5. 1 Drag coefficient comparison for a torus in a radial flow.

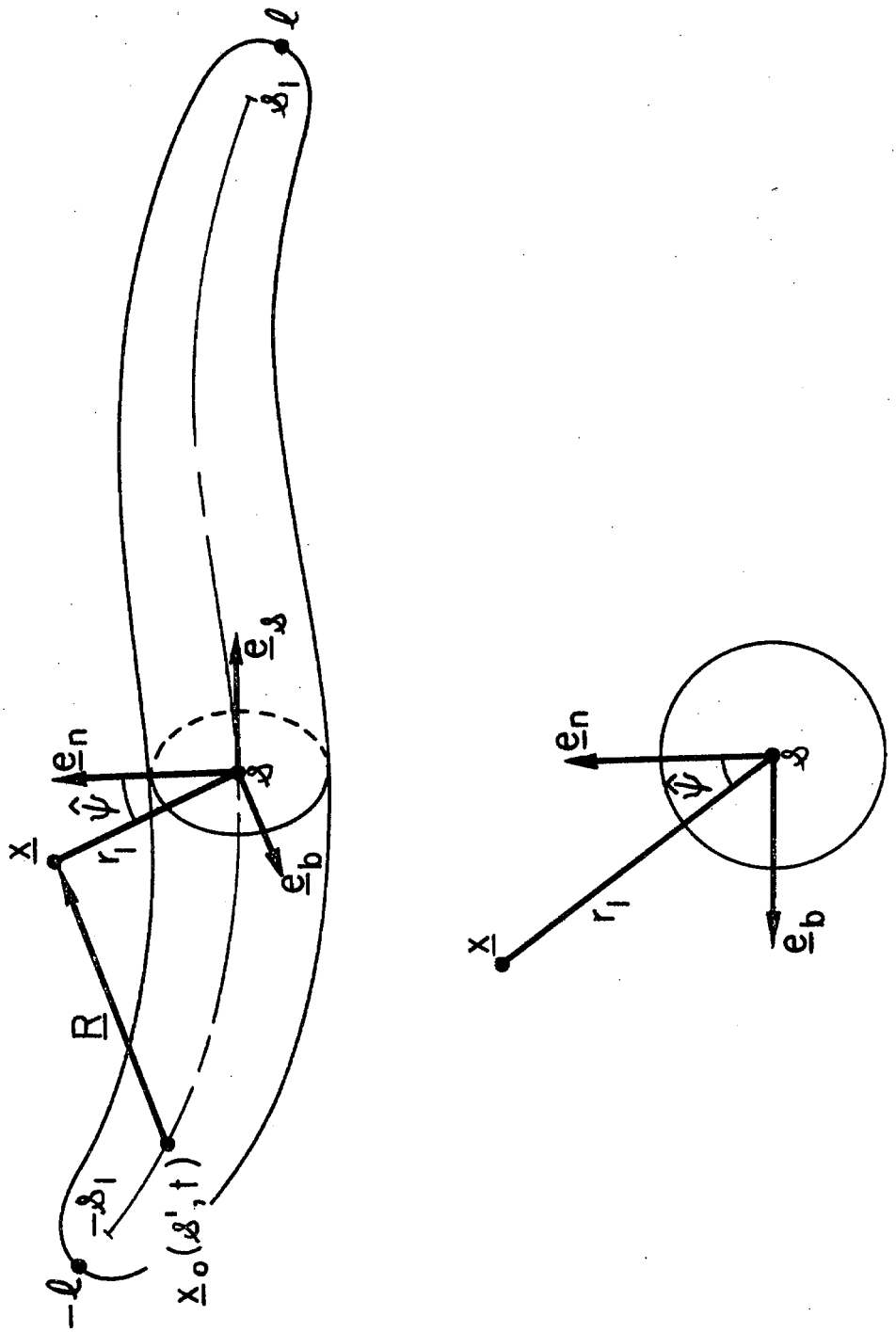

Figure 3.1.1 The geometry and coordinates used for the arbitrary movement of a slender body; note $\hat{\psi} = \pi - \psi$.

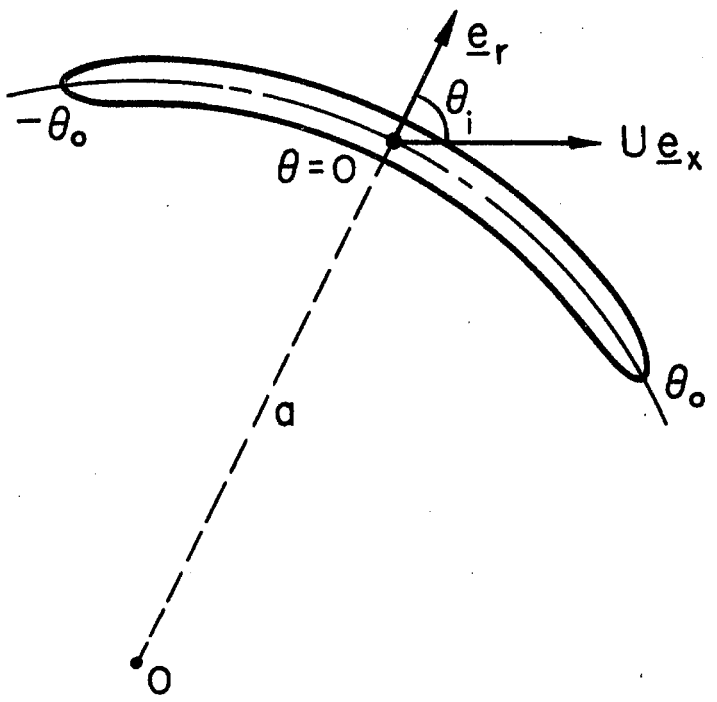

Figure 3. 3. 1 Description of geometry used for a partial torus.

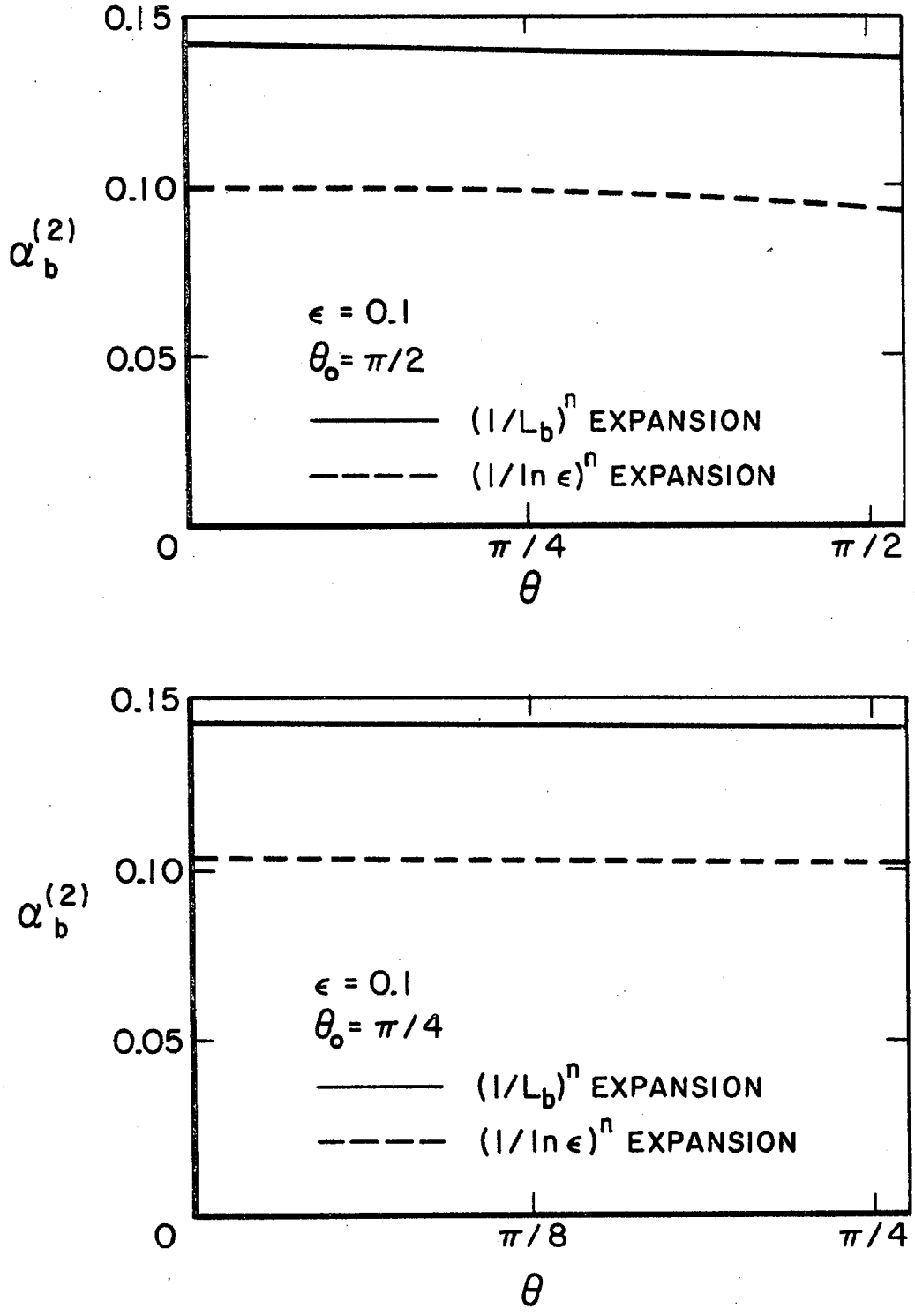

Figure 3.3.2 Second iterate of the Stokeslet strength found using the present theory (L_b^{-n} expansion) and the previous methods for the translation of a partial torus perpendicular to its plane.

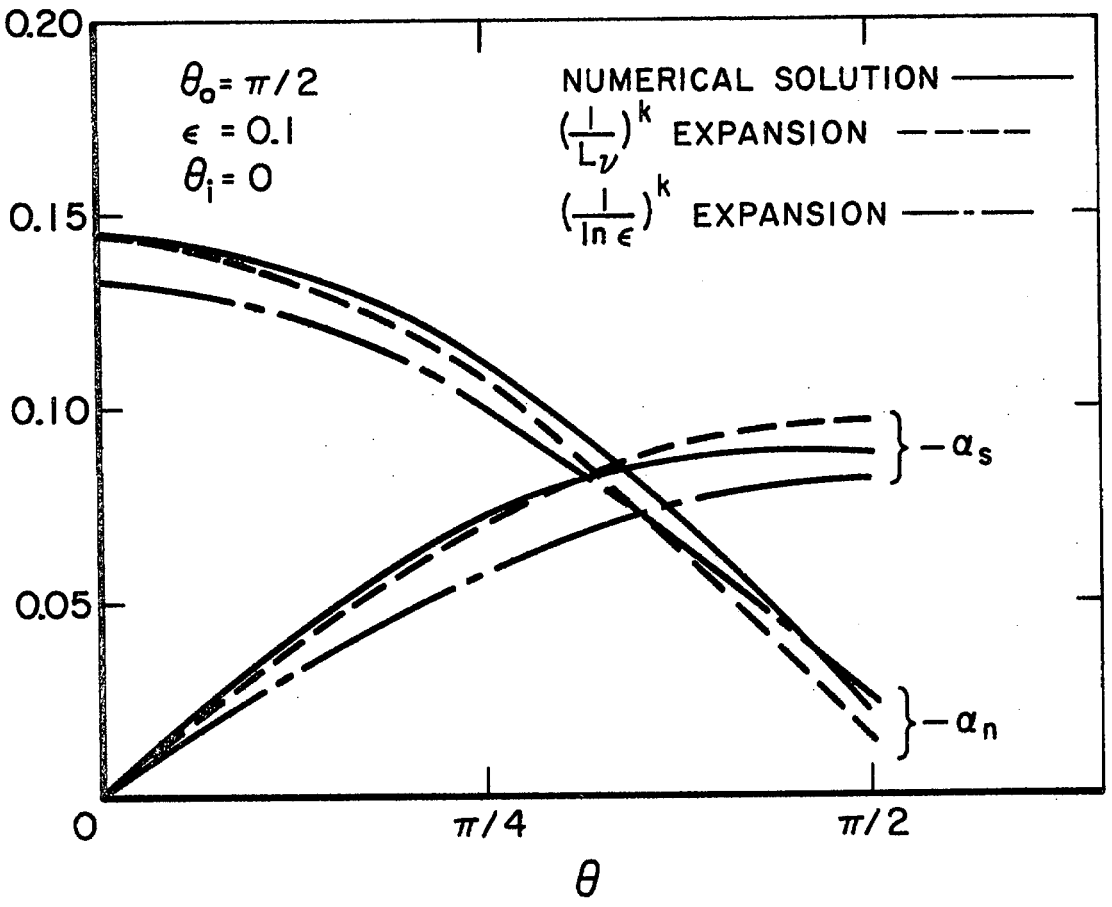

Figure 3. 3. 3 Second iterate of the Stokeslet strength found using the present theory (L_b^{-k} expansion) and the previous methods compared to the numerical solution for the translation of a partial torus in its plane.

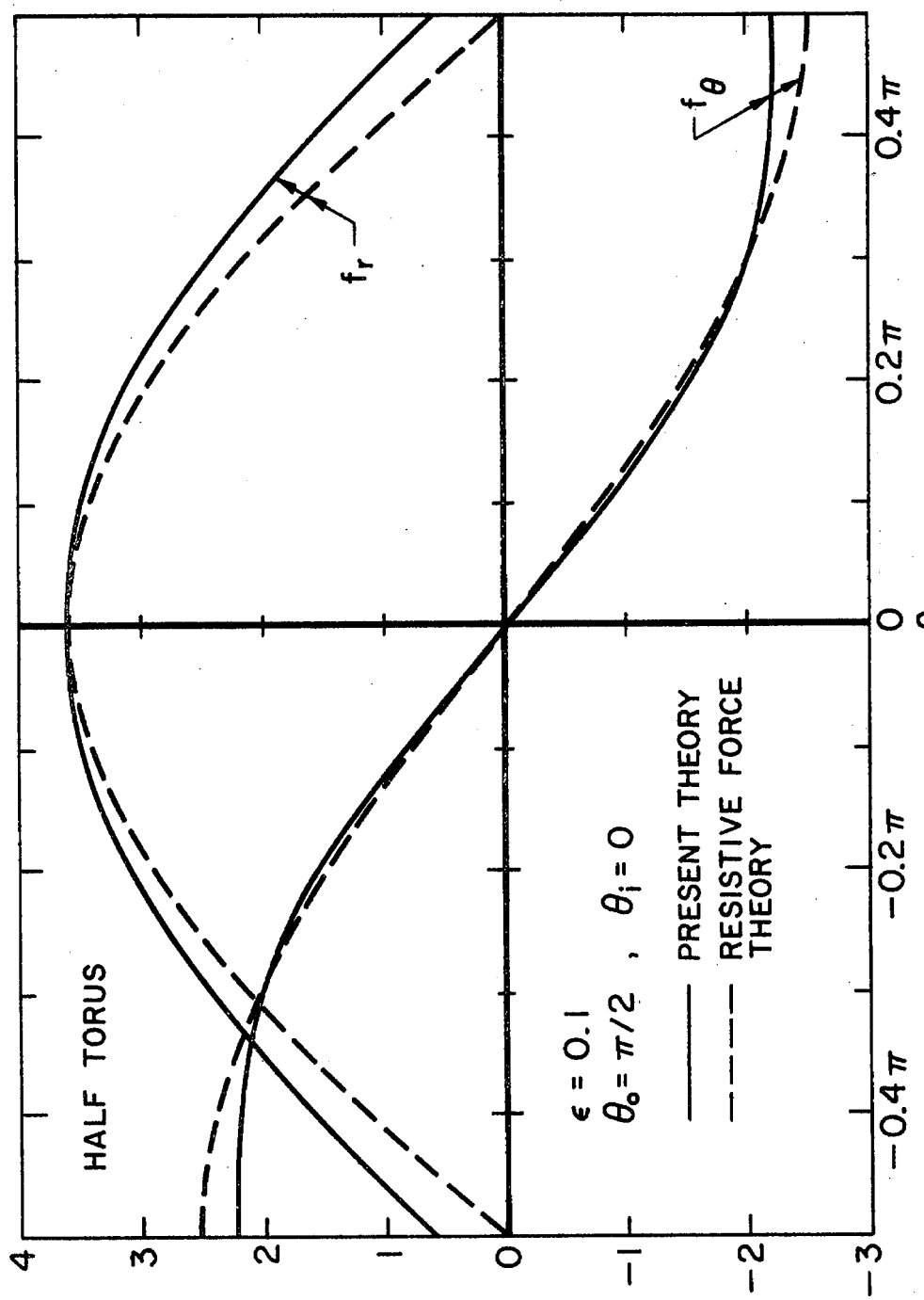

Figure 3.3.4 Comparison between the classical resistive-force theory and the numerical results for the translation of a partial torus in its plane (force/length nondimensionalized by μU).

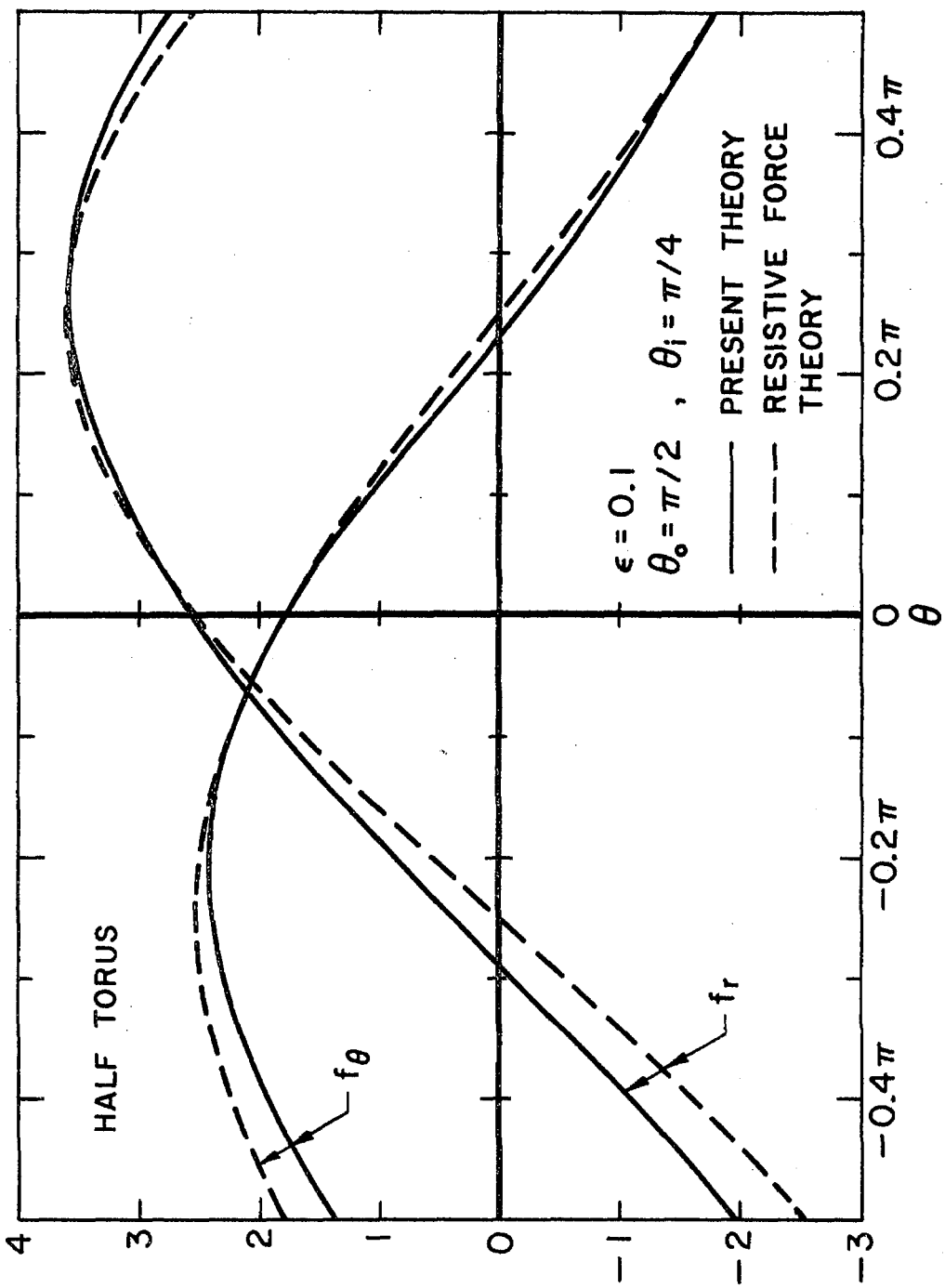

Figure 3.3.5 Comparison between the classical resistive-force theory and the numerical results for the translation of a partial torus in its plane (force/length nondimensionalized by μU).

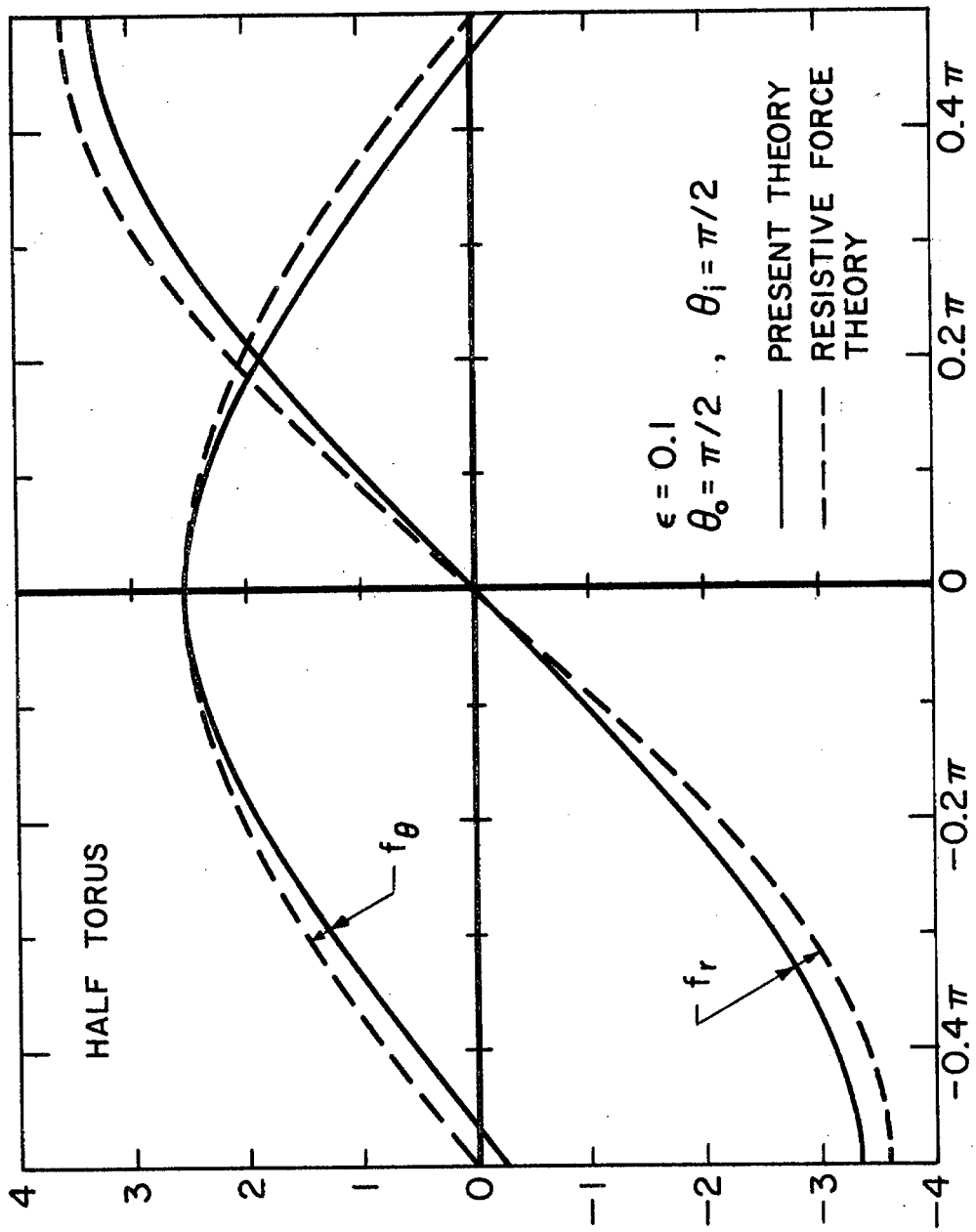

Figure 3.3.6 Comparison between the classical resistive-force theory and the numerical results for the translation of a partial torus in its plane (force/length nondimensionalized by μU).

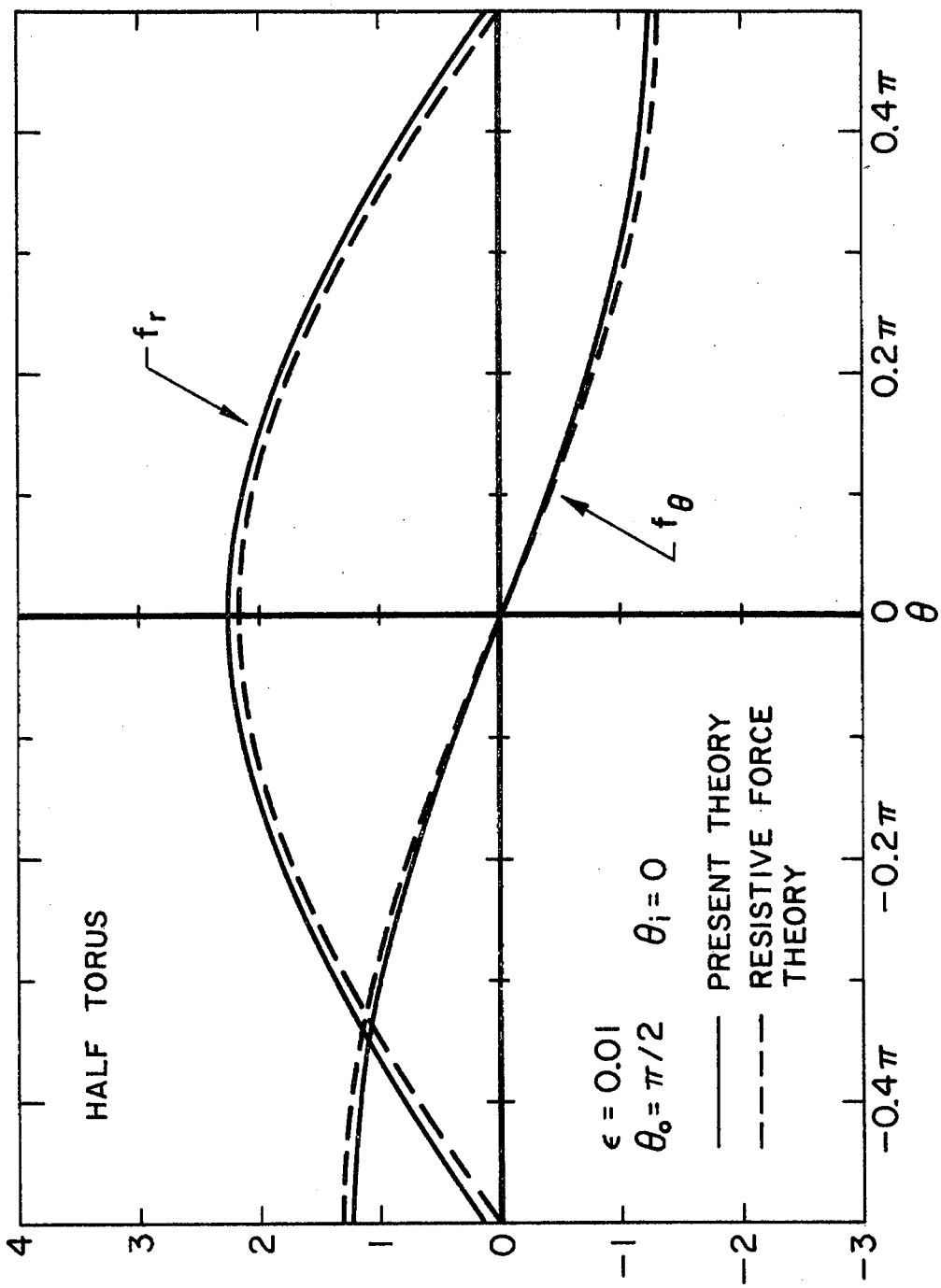

Figure 3.3.7 Comparison between the classical resistive-force theory and the numerical results for the translation of a partial torus in its plane (force/length nondimensionalized by μU).

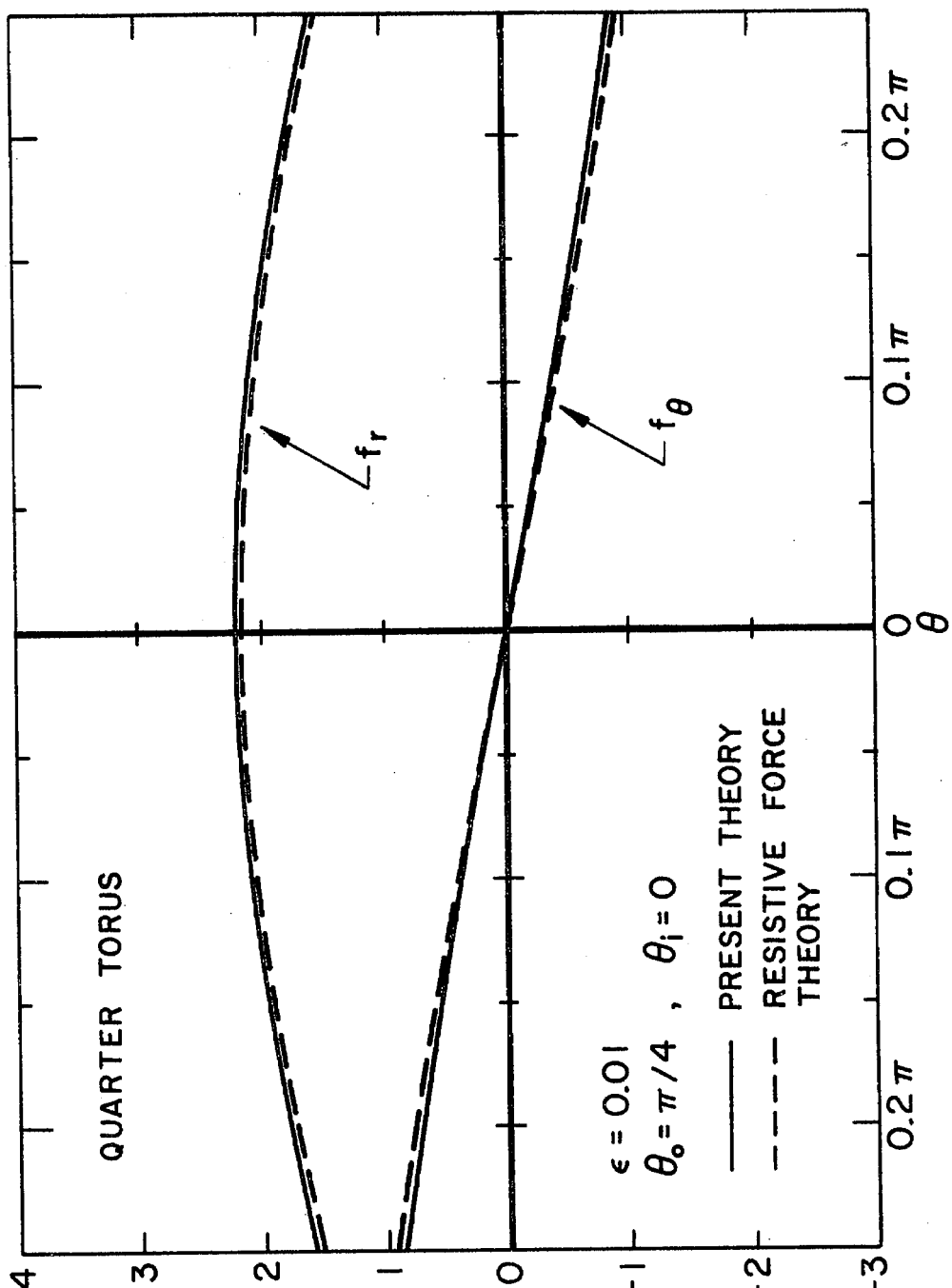

Figure 3.3.8 Comparison between the classical resistive-force theory and the numerical results for the translation of a partial torus in its plane (force/length nondimensionalized by μ U).

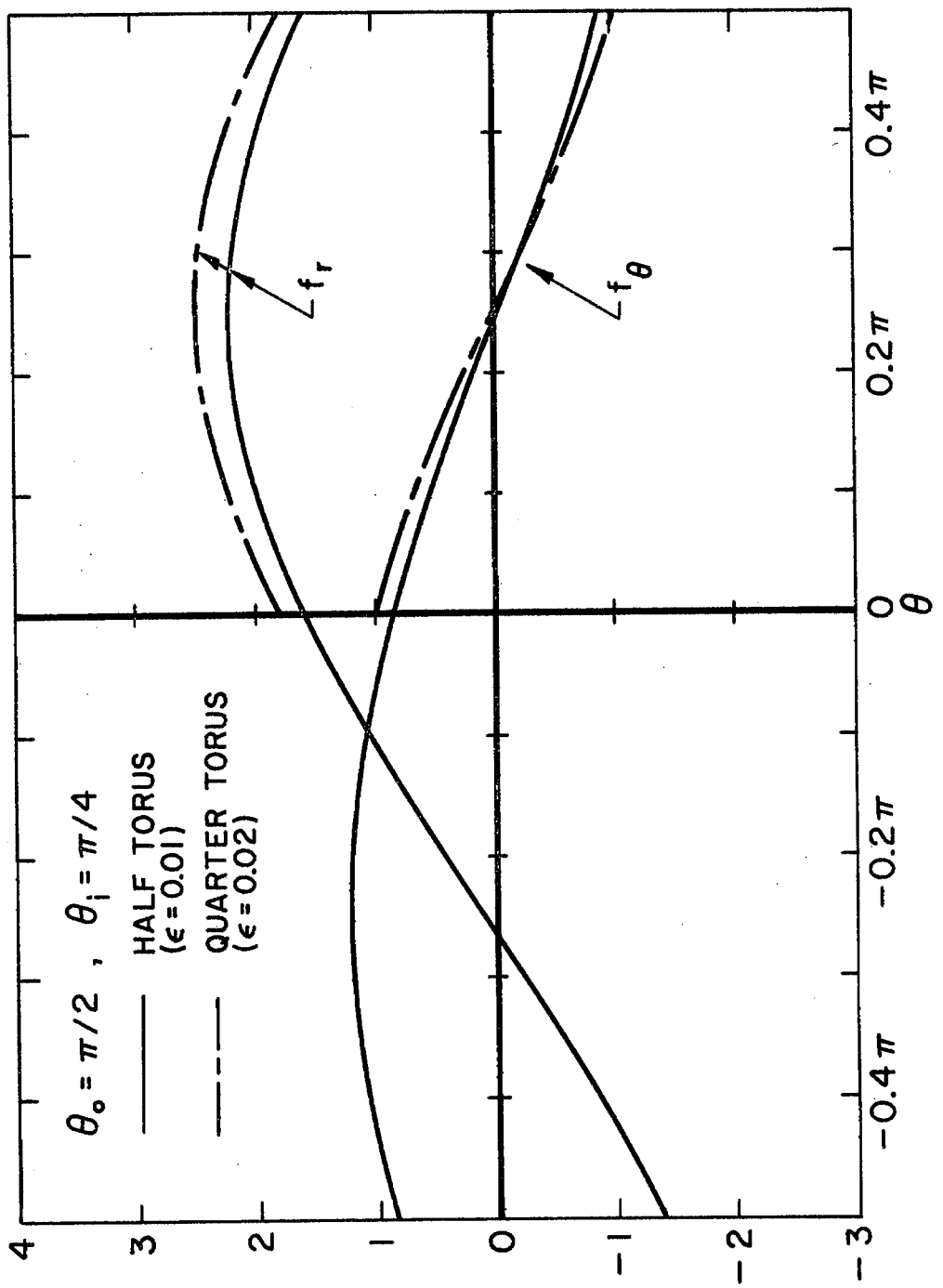

Figure 3.3.9 Comparison of the numerical results for a half torus and a quarter torus with overlapping centerlines for $0 \leqslant \theta \leqslant \pi/2$ (force/length nondimensionalized by μU).

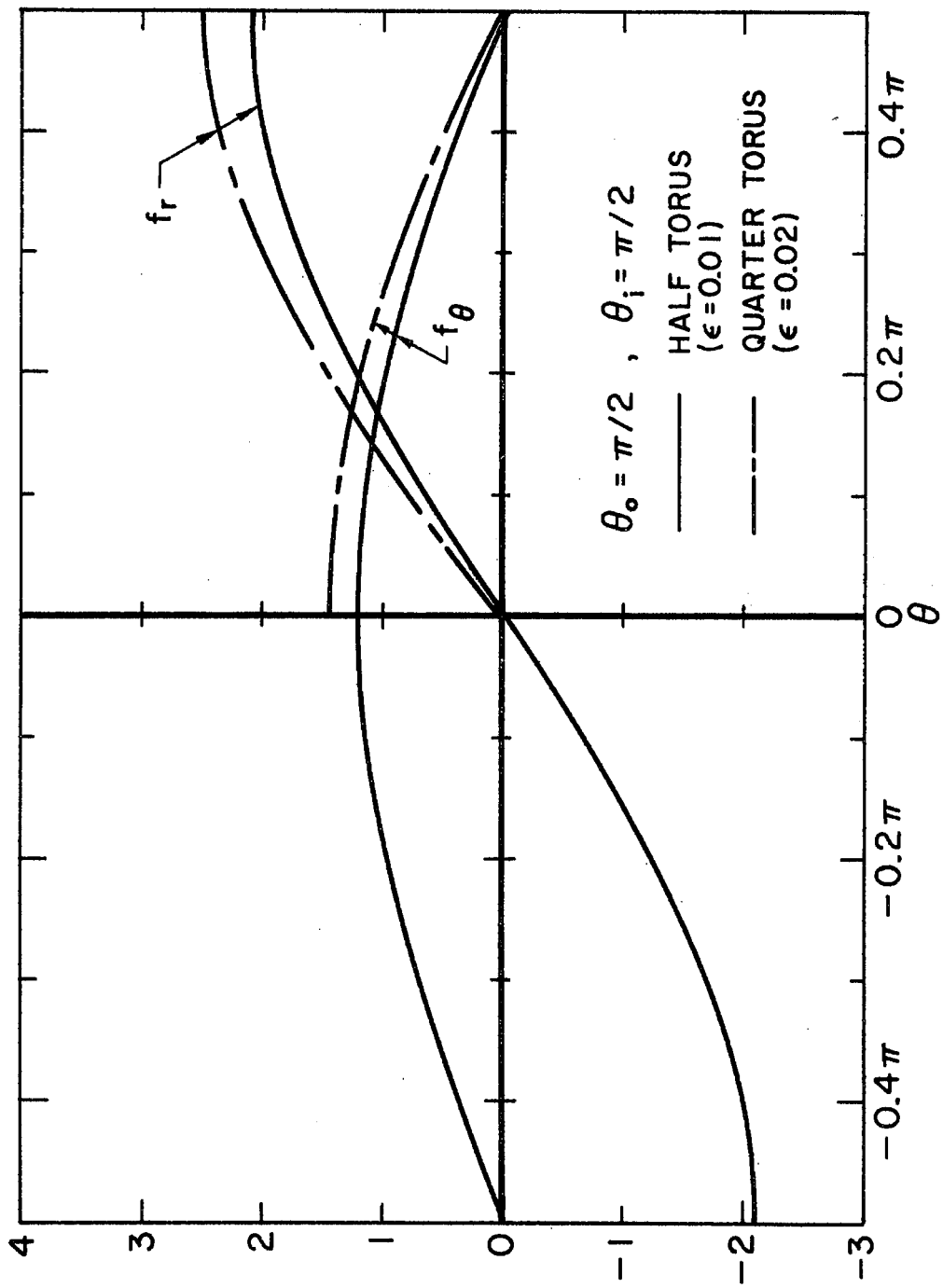

Figure 3.3.10 Comparison of the numerical results for a half torus and a quarter torus with overlapping centerlines for $0 \ll \theta \ll \pi/2$ (force/length nondimensionalized by μ U).

TABLE 4. 1. 1

Spermatozoa	b(μ)	ℓ(μ)	a(μ)	λ(μ)	n	C($\frac{\mu}{sec}$)	freq (sec^{-1})	U($\frac{\mu}{sec}$)
Chaetopterus	0. 1	15. 94	3. 8	19. 5	1. 25	517	26. 5	105
Oyster	0. 1	23. 5	4. 65	25. 6	1. 4	1100	43. 1	163. 8

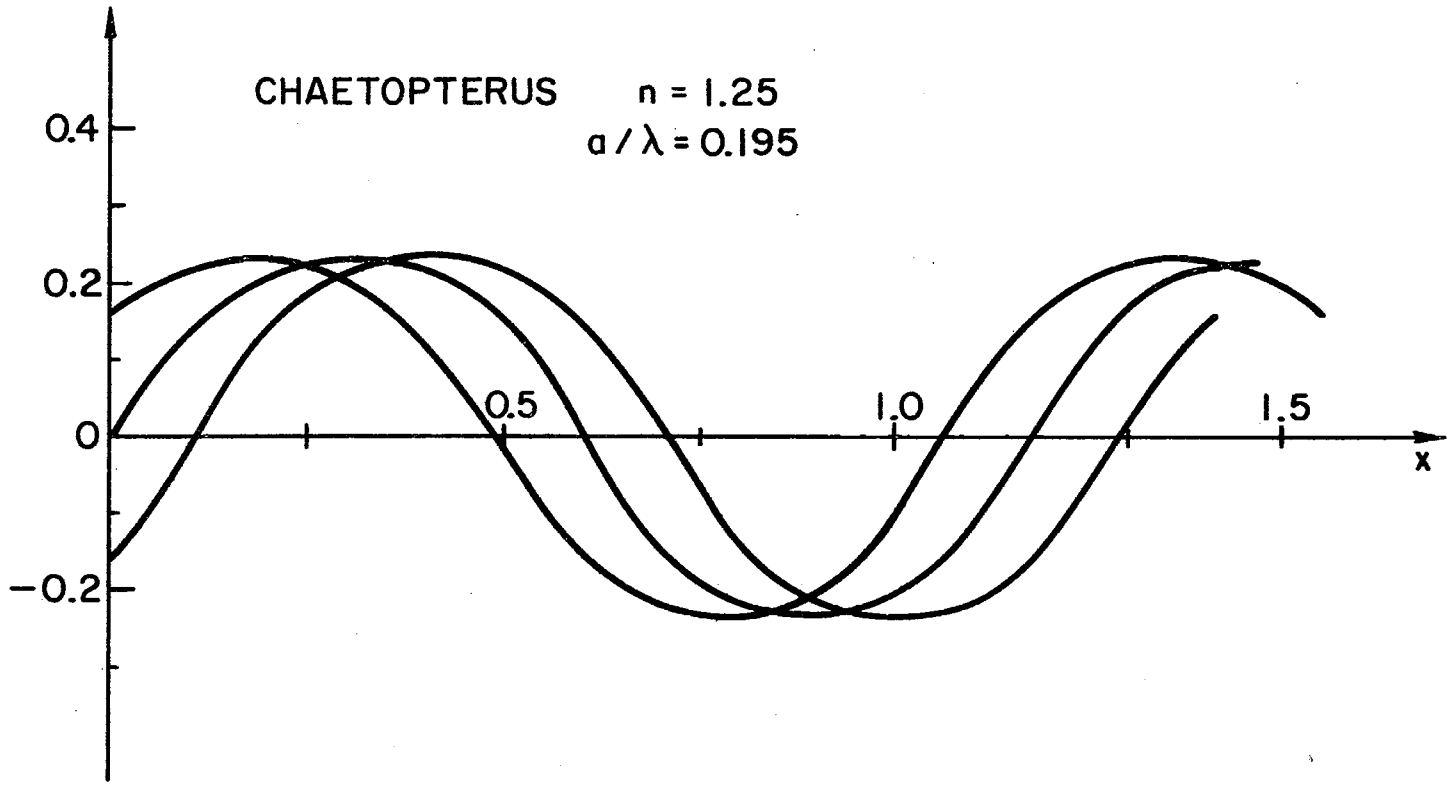

Figure 4. 1. 1 Typical waveform shown at a few instants in equal time progression for the spermatozoa Chaetopterus.

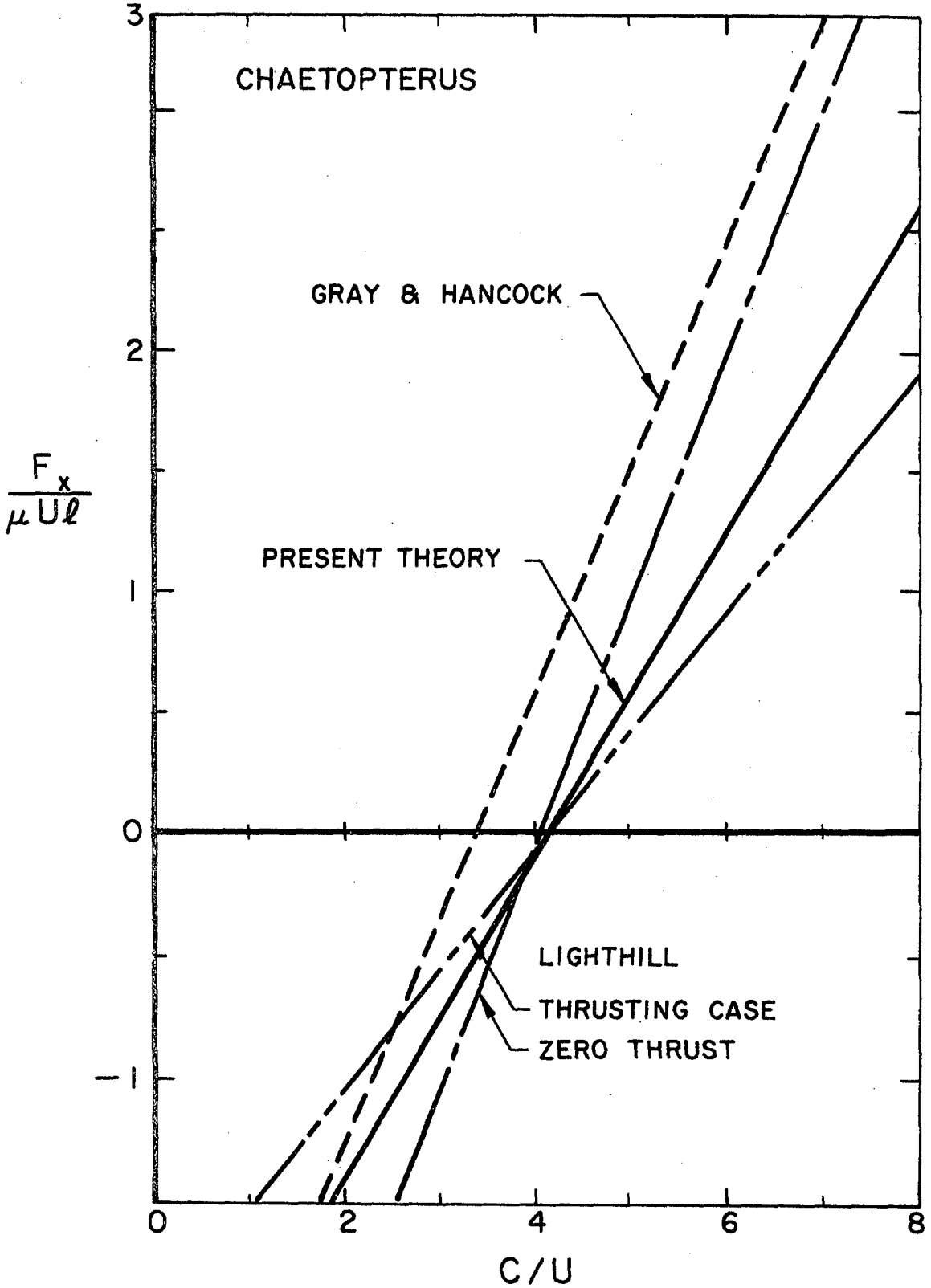

Figure 4. 1. 2 The average thrust/cycle calculated using the methods indicated for a headless spermatozoa.

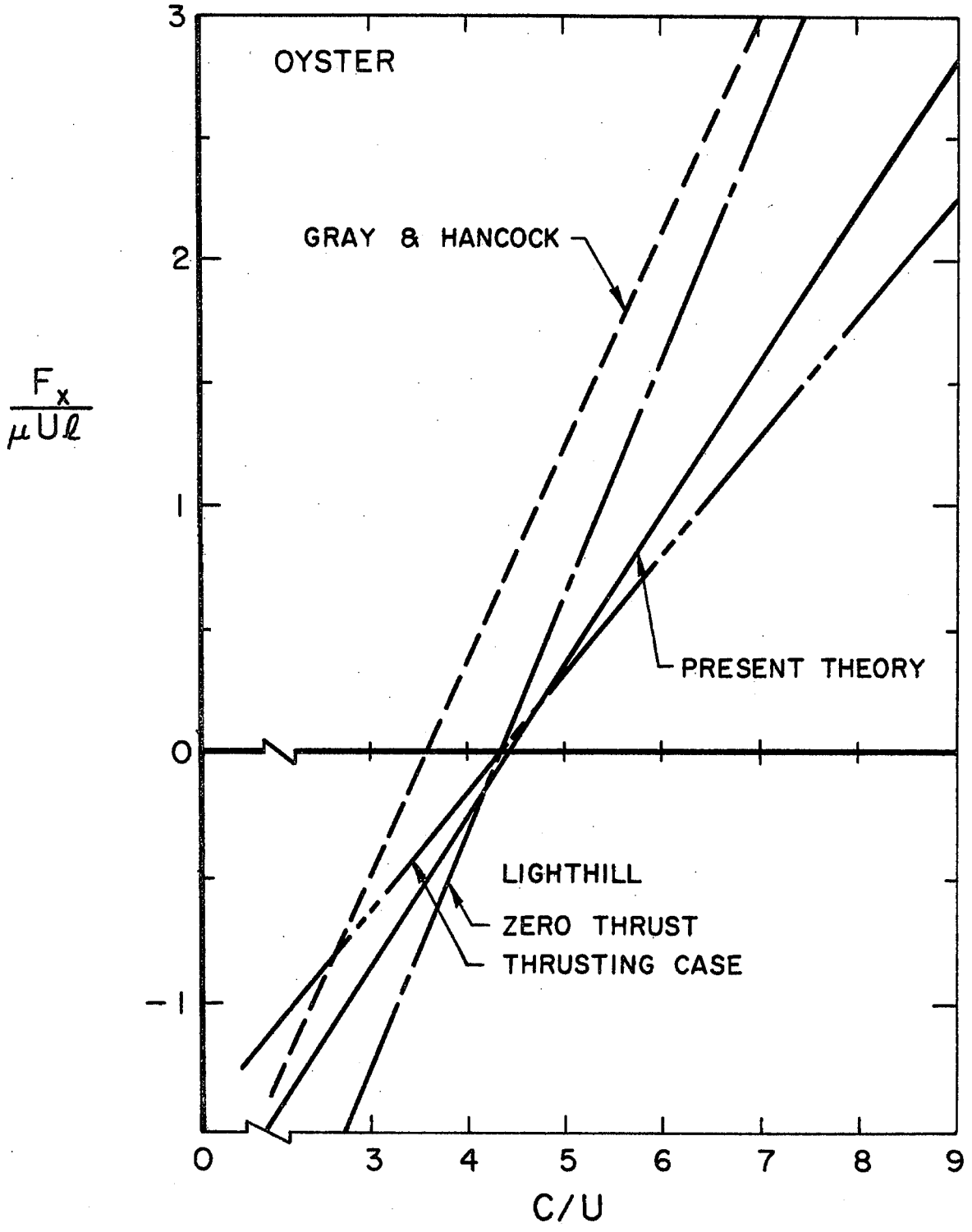

Figure 4.1.3 The average thrust/cycle calculated using the methods indicated for a headless spermatozoa.

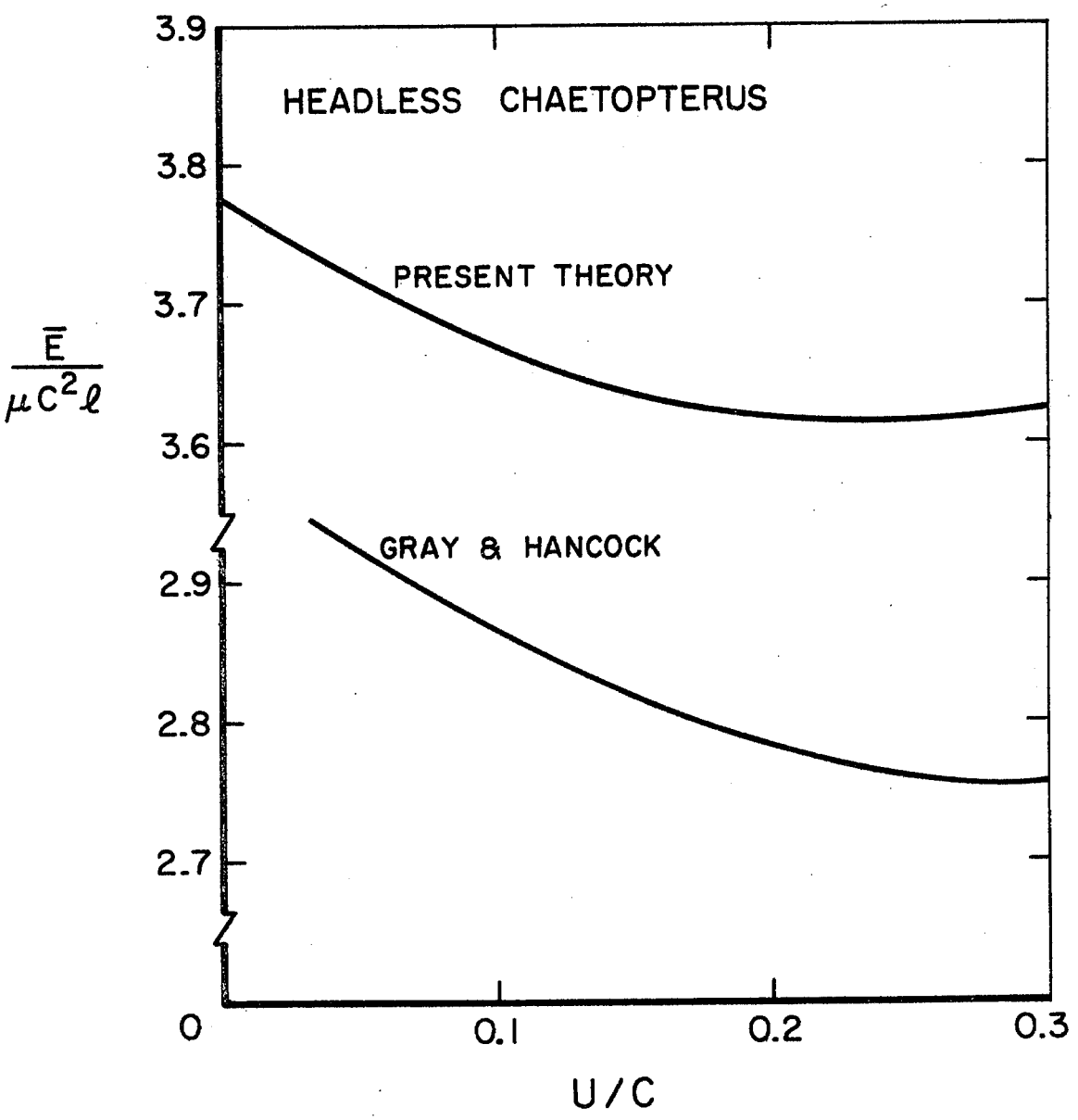

Figure 4. 1. 4 Average energy expended per cycle by the flagellum calculated using the present theory and the Gray and Hancock theory.

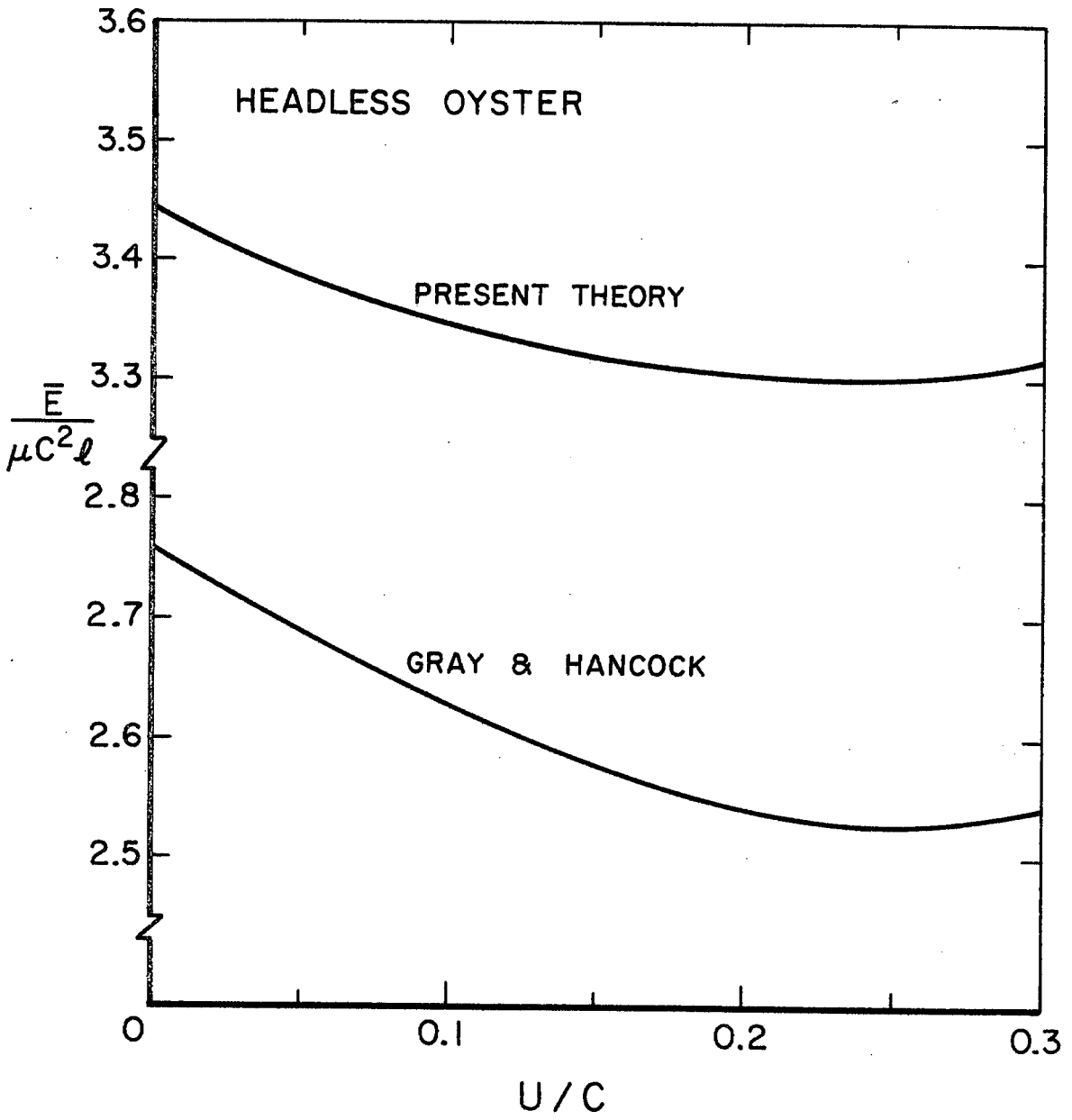

Figure 4.1.5 Average energy expended per cycle by the flagellum calculated using the present theory and the Gray and Hancock theory.

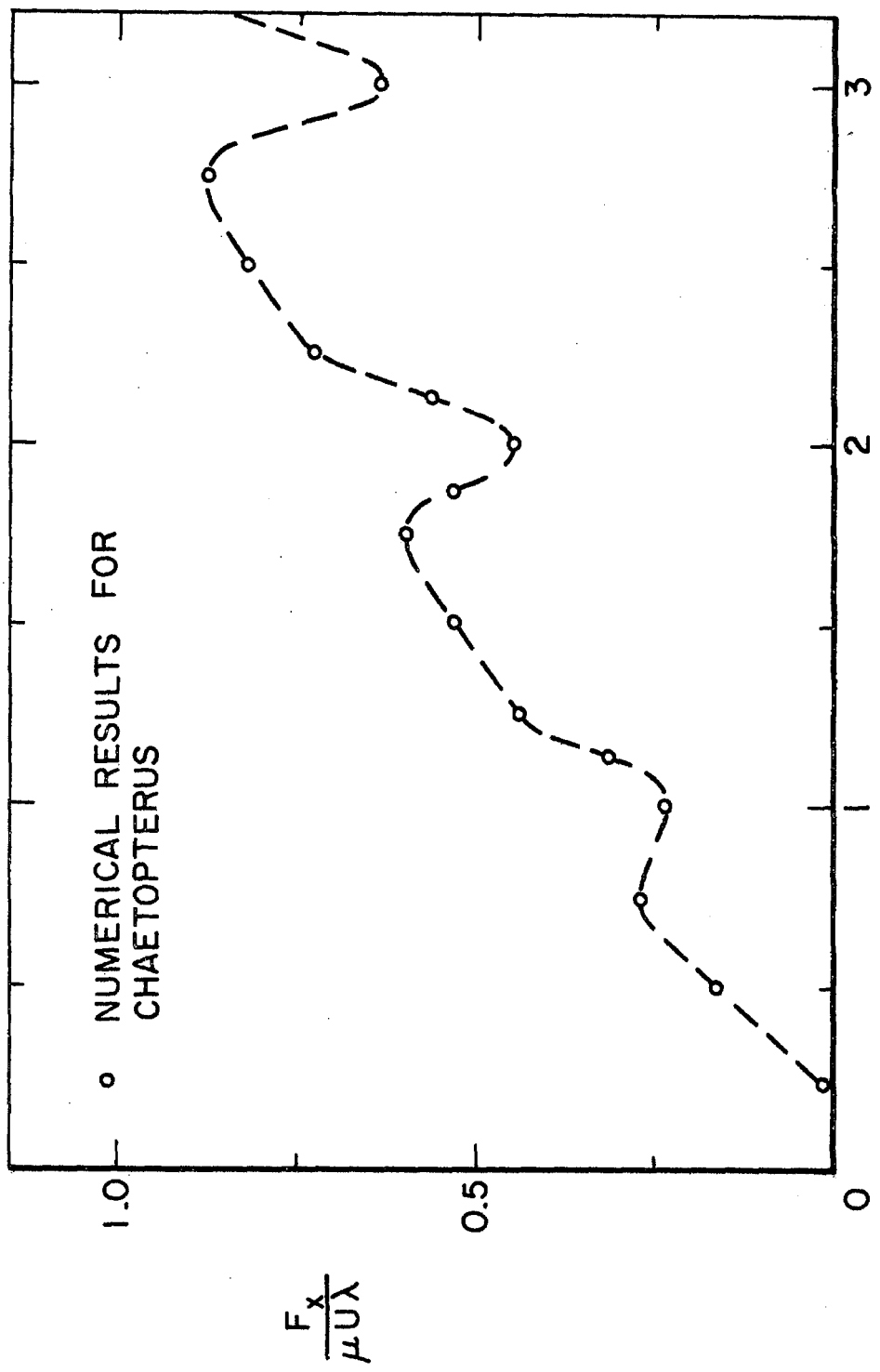

Figure 4.1.6 Average thrust per cycle versus number of waves, n, along the flagellum.

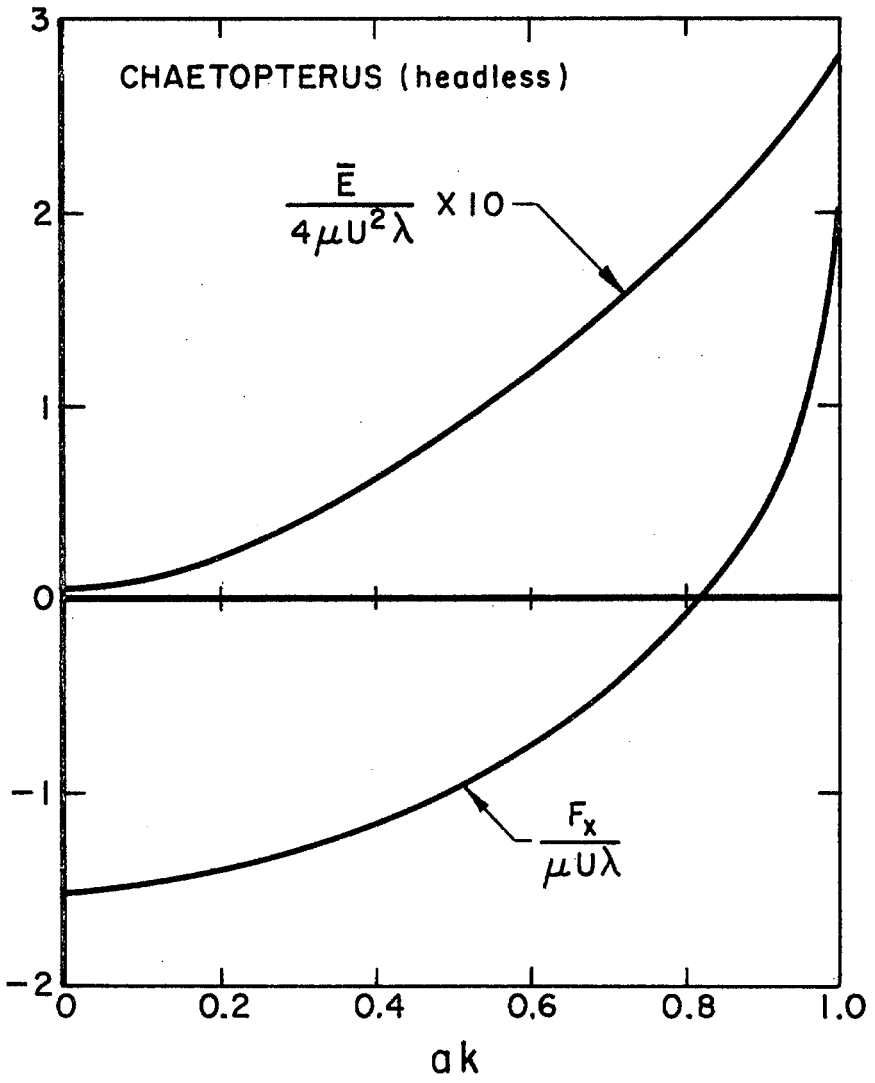

Figure 4.1.7 Average thrust and energy expenditure per cycle versus $ak = \frac{2\pi a}{\Lambda}$.

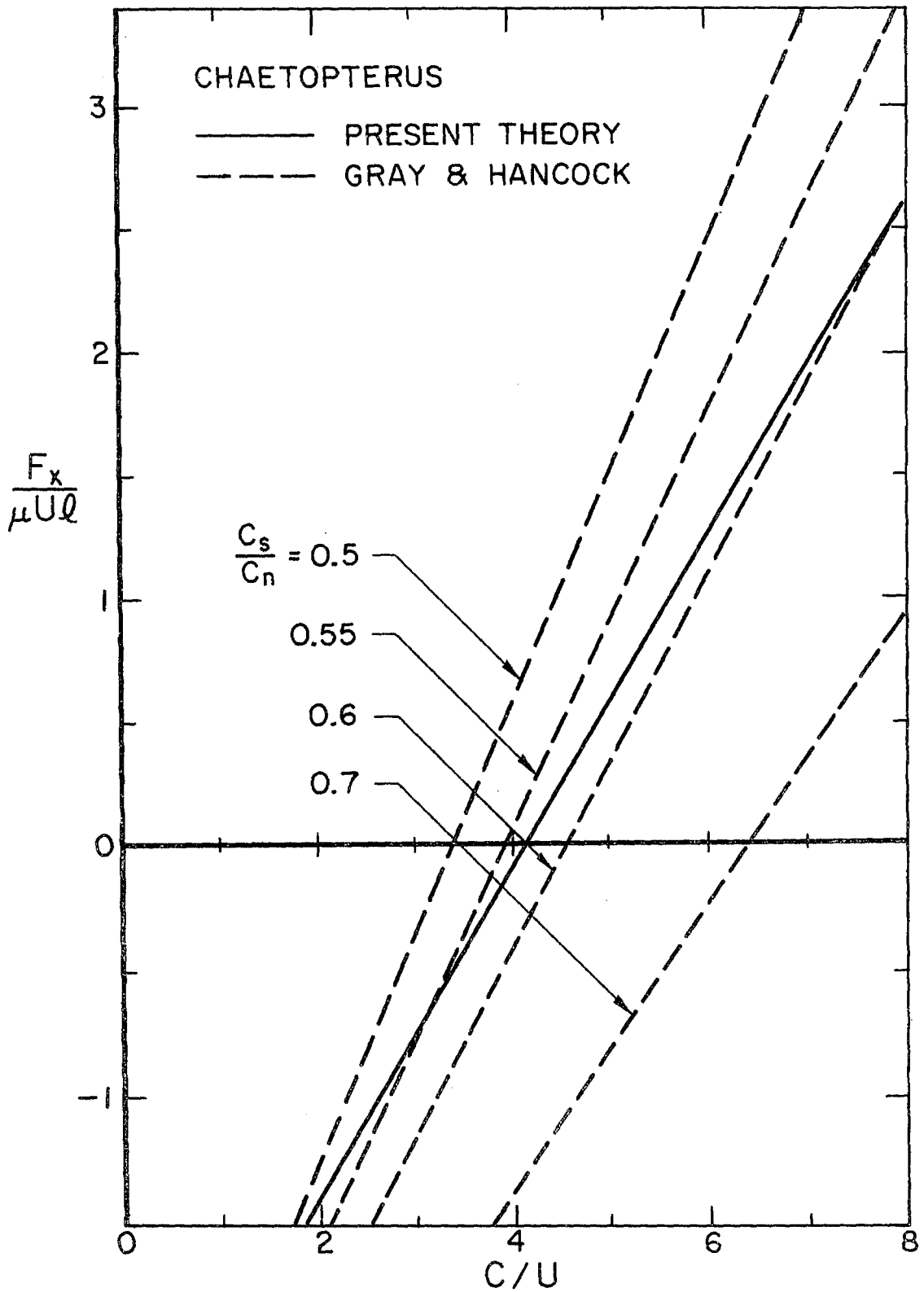

Figure 4.1.8 Comparison of present theory to Gray & Hancock theory with various values of C_s/C_n.

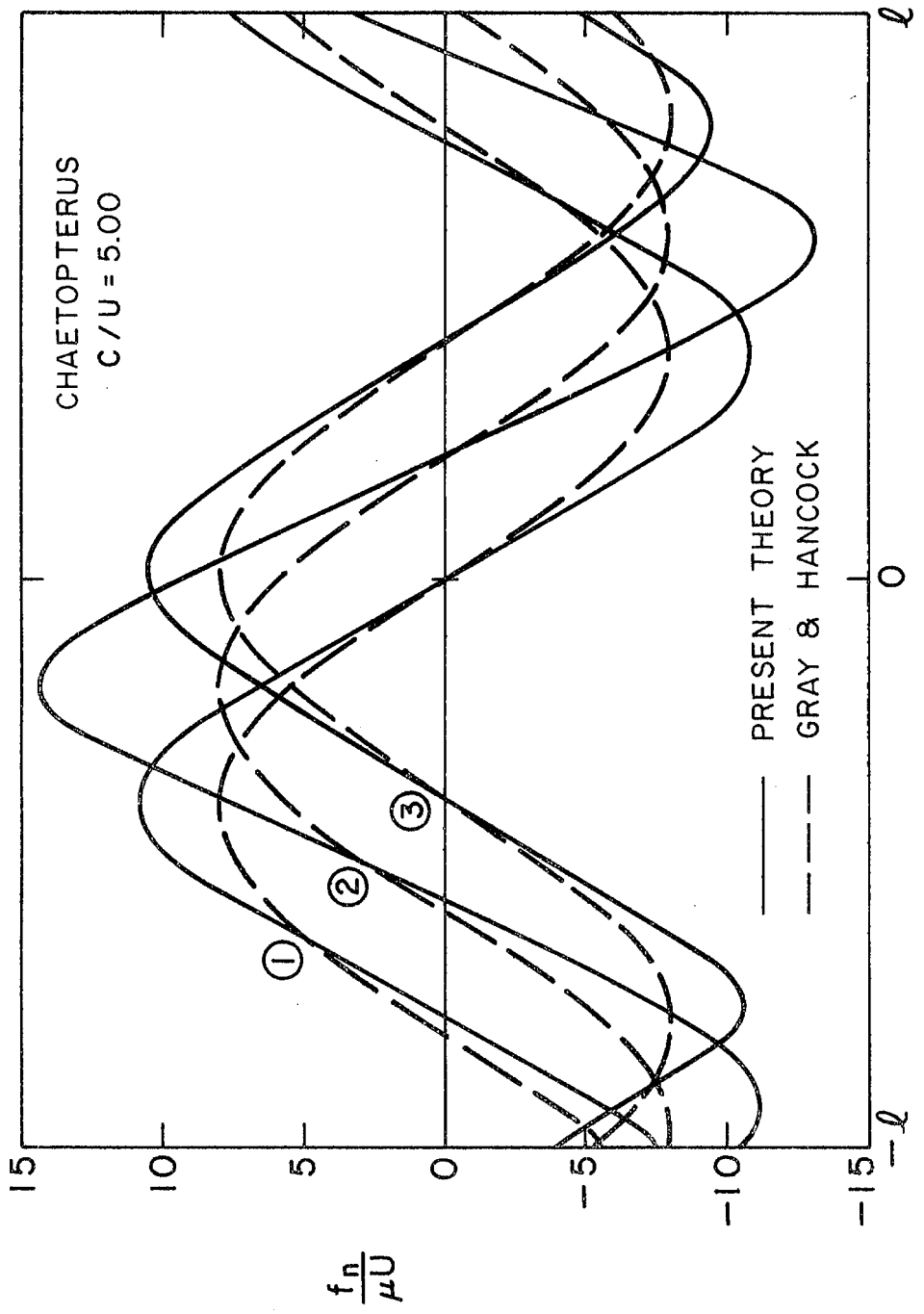

Figure 4.1.9 Comparison of the normal force/length at three instants in equal time progression for a typical case.

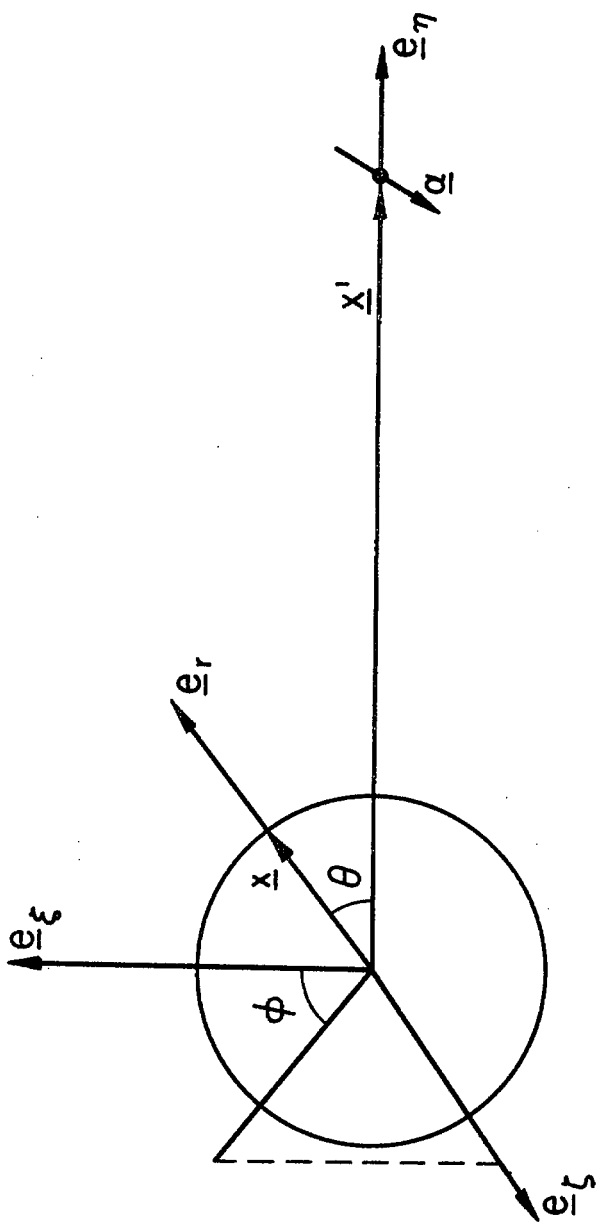

Figure 4.2.1 Coordinates used for calculating mean value of velocity on spherical surface due to a Stokeslet located at $\underline{x}'$.

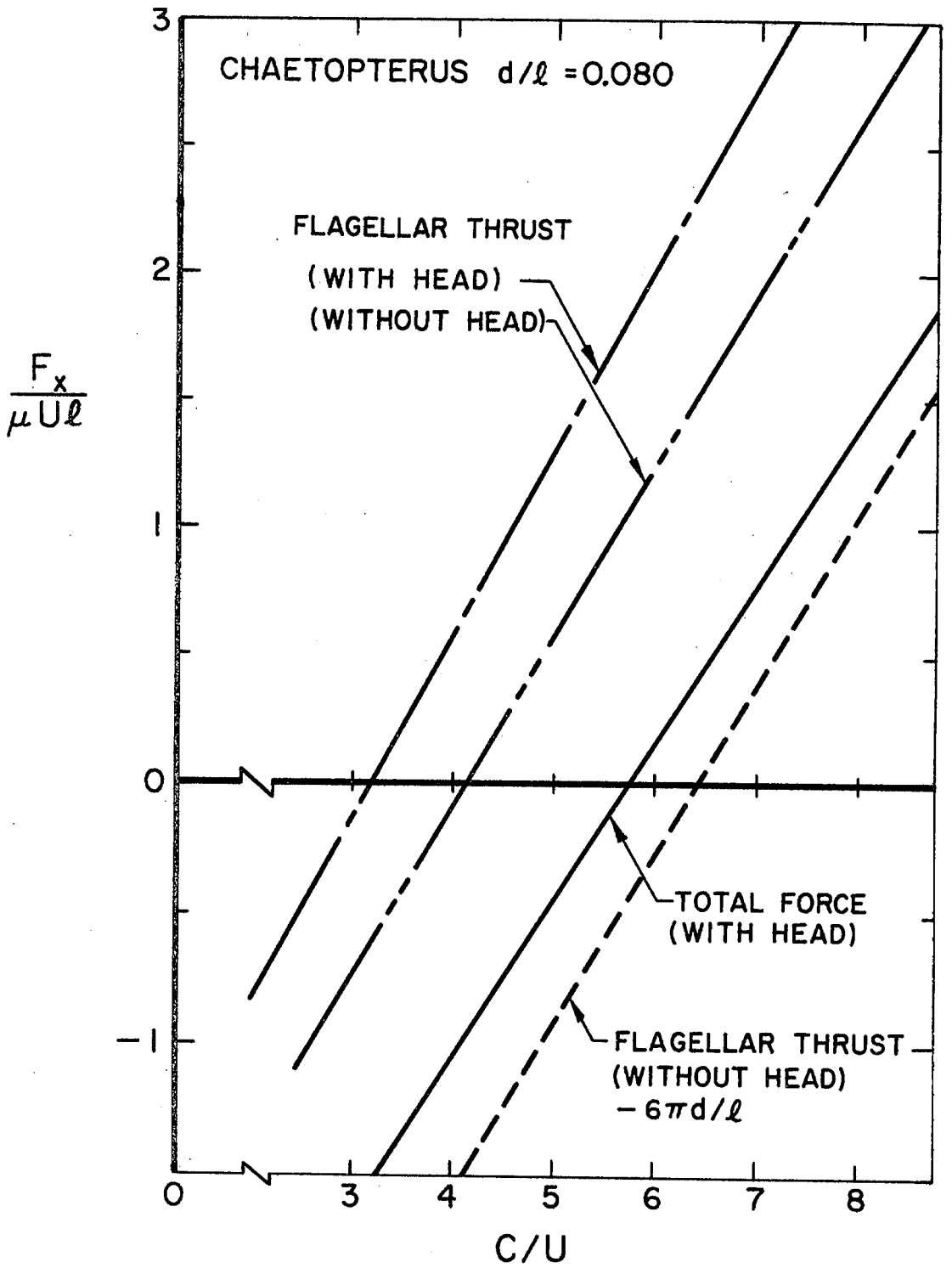

Figure 4.2.2 Average thrust force produced by a flagellum with and without a head present and the total average force on the organism with and without cell body-flagellar interactions.

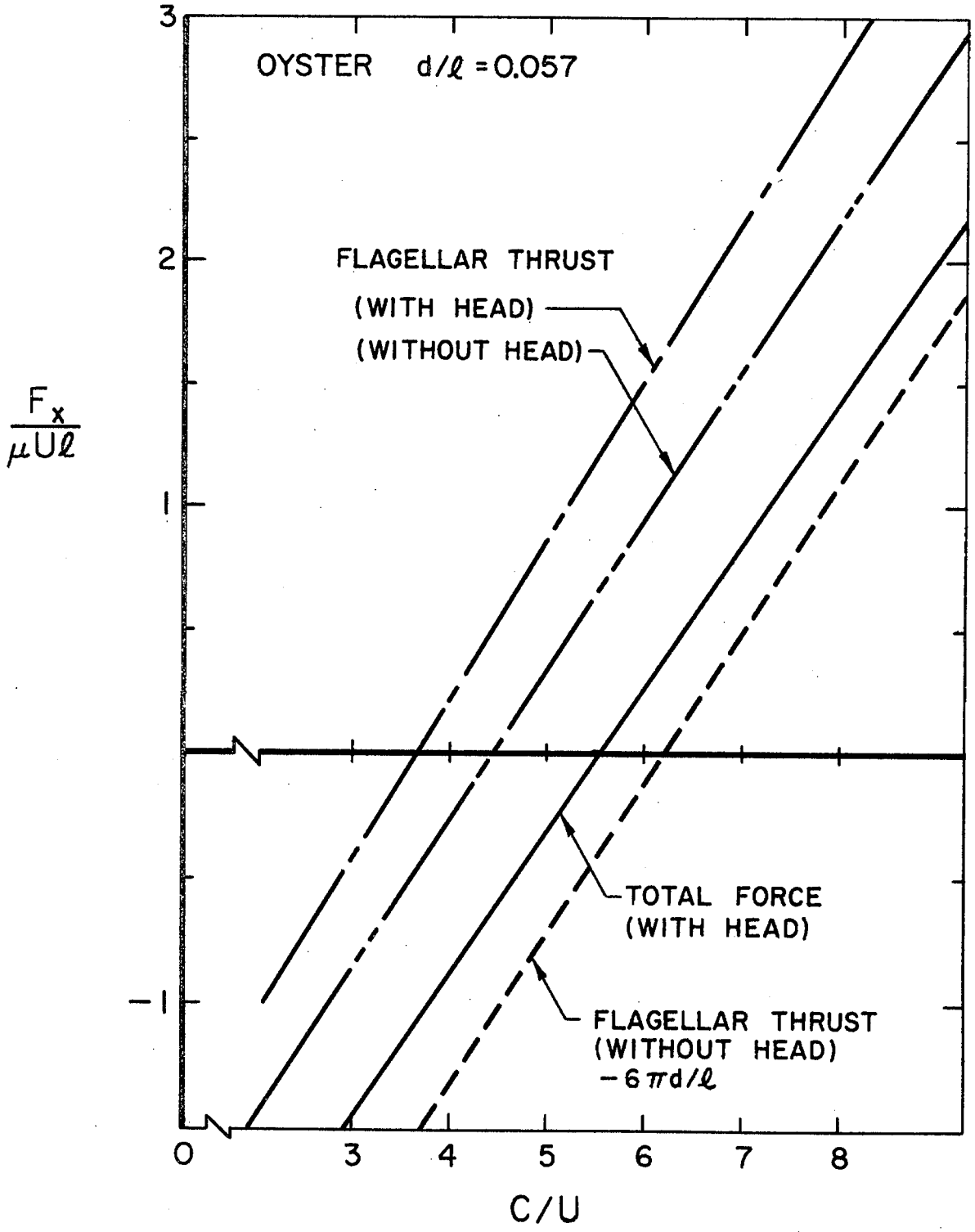

Figure 4.2.3 Average thrust force produced by a flagellum with and without a head present and the total average force on the organism with and without cell body-flagellar interactions.

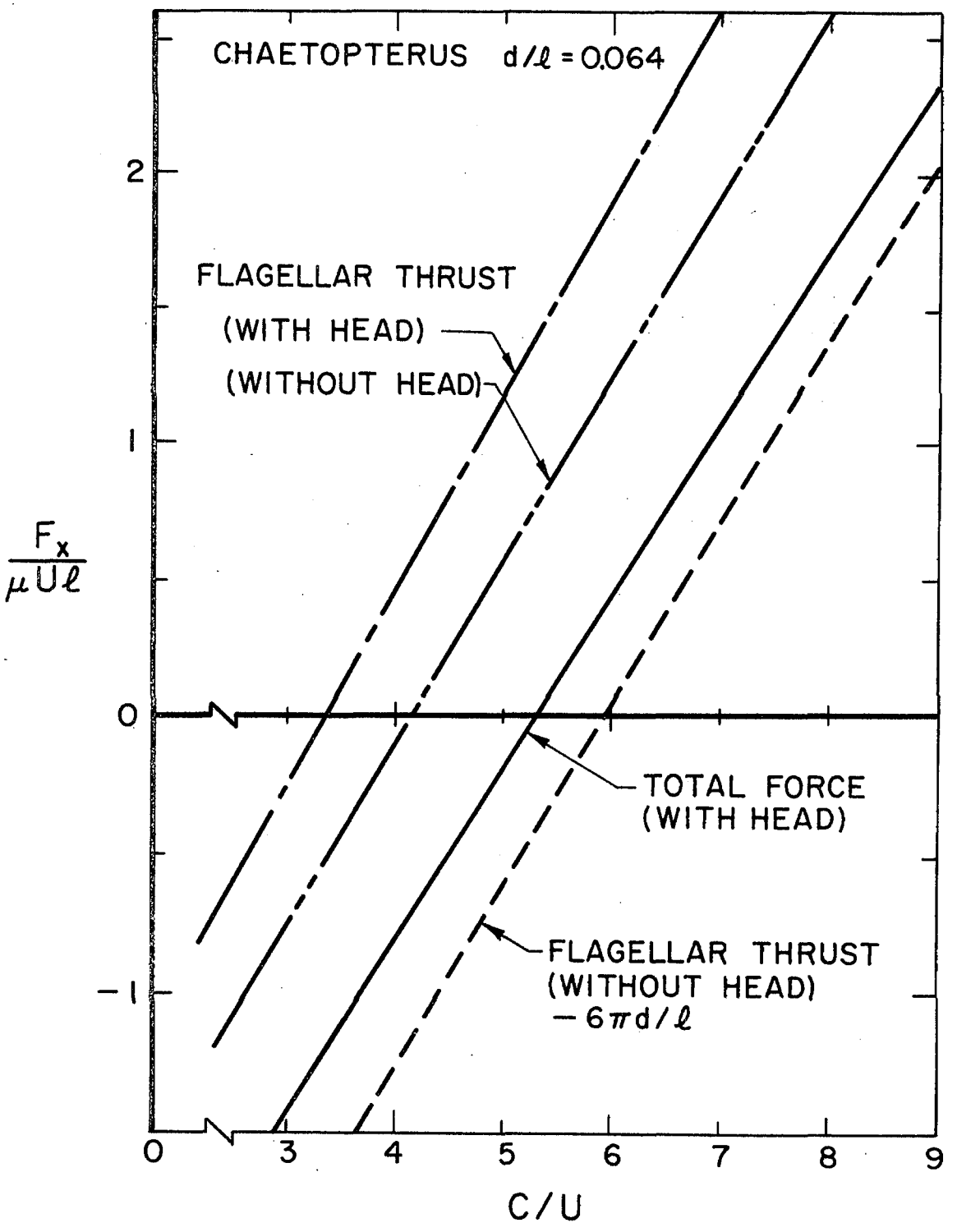

Figure 4. 2. 4 Average thrust force produced by a flagellum with and without a head present and the total average force on the organism with and without cell body-flagellar interactions (head size decreased by 20%).

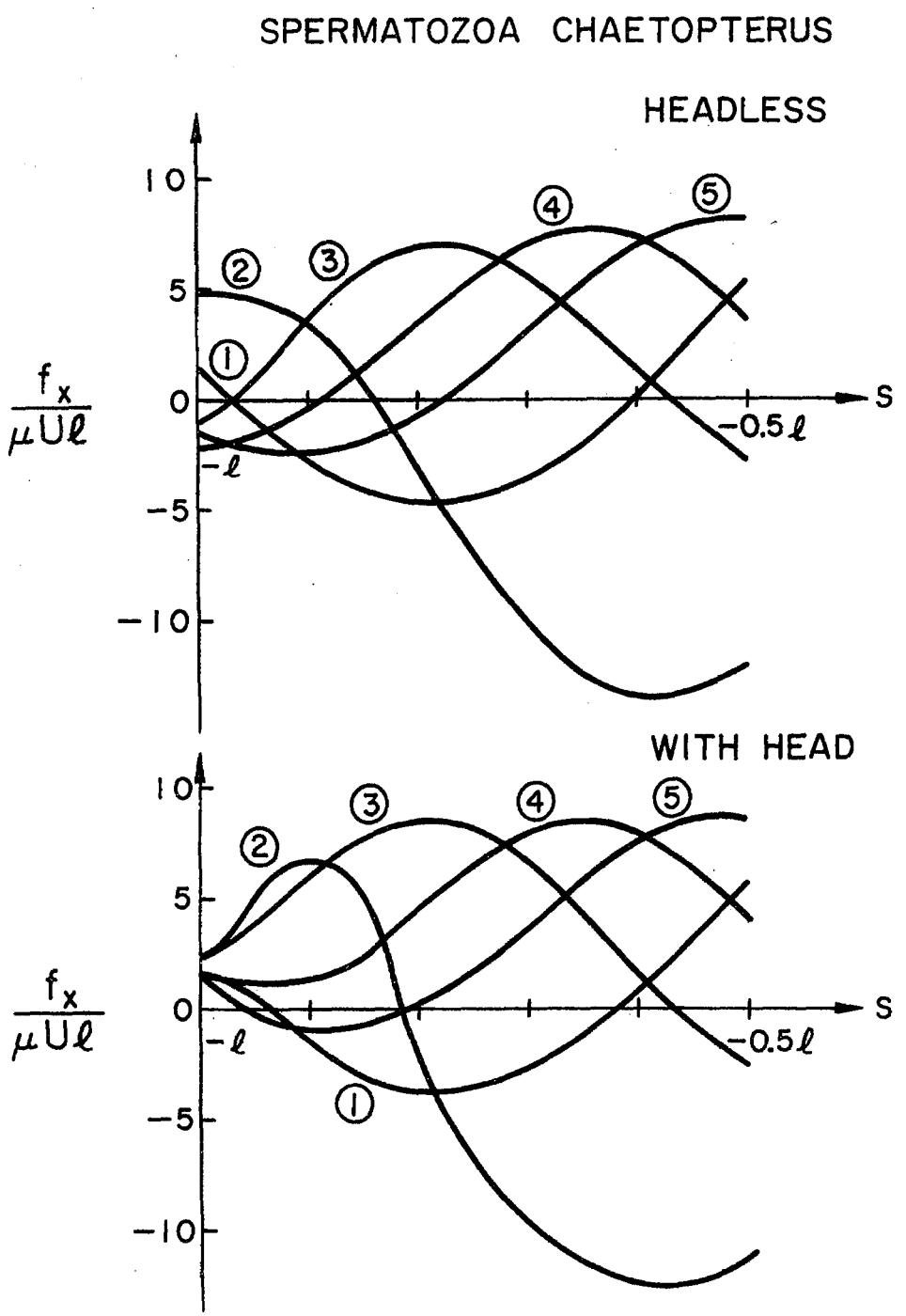

Figure 4. 2. 5 The instantaneous thrust/length at a few instants in time calculated with and without the cell body-flagellar interaction.

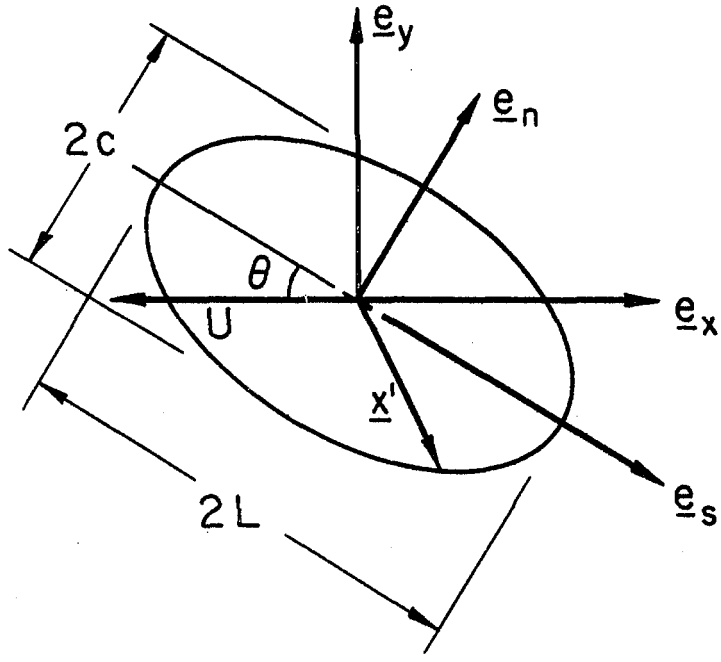

Figure 4. 3. 1 Cell body and coordinates used.

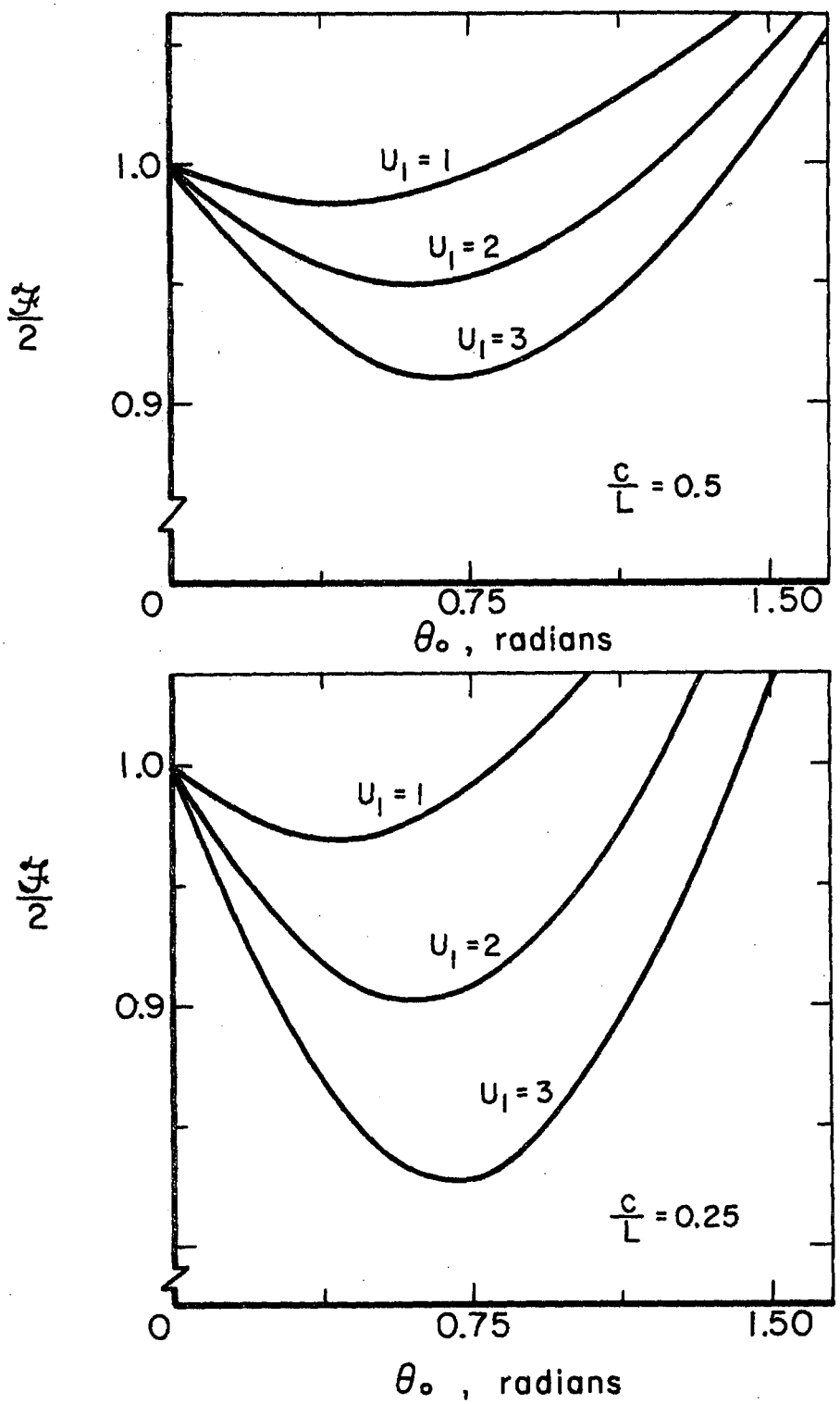

Figure 4.3.2 Drag reduction of a prolate spheroidal cell body that has a periodic transverse motion.